THE SOLVENT EXTRACTION OF CU (II) FROM CHLORIDE SOLUTIONS WITH CERTAIN NON-CHELATING NITROGEN DONOR LIGANDS

A thesis submitted to the

UNIVERSITY OF CAPE TOWN

in fulfilment of the requirements for the degree of

MASTER OF SCIENCE

by

KARIN SOLDENHOFF B.Sc (Hons.) (Witwatersrand)

Mineral and Process Chemistry
Council for Mineral Technology
Randburg
2125
Republic of South Africa

April 1986

CONTENTS

ACKNOWLEDGEMENTS

I would like to take this opportunity to thank :

- Dr J S Preston, my supervisor, whose advice and expert guidance have proved to be invaluable during the course of this work.
- Associate Professor M J Orren and Dr K Koch, my co-supervisors at U.C.T., for their time and helpful comments.
- Dr M J Nicol and Dr C A Fleming of MINTEK for their interest at all times.
- The Council for Mineral Technology (MINTEK) for allowing this work to be used to fulfil the requirements of this degree.

ABSTRACT

The extraction of copper from chloride solutions with some aliphatic oximes as well as some pyridine carboxylates was studied and the complexes formed in the organic phase identified. The association of octanal oxime in toluene was taken into account in the extraction studies and formation constants for dimers and trimers obtained. Copper (II), Nickel (II) and Cobalt (II) are extracted by a solvating mechanism in which only the neutral $MC\ell_2$ species is extractable. This reaction is largely independent of pH.

Studies were also carried out on the use of the commercial reagent ACORGA CLX-20, for the selective extraction of copper from a synthetic solution simulating leach liquors obtained by ferric chloride leaching of complex sulphide ores. Results show that separation of copper from iron is dependent on the amount of acid and chloride present in the aqueous phase.

LIST OF ABBREVIATIONS

LIX	copyright trade mark of General Mills Inc.
KELEX	copyright trade mark of the Ashaland Chemical Co.
SHE	copyright trade mark of Shell Chemicals.
Shellsal	2325 90% aromatic diluent marketed by Shell Chemicals.
P and ACORGA	copyright trade mark of ICI.

aq	aqueous
EDTA	ethylenediaminetetraacetic acid
2EHO	2-ethyl hexanal oxime
i	initial
K.F.	Karl-Fisher
L	ligand
LH	chelating ligand
M^{n+}	metal ion
MPO	2-methyl propanal oxime
NOPC	n-octyl-3-pyridine carboxylate
OCOX	octanal oxime
org	organic
OX	oxime
SWS	standard water solution

CHAPTER 1

CHAPTER 1

INTRODUCTION

1.1 Conventional Methods of Recovery and Processing cf Copper

Copper exists in the earth's crust as sulphide and oxide minerals of which the most common are chalcopyrite ($CuFeS_2$), covellite (CuS), malachite ($CuCO_3 \cdot Cu(OH)_2$) and crysocolla ($CuSiO_3 \cdot 2H_2O$). The major sources of copper are the low grade porphyry type deposits, where the mineral is distributed in fractures and small veins. Copper content is in the region of one percent. Conventional methods of recovery and processing are summarised in Figure 1.1.

Figure 1.1 - Schematic diagram for the treatment of copper ores. Adapted from Kirk-Othmer[1]

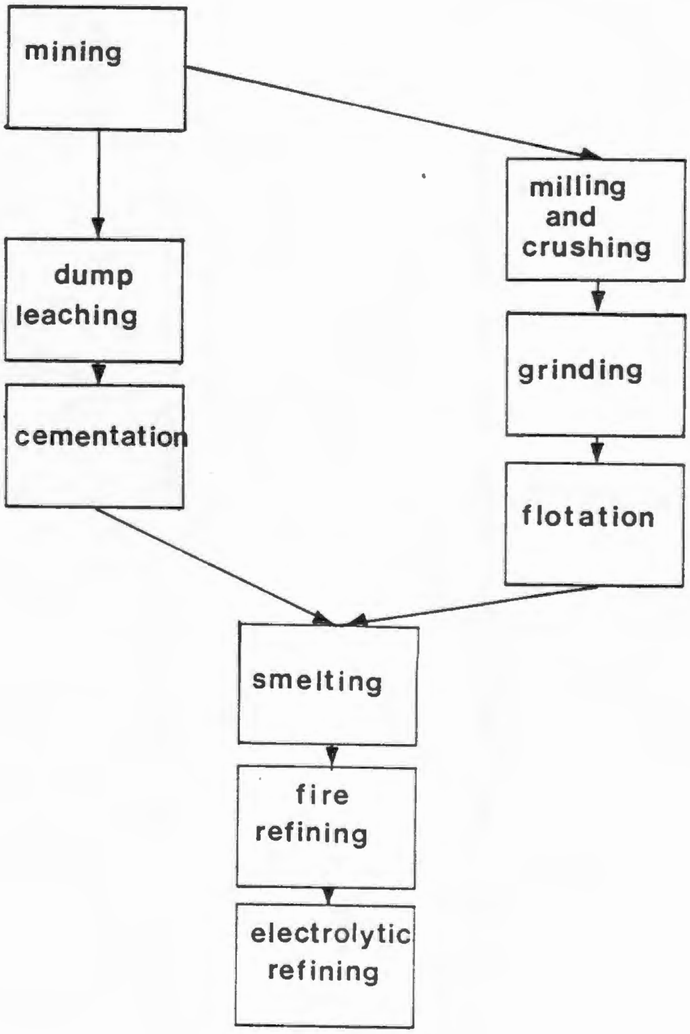

Copper ore, most commonly obtained from open-pit mines, is transported to concentrators where it is crushed and ground with water. The ore slurry is then passed through flotation cells where the mineral is removed as froth. After dewatering the concentrate is ready for smelting.

Dump leaching, a technique used to recover metal values from very low grade ores, is often used to treat waste remaining from mining. The material is piled into heaps and leached by percolation with dilute acid. This is followed by cementation, which consists of passing the pregnant solution over a bed of scrap iron and precipitating metallic copper. The copper obtained by this process needs further refining and is fed into smelters.

The concentrate is melted in reverberatory furnaces to produce a matte containing mixed sulphides of copper, iron and metallic impurities. The molten matte is then taken to converters where oxygen and fluxes react with the metal sulphides to produce inpure metallic copper, SO_2 being the main by-product. The copper obtained from the convertors is known as blister copper and requires further fine-refining and electrolytic refining stages before it can be marketed for industrial use.

The pyrometallurgical techniques described above suffer from the disadvantage of producing large quantities of sulphur dioxide as well as metallic fumes containing amongst others lead, arsenic and antimony. The problem of sulphur dioxide pollution is partially solved by the construction of sulphuric acid plants, next to the smelters. The process economics are however not always favourable, as other factors such as market for the acid near the smelter or treatment of dilute off-gas streams have to be taken into account.

Because conventional metallurgical processing demands the production of separate metal concentrates, it is ineffective in the treatment of complex sulphide ores[2,3]. These consist of very fine-grained mixtures of various minerals, the main components being : chalcopyrite ($CuFeS_2$), sphalerite (ZnS), galena (PbS), pyrite (FeS_2) and pyrrhotite (FeS). As a consequence of their peculiar mineralogical association, selective flotation is unattractive and leads to contaminated concentrates and low metal recoveries. Nevertheless, differential flotation for the recovery of copper, lead and zinc metal values from complex ores has been used, but the processes are complicated[4,5,6].

Hydrometallurgical techniques, on the other hand can easily handle bulk concentrates and many alternative processes have been proposed. They all consist of basically three steps :

1. Leaching of ore or concentrate followed by liquid/solid separation.
2. Purification which may include precipitation, crystallization, cementation, ion-exchange or solvent extraction.
3. Electrowinning

These steps can be modified to suit the particular mineral being treated. For example, a variety of leach regimes are available such as bacterial, chloride, sulphide, acid or ammonia pressure leaching, etc. Recent developments in copper hydrometallurgy are well documented[3,7,10,11].

Of particular interest are the chloride leaching processes which offer high leaching rates and efficiencies for chalcopyrite[8,9], a mineral which is not easily leached by other reagents. In addition, the sulphide in the ore is transformed mainly into elemental sulphur if, for example, ferric or cupric chloride are used as lixiviants[12].

1.2 The Role of Solvent Extraction in Copper Hydrometallurgy

Solvent extraction offers the means to upgrade leach liquors for the production of pure electrolytes. It has been extensively used in the past twenty years, mainly on solutions obtained by the leaching of oxide ores with dilute sulphuric acid. Much research has gone into the development of suitable copper selective extractants, and many reagents are now commercially available[10,11].

The first extractants to be used were of two types[13,14,15].

a) Substituted aliphatic and aromatic o-hydroxyoximes, which includes LIX 63 and the LIX 64, 65, 70 hydroxybenzophenone oximes, the P5000 salicyladoxime series, as well as the SME 529, alkylated acetophenone oximes.

b) The substituted 8-hydroxyquinoline e.g. KELEX 100.

More recently, modified aldoximes as well as ketoxime-aldoxime[16] mixtures have been developed with improved performances in operating plants.

Most of these reagents function as monoprotic acids (LH) so that extraction of divalent metals can be represented by the following equation :

$$2\,\overline{LH} + M^{2+} \rightleftharpoons \overline{ML_2} + 2H^+ \qquad \text{.... (1)}$$

where the bars denote the presence of species in the organic phase.

The nature of the organic extracts as well as the extraction reaction have been extensively studied[17,18,19]. As can be gathered from equation (1) the performance of these extractants is governed above all by the hydrogen ion concentration at the extraction stage. With the development of chloride leaching processes it would be attractive to find extractants that could extract from chloride solutions without the need for pH control. LIX 64N[20] and KELEX 100[21] have been shown to extract copper in the presence of chloride ion. However, hydrochloric acid has a very high activity in concentrated chloride media and thus constraints on the chloride concentration have to be applied.

1.3 The Use of Non-Chelating Nitrogen Donor Ligands for the Extraction of Cu(II) from Chloride Solutions

It is well known that nitrogen donor ligands form stable complexes with copper. The pyridine complexes of copper (II) are a good example, but these are soluble in the aqueous phase and are thus of no use as extractants unless another liquid which is only soluble in the organic phase is used in addition. Thus, Cu(II) pyridine complexes are extracted into organic phases in the presence of salicylic acid[22] or oxygen containing solvents[23].

The new reagent developed by ICI[24], a pyridine dicarboxylic ester known as ACORGA CLX-20, functions as a nitrogen donor. It is able to extract copper from chloride solutions by a mechanism that is largely independent of pH, but that is markedly dependent on chloride concentration. Thus extraction will occur at high chloride concentrations while stripping can be carried out by contacting the metal containing organic phase with water (i.e. the reversal of the extraction process).

$$2\overline{L} + Cu^{2+} + 2Cl^- \leftrightharpoons \overline{CuCl_2L_2}$$

L = ACORGA CLX-20

1.4 Some Theoretical Aspects of Solvent Extraction

Solvent extraction involves the distribution of metal species between two immiscible liquid phases. This distribution may be physical or chemical, but only the latter is of concern in this work. Normally a metal ion exists in solution as an hydrated ion with no tendency to transfer into a non-polar organic phase. To make the metal ion compatible with such an organic phase, its charge has to be neutralized and some or all of its water of hydration substituted by relatively hydrophobic ligands. Extraction systems can be divided into three broad classes, according to the way in which the above requirements are satisfied :

1. Systems involving compound formation such as those using chelating or acidic extractants. These act by a cation exchange mechanism, and it is to this class that the hydroxyoxime extractants belong. The extracted complex is electrically neutral and therefore a cation (generally a proton) must be displaced from the organic phase.

$$M^{n+} + \overline{nHL} \rightleftarrows \overline{ML_n} + nH^+$$

2. Systems involving ion association, resulting from physical attractive forces between oppositely charged species. The extraction of divalent metals from chloride solutions with high molecular weight amines[25] is a good example of an anion-exchange process forming ion-association complexes in the organic phase. The metal is extracted as an anionic species.

$$MCl_n^{(2-n)} + (n-2)\,\overline{R_3NHCl} \rightleftarrows \overline{((R_3NH)_{n-2}\,M\,Cl_n)} + (n-2)\,Cl^-$$

$$n>2 \qquad \ldots.\ (2)$$

3. Systems involving neutral extractants or solvation of the metal ion. In these systems only neutral metal species are extractable. The electron donating properties of the ligands are used either for direct coordination with the metal complex, as is the case for non-chelating nitrogen donor ligands, or for solvation, which occurs with oxygen - containing organic solvents such as ethers.

1.5 Objectives of Research

A considerable amount of work has been done on hydroxyoximes of the type used for the commercial extraction of copper. Other chelating oximes such as α-dioximes[26, 27, 29], azo-oximes, carbonyl oximes, nitrosophenols, amido oximes, α-amino oximes[28] and cyclic trioximes[30] have also been studied[18], but little work has been done on the behaviour of oximes containing no other functional group. Preston studied the effect of non-chelating oximes on the extraction of base metals when used as an additive in organophosphorus[31], carboxylic[32] and sulphonic acid[33] systems. He also reported that these compounds are able to extract copper from chloride solutions without any auxiliary extractants. It was thus decided to examine in greater detail the factors influencing the extraction of copper with aldoximes as well as to compare the behaviour of these extractants with other nitrogen-donor ligands such as n-octyl-3-pyridine carboxylate and ACORGA CLX-20.

The objectives of this work can thus be summarized as follows :

a) To study the extraction of copper from chloride solutions with a typical aliphatic aldoxime (octanal oxime) by examining :

    i) the effect of chloride concentration

    ii) the effect of extractant concentration

    iii) the effect of copper concentration

    iv) the effect of pH

    v) the stoichiometry of the extraction reaction

    vi) the association of extractant in the organic phase

b) To investigate the extraction of copper from chloride solution with n-octyl-3-pyridine carboxylate by similar means as for octanal oxime.

c) To investigate the selectivity of the above extractants for copper over other metals such as Ni^{2+}, Co^{2+} and Fe^{3+} and examine their respective extraction reactions.

d) To test the effectiveness of ACORGA CLX-20 in dealing with solutions simulating liquors obtained from the leaching of complex sulphide ores.

CHAPTER 2

CHAPTER 2

EXPERIMENTAL SECTION

2.1 Chemicals, Reagents and General Procedures

All chemicals and reagents used were analytically pure and obtained from various suppliers. $Ni(NO_3)_2 \cdot 6H_2O$, $AgNO_3$, naphthalene and toluene were obtained from BDH Chemicals, England. $Co(SO_4)_2 \cdot 7H_2O$, $CoCl_2 \cdot 6H_2O$, Cu and Fe were supplied by E. Merk, Darmstad; $FeCl_2 \cdot 4H_2O$, $FeCl_3 \cdot 6H_2O$, and $HClO_4$ by PAL Chemicals, Protea, SA; ZnO by B. Owen Jones, Johannesburg; NaCl, ethylenediaminetetraacetic acid and KI by NT Laboratory Suppliers; LiCl by J.T. Backer Chemical Co, Phillipsburg; $Cu(NO_3)_2 \cdot 3H_2O$ and 8-hydroxyquinoline by Riedel-De Haën AG, Seelze-Hannover and finally nicotinic acid, octan-1-ol, anhydrous methanol, Karl-Fisher reagent, hexamine, KBr and $Na_2S_2O_3$ were obtained from SA AR Chem, Krugersdorp, SA.

Water used to make up all aqueous solutions was triply distilled and filtered by a Millipore system.

n-Octyl-3-pyridine carboxylate was prepared by esterification of nicotinic acid. Octan-1-ol (1,0 mol) and nicotinic acid (0,25 mol) were refluxed for 36 hours at approximately 150 °C, with continuous distillation of the water formed in the reaction. An ~ 80% yield was obtained. The reaction mixture was washed with Na_2CO_3 and filtered. Excess octanol was removed by distillation (b.p. 94 °C, 20 mm Hg) and the ester was distilled at reduced pressure (b.p. 110 °C at 0,15 m bar) (n_D^{18} 1,4883).

Octanal oxime, 2-ethyl hexanal oxime and 2-methyl propanal oxime were prepared as described elsewhere[31].

ACORGA CLX-20 was used as supplied by ICI, England. Its percentage purity was determined as 88,8% by the potentiometric titration of a weighed sample (approximately 2 mmol) dissolved in glacial acetic acid, versus a solution of $HClO_4$ (2mℓ of 70% (w/w) in 50 mℓ acetic acid). Standardisation of acid was done with 8-hydroxyquinoline.

Ultraviolet-visible spectra were run on a Beckman ACTA MIV Spectrophotometer.

Micro analyses were performed by the microanalytical section of MINTEK.

Aqueous metal concentrations ($< [10^{-4}]$M) were determined by atomic absorption using a VARIAN AA-1275 series spectrophotometer. Both sample and standard solutions of Cu, Pb, Zn and Fe were made up in 4% (w/w) HNO_3. The operating conditions recommended by the manufacturers were used.

For metal concentrations higher than $[10^{-3}]$M, the following titration procedures were employed :

a) Titration against[58] ethylenediaminetetraacetic acid

Metal	pH of Titration	Indicator	Buffer
Cu^{2+}	10	Murexide	NH_4^+/NH_3
Ni^{2+}	10	Murexide	NH_4^+/NH_3
Zn^{2+}	6	Xylenol Orange	Hexamine
Co^{2+}	6	Xylenol Orange	Hexamine

b) Iron (III) concentrations (~ 0,05M) were determined by the iodometric titration[62] of iron solutions with excess potassium iodide against a sodium thiosulphate solution (0,1M). Cuprous iodide was added to speed up the reduction of iron (III). Starch was used as the indicator, for monitoring the consumption of iodine.

i.e. $$Fe^{3+} + I^- \leftrightarrows Fe^{2+} + 1/2\ I_2$$

$$2\ Na_2S_2O_3 + I_2 \leftrightarrows Na_2S_4O_6 + 2NaI$$

c) Iron (II) concentrations were determined by titration against tetra ammonium sulphatocerate[63]. A 5 ml sample of ~ 0,05M Fe(II), dissolved in 25 ml of (0,5M) H_2SO_4 was titrated against (0,02M) $(NH_4)_4Ce(SO_4)_4$ solution using (1/40 M) Ferroin solution as indicator.

$$\text{i.e.}\quad 2\,FeSO_4 + 2\,Ce(SO_4)_2 \leftrightarrows Fe_2(SO_4)_3 + Ce_2(SO_4)_3$$

2.2 Vapour Pressure Osmometry Measurements

The mean aggregation numbers of various concentrations of octanal oxime, 2-ethylhexanal oxime and n-octyl-3-pyridine carboxylate were determined with a vapour pressure osmometer constructed at MINTEK.

The measurements were carried out at 25 °C and 1 hour equilibration time was allowed. Naphthalene was used as the standard material for calibration.

Solutions of octanal oxime, 2-ethyl hexanal oxime, n-octyl-3- pyridine carboxylate and Naphthalene were prepared by weighing. Concentrations varied from 0,01 to 1,4 mol kg^{-1}. All measurements, (except those of naphthalene) were carried out with freshly prepared solutions. The instrument was calibrated daily and average readings were used for the calibration curve. For each concentration measurement, readings of ΔR were taken at two minute intervals up to sixteen minutes. ΔR drops linearly with time and the reading for $t = 0$ was obtained by extrapolation. Apparent molalities were read off the calibration curve. The degree of association $\bar{n}$, is then given by :

$$\bar{n} = \frac{\text{analytical molality}}{\text{apparent molality}}$$

$n = 1,0$ where no aggregation occurs

$n > 1,0$ where there is some degree of association.

2.3 Solvent Extraction Procedures

2.3.1 Metal Distribution Equilibria

Aqueous phases contained (0,008M or 5×10^{-4} M) metal; NaCl, KBr or LiCl (0,01 to 5M NaCl or KBr; 5 to 14 M LiCl), and ($1,6 - 2,0 \times 10^{-3}$ M) nitric acid for all metals except iron solutions which contained up to 0,1M acid. Stock solutions of Cu(II) and Ni (II) were made up from their metal nitrate reagents, while those of Fe(III), Fe(II) and Co(II) from the metal chlorides. Zn(II) solutions were made up from ZnO (0,1M) and HNO_3 (0,2M) according to reaction :

$$ZnO + 2\ HNO_3 \leftrightarrows Zn\ (NO_3)_2 + H_2O$$

Fe(II) solutions were made up from Fe powder and hydrochloric acid in the stoichiometric amount according to reaction :

$$Fe + 2\ HCl \leftrightarrows FeC\ell_2 + H_2\uparrow$$

Boiled water was used to prevent oxidation of Fe(II) to Fe(III).

Cu(I) solutions were made up from CuCl, and copper metal was added in excess to reduce any Cu(II) present.

$$Cu^0 + Cu^{2+} \leftrightarrows 2\ Cu^{1+}$$

Reagent concentrations for individual experiments are given in their respective graphs.

The extractants were dissolved in toluene and an approximate ten fold excess extractant to metal concentration was used. Equal volumes (25 ml) of organic and aqueous phases were shaken until equilibrium was reached. (At least 15 min for Cu, Co, and Fe and 1 hour for Ni and Zn). Contact times were determined by preliminary experiments. When the two phases were clearly separated, metal concentrations in the aqueous phase were determined by titration against EDTA, if the initial aqueous metal concentrations were (0,008M) or by atomic absorption if $[M^{2+}]_{aq}$ init. = $5x10^{-4}$M. Iron determinations were done by titration against sodium thiosulphate or tetra ammonium sulphatocerate. The difference between initial and final aqueous metal concentrations was assumed to be equal to the metal concentration in the organic phase. The percentage extraction and the distribution coefficient was calculated as shown :

$$\% \text{ Extraction} = \frac{[\text{metal}]_{\text{org}}}{[\text{metal}]_{\text{aq initial}}} \times 100$$

$$D = \frac{[\text{metal}]_{\text{org}}}{[\text{metal}]_{\text{aq}}}$$

$$= \frac{[\text{metal}]_{\text{aq initial}} - [\text{metal}]_{\text{aq final}}}{[\text{metal}]_{\text{aq final}}}$$

2.3.2 Determination of Halogen to Metal Ratio in the Extracted Complexes

Aqueous solutions containing (0,004 - 0,016M) Cu^{2+}, (2,0M) NaCl or KBr and (0,0016M) HNO_3 were contacted with (0,2M) extractant solutions (OCOX, 2EHO) dissolved in toluene or n-heptane as described in section 2.3.1. After equilibrium had been reached a known volume of organic phase (20 ml) was stripped with 0,01M HNO_3 (20 ml). The copper content in the stripped solution was determined by titration against EDTA and the halogen content by potentiometric titration with silver nitrate.

2.3.3 Determination of Extractant to Copper Ratio in the Extracted Complex - Loading Curves

i) Loading Curve of Copper with 0,05M Octanal Oxime

Aqueous solutions (25 ml) containing (4,0M) NaCl or (3,6M) KBr, (0,02M) HNO_3 and $Cu(NO_3)_2$ concentrations varying from 0,004M to 2,8M were contacted with (0,05M) octanal oxime solutions (25 ml) in toluene. The amount of copper extracted into the organic phase was then determined as follows :

A known amount of organic phase (20 ml) was heated until most of the toluene was evaporated. 10 ml of 25% (w/w) HNO_3 were then added and the solution was boiled for ~15 minutes. Upon addition of acid the Cu/oxime complex breaks down, the copper goes into solution and the remaining solvent is evaporated. The aqueous solution was then transferred into a 50 ml volumetric flask and its metal content determined by titration against EDTA.

With this method one hopes to fully saturate the organic phase with copper so that one reaches a point where no matter how much copper is present in the aqueous phase, the copper concentration in the organic phase remains constant.

ii) Loading Curve of Copper with n-octyl-3-pyridine carboxylate

Organic phase : (0,05M) NOPC
Aqueous phase : (4,0M) NaCl, (0,02M) HNO_3, (0,004 - 2,9M) $Cu(NO_3)_2$.

The experimental details are the same as for section 2.3.3 (i). At $[Cu]_{aq\ i} > 0{,}05M$ a blue precipitate appeared in the organic phase. This was filtered, dried and weighed. The total amount of copper in the aqueous phase was then calculated as :

$$[Cu]_{org}\ (total) = [Cu]_{org}\ (soluble) + [Cu]_{org}\ (precipitate)$$

where the $[Cu]_{org}$ (soluble) concentration was determined in the same manner as in 2.3.3 (i).

2.3.4 Loading and Stripping Isotherms

Loading isotherm : Aqueous solutions of (0,4M $CuCl_2{\cdot}2H_2O$, 0,3M $ZnCl_2$, saturated $PbCl_2$ (<0,05M), 3M $FeCl_2$ and (0,1/0,5M HCl) were contacted with 26% by volume ACORGA CLX-20 dissolved in Shellsol 2325. Aqueous to organic phase ratios varied in the following manner :

Vol aq (ml)	5	5	5	5	10	20
Vol org (ml)	25	15	10	5	5	5

The copper content in the organic phase was determined by titration against EDTA, and the aqueous copper content was calculated from the initial copper concentration.

Stripping isotherm : Aqueous solutions contained (0,394M) $CuCl_2$ and (0,15M) HCl. These were contacted with organic phases of 26% by volume ACORGA CLX-20 in Shellsol 2325 loaded with 14,2 gl^{-1} (0,22M) copper. Phase ratios used were :

Vol org (ml)	50	25	10	10	10	5
Vol aq (ml)	5	5	5	10	20	20

2.3.5 Determination of the Percentage Protonation of ACORGA CLX-20

The amount of acid extracted from aqueous phases containing (6,4-7,9 M) LiCl, (5 x 10^{-3} M) HCl and (8mM) Fe^{3+} into the organic phase by toluene solutions of ACORGA CLX-20 (0,2M), was determined by taking a 4 ml sample from the organic phase, dissolving it in ethanol and titrating against 0,01M NaOH. Bromothymol blue was used as an indicator.

2.4 Determination of the Relative pKa of Extractants in Ethanol

Octanal oxime and n-octyl-3-pyridine carboxylate solutions contained 0,05M extractant, 5 x 10^{-3} M $NaNO_3$ and 80% (v/v) ethanol·ACORGA CLX-20 solutions were made up to 90% (v/v) ethanol in water. 40 mls of the above stock solutions were titrated against 1,868M $HC\ell O_4$ solution in water. The pH of the titration was monitored with a glass electrode. Calculation of pKa is shown in Appendix 2.

2.5 Determination of the Solubility of Extractants in Water

Solutions of the extractants in ethanol, (10,048 mg ml^{-1} OCOX, 5,232 mg ml^{-1} NOPC, 5,017 mg ml^{-1} ACORGA CLX-20) were added by means of a micro burette, to a well stirred water solution (200 ml) containing (2,0 M NaCl, 0,0016 M HNO_3). The absorbance in the ultraviolet region was monitored as a function of volume added, at the following wavelengths :

Octanal oxime	λ = 220 nm
n-octyl-3-pyridine carboxylate	λ = 280 nm
ACORGA CLX-20	λ = 350, 190 nm

2.6 Determination of Water Content in the Organic Phase

Water contents of organic phases were determined by the Karl Fisher method[60]. A schematic diagram of the apparatus is shown in Figure 2.1. The Karl-Fisher reagent consists of a mixture of iodine, sulphur dioxide, anhydrous pyridine and anhydrous methanol. One molecule of iodine reacts with one molecule of water. The end point of the titration is signalled by an excess of I_2, which is detected electrometrically using a dead-stop end point procedure. The Karl-Fisher reagent was used in conjunction with a standard water solution (SWS) in methanol (2,753 mg ml^{-1}). The sample containing water was over titrated with K-F reagent. At this point the solution had a dark brown colour and a current of approximately 60 mA was measured. As the SWS was added the current decreased and reached zero at the end point.

The water content in the extracted complex was determined as follows : An aqueous solution of known $Cu(NO_3)_2$, HNO_3 and NaCl concentration was contacted with a solution of octanal oxime in toluene and the amount of copper and water transferred into the organic phase determined. The experiment was repeated under the same conditions but with no copper present, to find out how much water is transferred into the organic phase by the action of oxime alone. This amount was then subtracted from the first result.

Figure 2.1 - Apparatus for Karl-Fisher titration

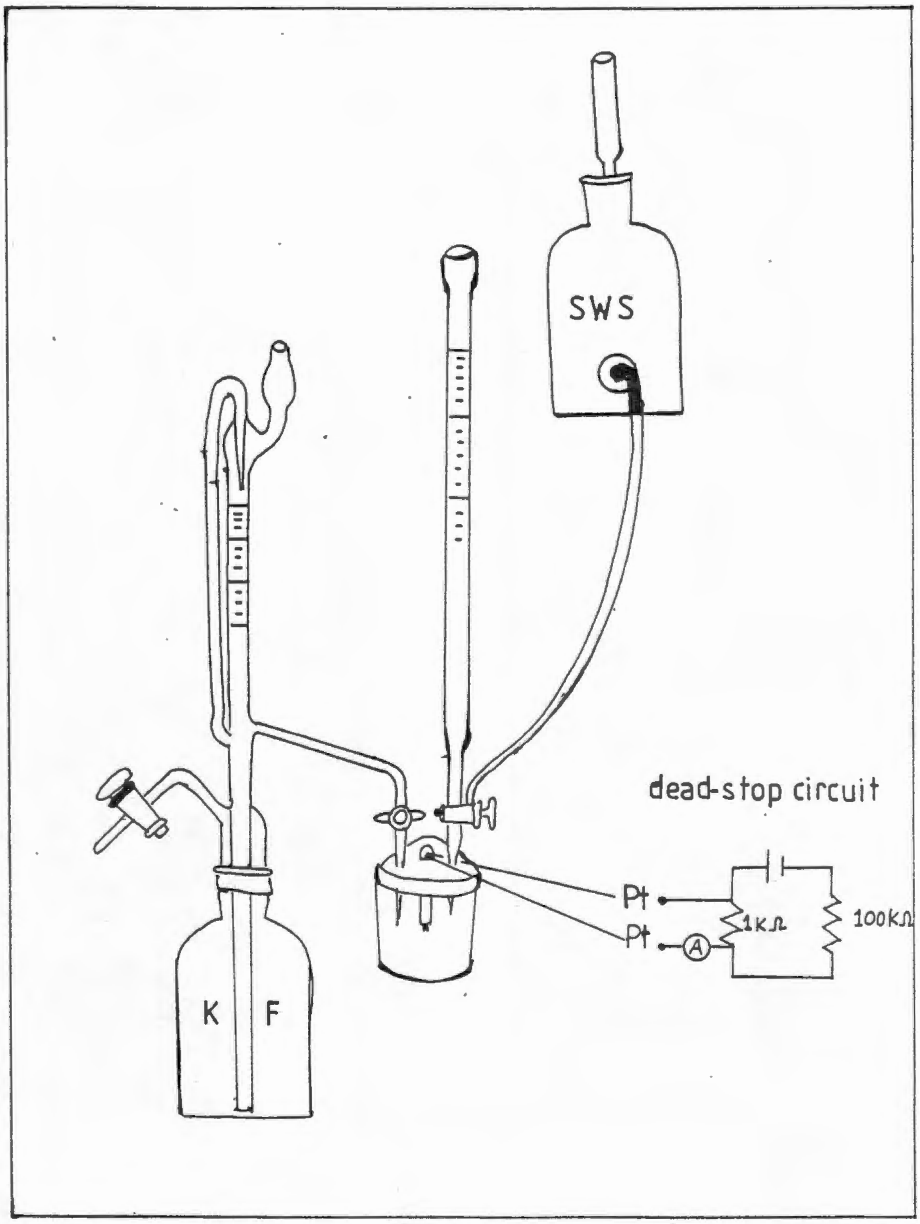

2.7 Batch Counter-Current Extraction of Copper with ACORGA CLX-20

Organic phases consisted of 26% by volume of ACORGA CLX-20 in an aromatic diluent, Shellsol 2325, as recommended by manufacturers. The aqueous feed solutions contained 22 gl^{-1} copper, 16,3 gl^{-1} zinc, saturated lead (< 10 gl^{-1}) 117,2 gl^{-1} iron and 0,5M HCl. The total chloride concentration was 6,0 M. The organic to aqueous phase ratio used was 2,5. Ten mls of aqueous phase were shaken with 25 ml of organic for ten minutes. The phases were allowed to settle. After separation they were transferred as described in Figure 2.2. Three stages and five cycles were used. The organic phases were then stripped with 0,1M nitric acid and the lead, zinc and iron content determined by atomic absorption. The copper remaining in the raffinate was also determined by A.A. The copper content in the organic phase was determined by taking 1 ml aliquot, buffering to pH 10, filtering the iron precipitate and titrating for copper with EDTA.

Figure 2.2 - Flow chart diagram for Copper batch countercurrent experiments

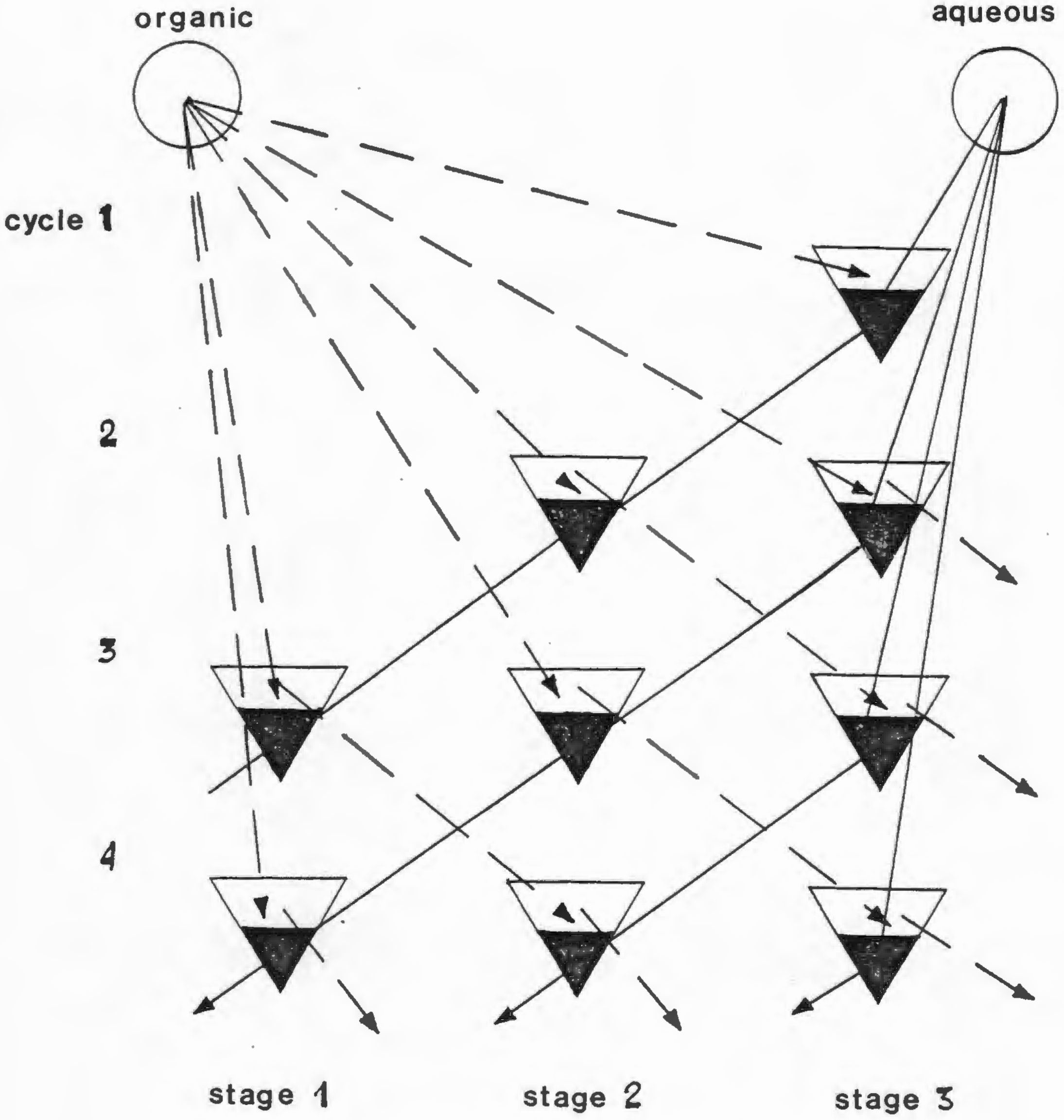

CHAPTER 3

CHAPTER 3

ASSOCIATION EQUILIBRIA OF OCTANAL OXIME IN TOLUENE

In order to fully understand the reaction occurring between metal complexes and extractants in liquid-liquid systems, one has to know how the extractant molecules themselves interact with each other, and to what extent these interactions interfere with the transfer of metal complexes from the aqueous to the organic phase.

The association of octanal oxime in chloroform has been studied by Geiseler and Stockel[34] by infra-red spectroscopy, but no formation constants are given for the proposed dimers and trimers. In this work, the aggregation equilibria of octanal oxime in toluene was studied by vapour pressure osmometry. This method has been widely used for the determination of association constants of certain phosphates[35], ammonium[35 36], and hydroxyoxime[37] complexes.

The technique involves measuring the differences in electrical resistance experienced by two thermistors placed in a cell saturated with solvent vapour. A drop of sample solution is placed on one thermistor and a drop of solvent on the other. The vapour pressure around the sample drop is smaller than the vapour pressure of the solvent due to the lowering of its chemical potential, i.e.

$$u_A(\ell) = u_S^* (\ell) + RT \ln x_S$$

$u_A(\ell)$ = chemical potential of sample drop

$u_S^*(\ell)$ = chemical potential of pure solvent

x_S = mole fraction of solvent.

As a consequence, solvent molecules diffuse out of the solvent drop and into the sample drop generating a difference in temperature which is measured in ohms (ΔR). The temperature shift is proportional to the molality of the dissolved substance.

The vapour pressure osmometer must be calibrated with a standard of known concentration in the solvent being used; in this case, toluene.

The differences in resistance, ΔR, observed for various concentrations of naphthalene in toluene are shown in Table 3.1. The plot of ΔR versus analytical molality (C), Figure 3.1, should be linear with zero intercept since naphthalene is not expected to associate in solutions of toluene. Experimentally a small deviation from linearity can be seen which can be described by

$$\Delta R = k_1C + k_2C^2 \qquad \ldots. \ (3.1)$$

where C = analytical molality
$k_1 = 990 \pm 7\ \Omega\ 1\ \mathrm{mol}^{-1}$
$k_2 = -104 \pm 3\ \Omega\ 1^2\ \mathrm{mol}^{-2}$

Calibration constants k_1 and k_2 were determined by general least squares treatment of the data.

Table 3.1 - Osmometric Data for Naphthalene in Toluene at 25 °C

C mol.kg^{-1}	ΔR Ohm	C mol.kg^{-1}	ΔR Ohm	C mol.kg^{-1}	ΔR Ohm
0,0115	11,1	0,0820	81,7	0,4876	452,8
0,0232	23,2	0,1192	117,9	0,5842	525,0
0,0347	34,1	0,1764	160,2	0,7565	701,2
0 0463	45,4	0,2357	228,8	1,0105	898,0
0,0582	58,3	0,3591	345,0	1,3141	1130,0

The experimental data points (ΔR, C) obtained for the octanal oxime solution are also shown in Figure 3.1 and it is evident from the plot that they deviate from monomeric behaviour. The apparent molality (S) is then calculated from the calibration equation (3.1).

Figure 3.1 - ΔR as a function of total concentration of Octanal Oxime in Toluene ⊙. Naphthalene calibration curve (full line) represents monomeric behaviour

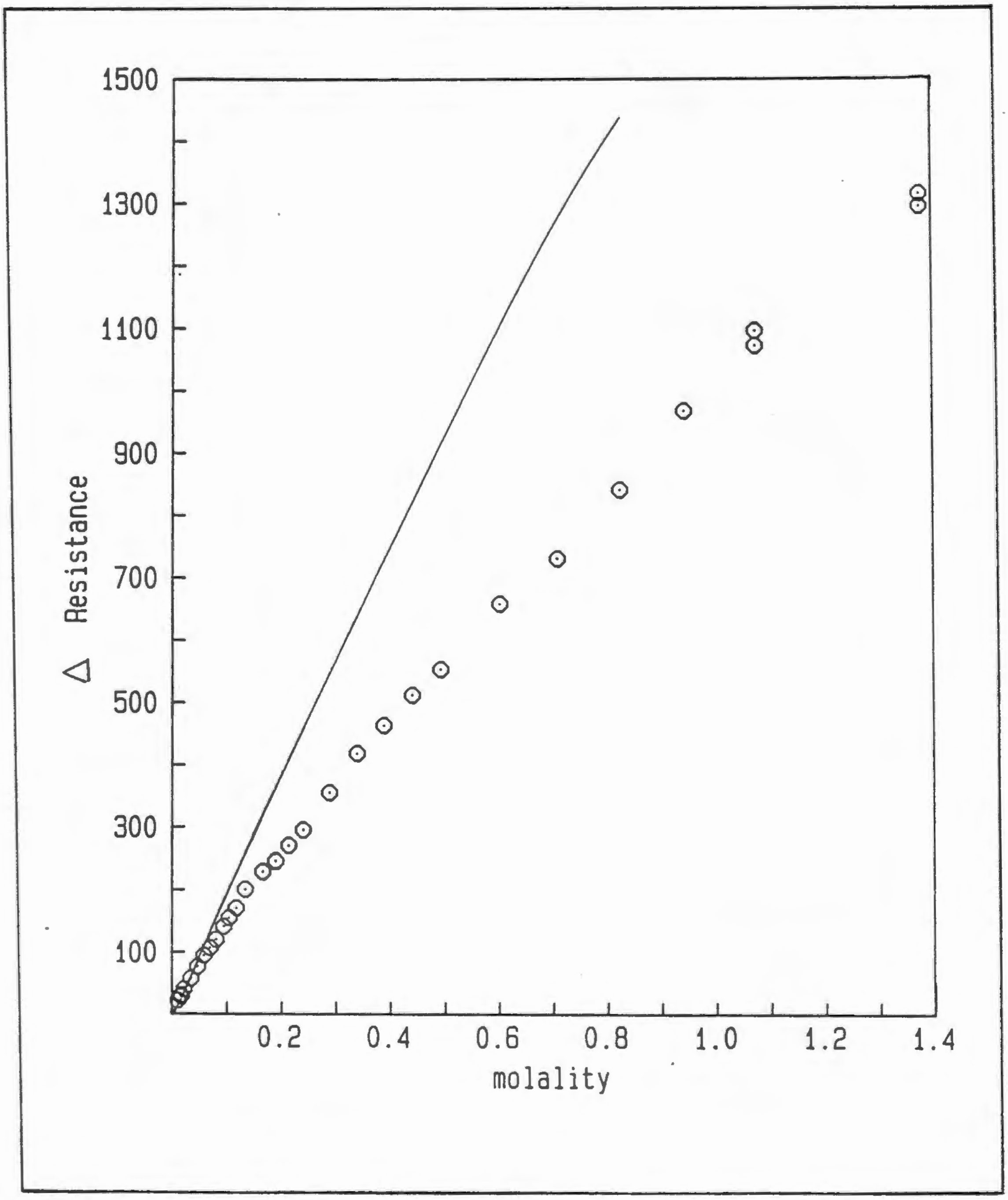

The aggregation process can be represented by the general equation :

$$n\ b \leftrightarrows b_n \qquad \text{.... (3.2)}$$

where b = monomeric concentration and $n > 2$

The corresponding formation constants are given by :

$$\beta n = \frac{[b_n]}{[b]^n}$$

The apparent and analytical concentrations can be written in terms of the monomeric concentration as shown in the following mass balance equations :

Analytical concentration $C = b + 2b_2 + \ldots nb$

$$= b + 2\beta_2 b^2 + \ldots n\beta_n\ b^n$$

$$= \sum_1^n n\beta_n\ b^n \qquad \text{.... (3.3)}$$

Apparent concentration $S = b + b_2 + \ldots b_n$

$$= b + \beta_2 b^2 + \ldots \beta_n\ b^n$$

$$= \sum_1^n \beta_n\ b^n \qquad \text{.... (3.4)}$$

The degree of association $\bar{n} = \dfrac{\text{analytical concentration}}{\text{apparent concentration}}$

$$= \frac{C}{S} \qquad \text{.... (3.5)}$$

Differentiating equation (3.4) and incorporating (3.5) one obtains

$$\frac{dS}{db} = \sum_1^n n\ \beta_n\ b^{n-1} = \frac{C}{b} = \frac{S\bar{n}}{b}$$

or

$$\frac{dS}{S}\bar{n}^{-1} = \frac{db}{b}$$

Therefore $\log b - \log b_o = \int_{S_o}^{S} (n)^{-1}\ d \log S$ .... (3.6)

The monomer concentration[36] can be calculated from the area underneath the curve $(\bar{n})^{-1} = f\ (\log S)$, where S_0 is sufficiently small so that one can safely assume that no association occurs, i.e. (a value of S where $b_0 = S_0$). Experimentally below molalities of 0,01 no difference could be found between ΔR readings given by napthalene and those given by octanal oxime solutions. The S_0 value was set at 0,005 molal. The area under the curve $(\bar{n})^{-1} = f\ (\log S)$ was calculated using the trapezoidal rule.

$$\text{Area} = \Delta x_i\ f\ (x_{i-1}) + 1/2\ [f(x_i) - f(x_{i-1})]\ \Delta x_i$$

where $f(x_i) > f(x_{i-1})$

and x_i is given by experimentally determined log S.

By using numerical integration one avoids smoothing the data to fit a specific function and then introduce further errors.

3.1 Determination of Highest Aggregate

Considering equilibria of the type shown in equation (3.2), one has to find a limiting value for n. This can be done by considering equation (3.3) rearranged as :

$$\log\left(\frac{C}{b} - 1\right) = \log\left(\sum n\beta_n\right) + (n-1)\log b \qquad \ldots .\ (3.7)$$

A plot of log (C/b - 1) versus log b is shown in Figure 3.2. The highest slope obtained is 1,6 and thus the upper limit of (n-1) equals 2, representing the formation of a trimer.

This is confirmed by considering as an approximation the formation of dimers exclusively. From equations (3.3) to (3.5) one can obtain an expression for C in terms of $\bar{n}$.

Figure 3.2 - Determination of limiting slope of plot log (C/b - 1) versus log b

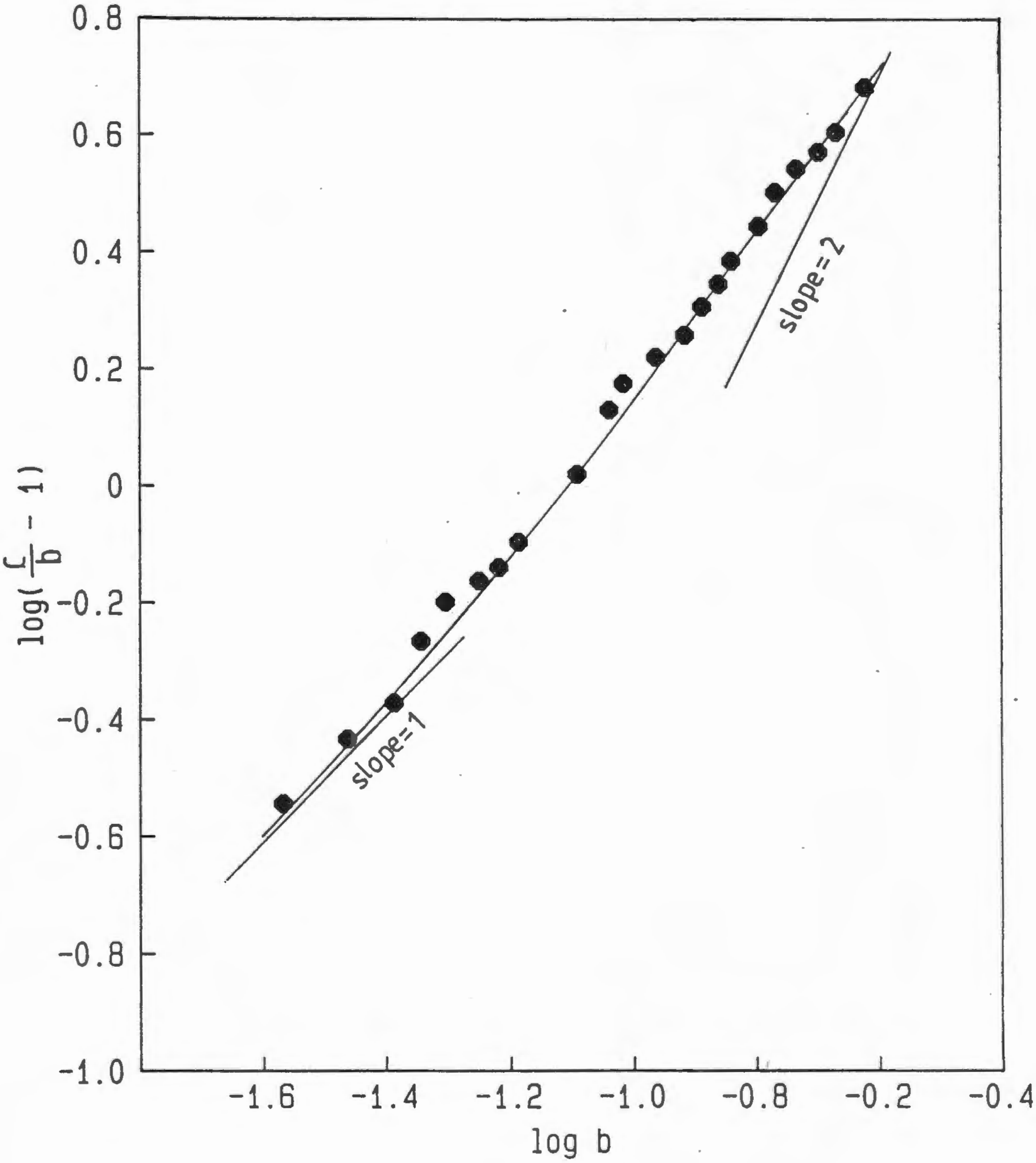

$$\text{ie. } \beta_2 C = \left(\frac{\bar{n}\ (\bar{n}-1)}{(2 - \bar{n})^2}\right) \qquad \ldots. \ (3.8)$$

If the assumption is correct then a plot of $\bar{n}(\bar{n}-1)/(2-\bar{n})^2$ versus C should be a straight line. Such a plot is shown in Figure 3.3 and one can see that the curve is by no means linear. However, if a similar plot is made based on the assumption that only trimers are formed one obtains a reasonable linear correlation based on equation (3.9). This confirms the presence of trimers.

$$\beta_3{}^{1/2}C = (2\bar{n}(\bar{n}-1)^{1/2})/((3-\bar{n})^{3/2}) \qquad \ldots. \ (3.9)$$

It is therefore reasonable to assume that the system can be described by a monomer-dimer-trimer equilibrium.

3.2 Calculation of Formation Constants for $(OCOX)_2$ and $(OCOX)_3$ SPECIES

3.2.1 Graphical treatment : Formation constants β_2 and β_3 can be determined by the projection maps method[43],by the introduction of the following normalised functions :

$$u = \beta_2 b \qquad \ldots. \ (3.10)$$

$$L = \beta_3\ \beta_2{}^{-2} \qquad \ldots. \ (3.11)$$

where $\log (C/b - 1) = \log (2\beta_2\ b + 3\ \beta_3 b^2)$ becomes

$$y = \log (2u + 3Lu^2) \qquad \ldots. \ (3.12)$$

Figure 3.4 shows a family of Y curves, determined for various values of L, superimposed on the experimental y = f(log b) plot. The best fit was found for L = 0,5, but as can be appreciated from the closeness of the curves, y values are not very sensitive to the L constant. Formation

Figure 3.3 - Analytical concentration as a function of degree of association ($\bar{n}$), for formation of Dimers (curve a) and Trimers (curve b) exclusively

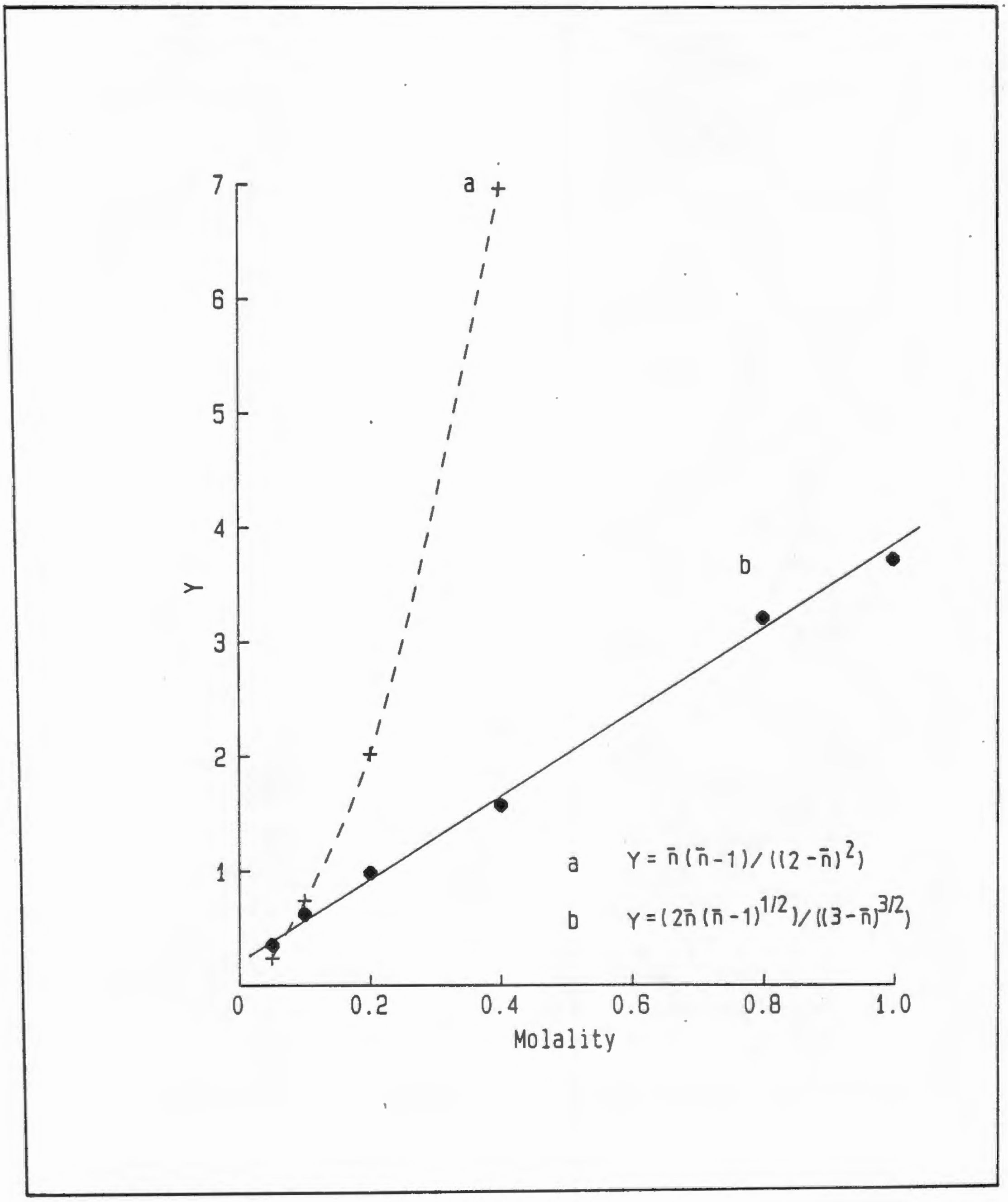

constant β_2, is then equal to the difference in x values between y = f(log b) and y = f(log u). This is apparent from equations (3.10), where

$$\log u = \log \beta_2 + \log b \qquad \ldots (3.13)$$

β_3 is simply calculated from equation (3.11). Formation constants β_2 and β_3 are shown in table 3.3.

3.2.2 Numerical treatment : Least squares treatment was used to fit a third order polynomical to the experimental data (C,b), i.e.

$$C = P_1 + P_2b + P_3b^2 + P_4b^3$$

where P_1 and P_2 were set at 0 and 1 respectively.

Trial runs assuming formation of other species were done.

Table 3.2 shows the various models tried out with their respective sums of squares error, u, which is smallest for the monomer-dimer-trimer model

$$u \text{ defined as } = \sum \left(\frac{C_{exp} - C_{cal}}{C_{exp}}\right)^2$$

Table 3.2 - Polynomial Fits

Polynomial	u	Equilibrium Assumed			
1,2	0,119	monomer	dimer		
1,3	0,276	monomer	trimer		
1,4	0,348	monomer	tetramer		
1,2,3	0,008	monomer	dimer	trimer	
1,2,4	0,029	monomer	dimer	tetramer	
1,2,3,4	0,033	monomer	dimer	trimer	tetramer

Figure 3.4 - log (C/b-1) versus log b plot superimposed on a family of $y = \log(2u + 3u^2 L)$ curves

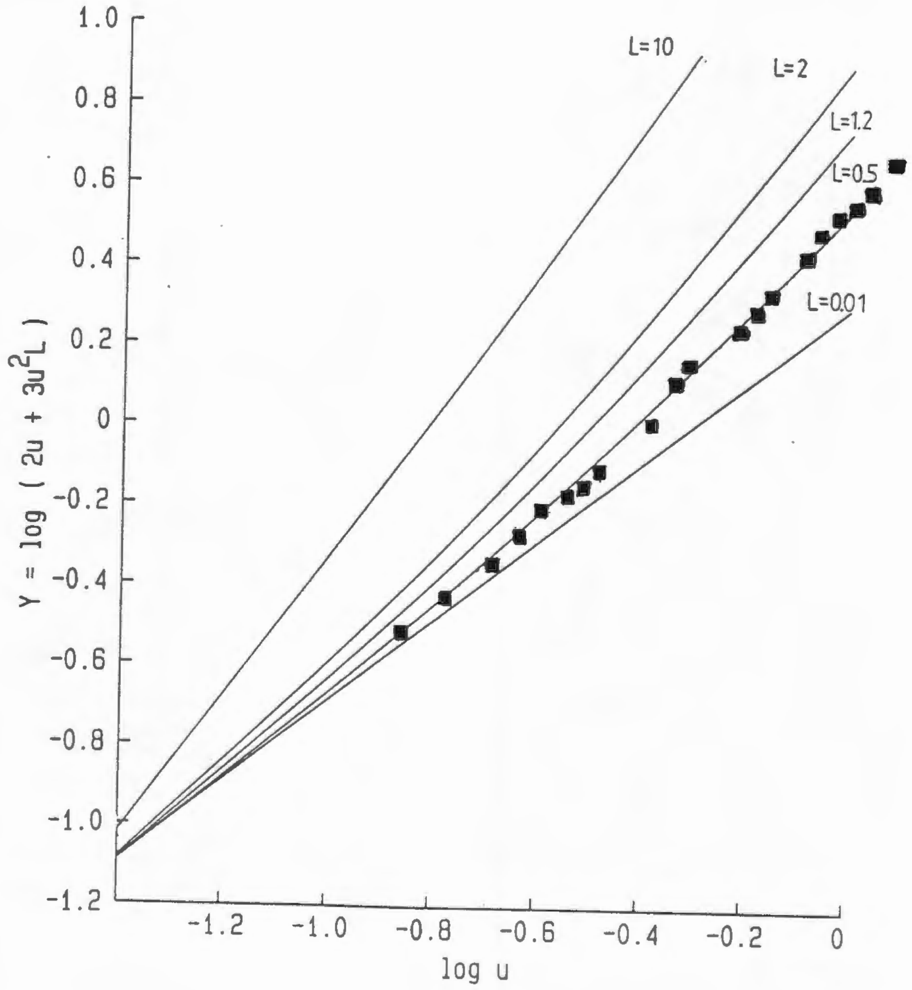

Table 3.3 - Formation Constants for Dimer (β_2) and Trimer (β_3)

Method	β_2	β_3
Graphical	5,24	13,77
Numerical	6,25	12,01

The final formation constants are shown in Table 3.3. From the species distribution diagram, (Figure 3.5), one can see that at concentrations between (0,2 - 1,4 molal), the trimer is formed at the expense of the monomer, while the dimer remains reasonably constant. The dimer stability can be explained in terms of the formation of a six-membered ring resulting from intermolecular hydrogen bonding between the nitrogen and the hydroxy hydrogen as shown in Figure 3.6.

The association of 2-ethyl hexanal oxime in toluene was not studied in detail as this reagent was only used on a few extraction experiments. The degree of association was found to be roughly similar to that of octanal oxime as shown in Table 3.4.

Table 3.4 - Mean Aggregation Numbers of Oxime Solutions in Toluene

Molarity	Octanal Oxime	2-Ethyl Hexanal Oxime
0,1	1,35	1,25
0,2	1,54	1,43
0,4	1,69	1,60
0,8	1,81	1,85

3.3 <u>Summary</u> : The aggregation of octanal oxime in toluene was studied by vapour pressure osmometry at 25 °C. It was found that at concentrations up to 1,4 molal monomers, dimers and trimers were present. The data was treated both graphically and numerically. Formation constants for dimers (β_2 = 6,25) and trimers (β_3 = 12,01) were obtained.

Figure 3.5 - Species distribution diagram for the association of Octanal Oxime in Toluene, 25 ° C

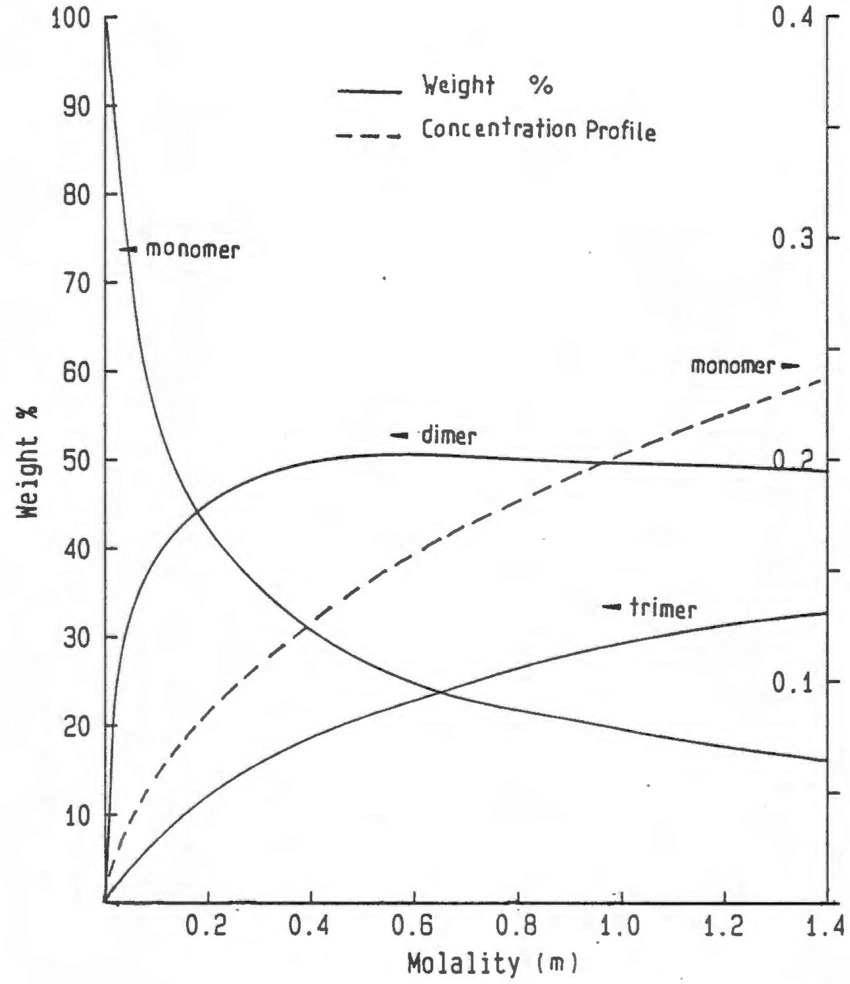

Figure 3.6 - Octanal Oxime Dimer structure

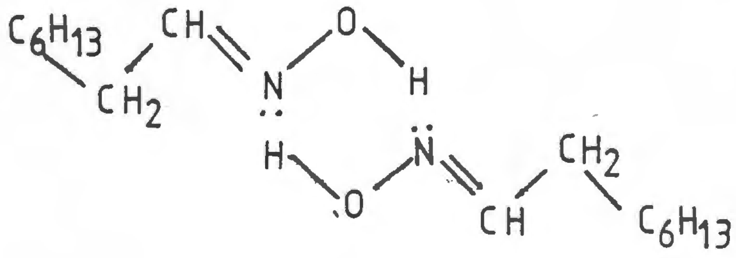

CHAPTER 4

CHAPTER 4

SOLVENT EXTRACTION OF COPPER FROM CHLORIDE SOLUTIONS WITH SOME ALIPHATIC OXIMES

4.1 Extraction of Copper with Octanal Oxime

Octanal oxime is a non-chelating ligand and is expected to extract copper from chloride solutions by the general reaction :

$$Cu^{n+} + n\,Cl^{-} + \overline{m\,OX} \rightleftarrows \overline{CuCl_n\,OX_m} \qquad \ldots\ (4.1)$$

where the bars indicate the presence of the species in the organic phase and OX represents the oxime. Incorporating the equilibrium constant and distribution coefficient into equation (4.1) one obtains the following expression :

$$\log D = \log K_{EX} + n \log \{Cl^{-}\} + m \log \{OX\} \qquad \ldots.\ (4.2)$$

$$\text{where} \quad K_{EX} = \frac{\gamma\,(MC\ell_nOX_m)}{\gamma(M^{2+})(\gamma(C\ell))^n\ (\gamma(OX))^m} \quad x \quad \frac{[MC\ell_nOX_m]}{[C\ell]^n\ [OX]^m[M^{2+}]}$$

$$= \frac{[MC\ell_nOX_m]}{\{Cl^{-}\}^n\ \{OX\}^m\ [M^{2+}]} \qquad \ldots.\ (4.3)$$

assuming

$$\gamma\ (MC\ell_nOX_m) = \gamma\ (M^{2+}) = 1$$

$$\text{and } D = [\text{Metal}]_{org}\ /\ [\text{Metal}]_{aq}$$

$$= \frac{[MCl_n\ OX_m]}{[M^{2+}]} \qquad \ldots.\ (4.4)$$

The extraction reaction can be studied using the slope analysis technique where the partial derivatives (4.5) and (4.6) will yield values for n and m respectively.

$$\left(\frac{\partial \log D}{\partial \log \{Cl\}} \right)_{\{OX\}} = n \qquad \ldots. (4.5)$$

$$\left(\frac{\partial \log D}{\partial \log \{OX\}} \right)_{\{Cl\}} = m \qquad \ldots. (4.6)$$

Meaningful results will be obtained as long as the constant conditions imposed by the derivatives are adhered to. For example, the chloride dependence can only be studied if the oxime concentration is kept constant. In general a ten-fold excess of extractant over metal is maintained so that the amount of reagent consumed will be small compared to the overall concentration. Another factor that is implicit in these equations is that the extractant is not soluble in the aqueous phase to any great extent. The solubility of octanal oxime in water under the conditions used for extraction studies was measured and found to be negligible (Appendix III).

4.1.1 The Effect of Chloride Concentration

Metal distribution experiments to determine the effect of chloride ion concentration on the extraction, involved varying the amount of NaCl present in the aqueous phase while keeping all other parameters constant. Experimental details are given in section (2.3.1). Chloride activities instead of concentrations were used throughout the work. Activity coefficients were obtained from the literature[38, 61]. Typical extraction curves are shown in Figures 4.1 and it can be seen that extraction increases with increasing chloride concentrations.

Figure 4.1 - Extraction of Cu(II) from Chloride solutions with Octanal Oxime. Aqueous phases : $[Cu^{2+}]_i$ = 0,008M, $[HNO_3]$ = 1,6 x 10^{-3}M, [NaCl] = 0,01 - 5,0M. Organic phases : (0,05M)a, (0,1M)b, (0,2M)c, (0,4M)d, (0,8M)e

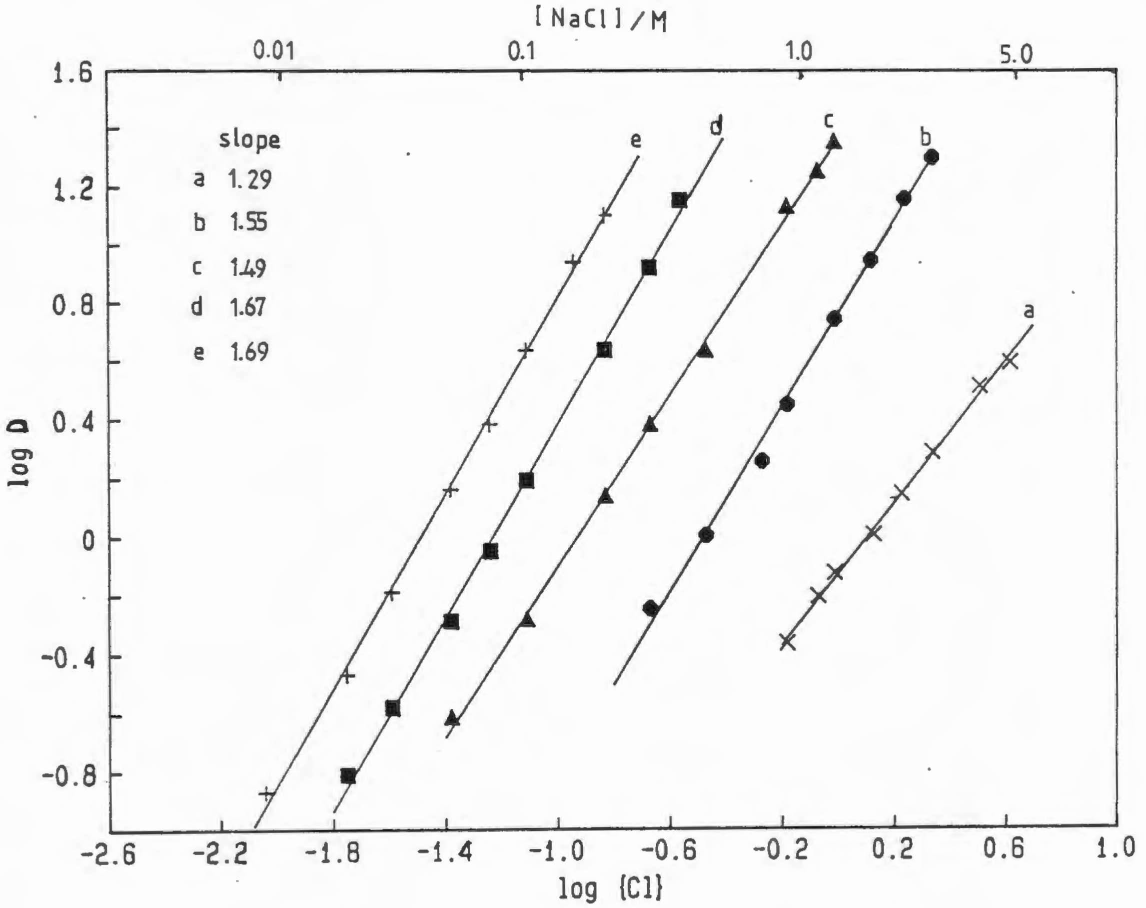

According to equation (4.5), the slope of the plot of logD versus log{Cl} will be equal to the number of chloride molecules present in the extracted complex.

A slope of two is expected for the formation of an electrically neutral complex. Straight line plots were obtained for various octanal oxime concentrations (0,05-0,8M) with slopes ranging from 1,69 to 1,29 (Figure 4.1). At the lower oxime concentration (0,05M), the constant [oxime] condition is not met since the latter is only six times in excess of the initial $[Cu]_{aq}$, and it is in this instance that the observed slope differs most from the expected value. At higher oxime concentrations slopes closer to the ideal value, are observed. The discrepancy is due to the formation of aqueous $(CuCl_n)^{2-n}$ charged complexes which are not extractable, but are present in the aqueous phase. Taking this factor into account, the distribution coefficient expression becomes :

$$D = \frac{[MCl_n\ OX_m]}{[M^{2+} + MCl^{+} + MCl_2 + MCl_3^{-}\ldots]}$$

$$= \frac{[MCl_n\ OX_m]}{[M^{2+}]\ (1 + \beta n\ \{Cl\}^n)} \qquad \ldots.\ (4.7)$$

$$\text{where } \beta n = \frac{[MCl_n{}^{2-n}]}{[M^{2+}]\ \{Cl\}^n}$$

Equation 4.2 is then equal

$$\log D = \log K_{EXT} + n \log \{Cl\} + m \log \{OX\} - \log (1 + \beta n\ \{Cl\}^n) \qquad \ldots.\ (4.8)$$

The slope of log D vs log $\{Cl\}$ plot is therefore decreased due to the last term in expression (4.8). Extraction data can be used to calculate values for (β_n) formation constants (Appendix I).

4.1.2 The Effect of Extractant Concentration

As indicated by equation (4.6), the number of extractant molecules coordinating to the metal complex in the organic phase can be determined by construction of log-log plots of the distributiuon coefficient versus the oxime activity. Aqueous solutions of constant chloride, acid and copper concentration were contacted with various concentrations of octanal oxime in toluene (Section 2.3.1).

Due to the association of octanal oxime in the organic phase the effective oxime concentration is much lower than the analytical concentration. To overcome this problem, monomer concentrations were calculated using data obtained from osmometric measurements (Chapter 1). Results are shown in Figure 4.2 (A,B). Corrections for association will be more pronounced at the higher oxime concentrations. Slopes of 3,0 and 3,5 were obtained for oxime concentration ranges of (0,01 to 0,025M) and (0,05 to 0,8M) respectively. This result suggests that $CuCl_2(OCOX)_3$ is the most stable complex and as the concentration of oxime is increased $CuCl_2(OCOX)_4$ is formed. A slope value of 3,5 would therefore represent an average value.

The formation of two different complexes is also suggested by the following : the octanal oxime extract, resulting from the extraction of copper from potassium bromide solutions is green at low extractant concentrations (0,05 to 0,2M) and blue above 1,0M. In contrast, extracts of copper from chloride media under similar conditions yield only bluish organic phases. This change in colour seems indicative of a change in the immediate surrounding of the copper ion. One such example is the effect of non-aqueous solvents on the colour of square-planar $Cu(tmen)(acac)ClO_4$ [39] complex, [tmen = tetramethylethylenediamine and acac = acetylacetonate). For instance the colour changes from redish-violet to turquoise to green as the solvent molecules (nitrobenzene, pyridine and piperidine) occupying the z-axial positions become progressively more basic, and the complex changes from a square planar configuration to an octahedral one.

Configurational changes of the Cu(II), d^9 ion, are difficult to detect since they give rise to a broad band envelope in the ultraviolet-visible absorption region. Both the chloride and bromide complexes exhibit similar changes in the UV-VIS spectra. In samples where the extractant is in large excess (0,8 - 1,0 M OCOX, 0,008M Cu) one peak is seen at approximately 625nm. This corresponds to the blue Cu/Br/OCOX complex. As the extractant to copper ratio is reduced (0,05M OCOX, 0,016 M Cu), the bromide complex turns green and the peak broadens and shifts to a maximum of 710 nm. This shift in wavelength also occurs in the chloride complex, even although no colour change is observed.

Figure 4.2 - log D Dependence on Octanal Oxime concentration. (-----) Analytical Oxime concentrations. (——) Monomer Oxime concentration. (A) Extraction from Chloride solutions. Aqueous phases: ($[Cu^{2+}]_i$ = 4,45 x 10^{-4} M, $[HNO_3]$ = 10^{-3} M, [NaCl] = 4,0M) (B) Extraction from Chloride solutions. Aqueous phase: ($[Cu^{2+}]_i$ = 8 mM, $[HNO_3]$ = 1,6 x 10^{-3}, [NaCl] = 0,4M) (C) Extraction from Bromide solutions. Aqueous phase: ($[Cu^{2+}]_i$ = 8 mM, $[HNO_3]$ = 1,6 x 10^{-3}M, [KBr] = 0,6M)

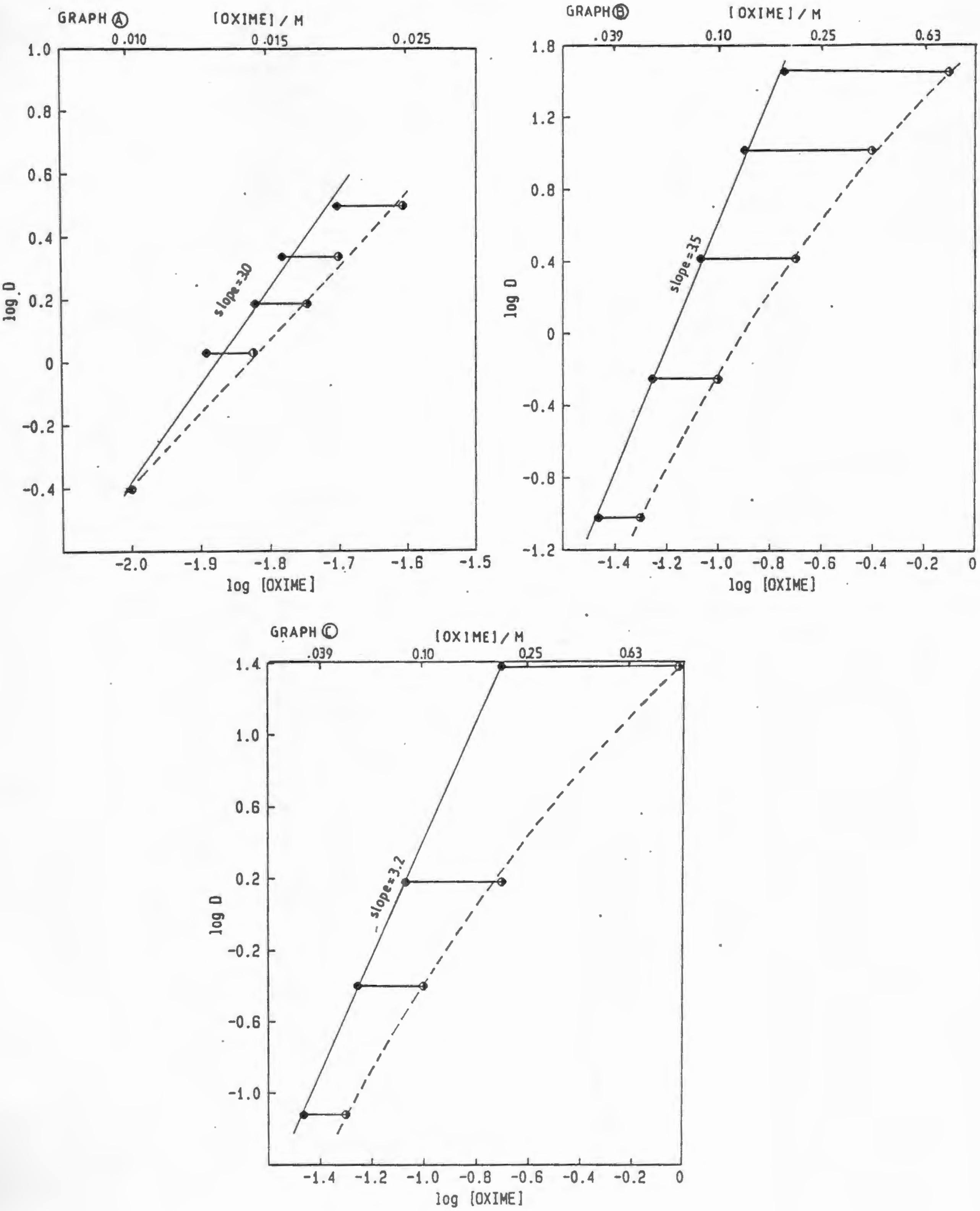

The complexes must be at least five coordinate because a minimum of three oxime molecules are present in both chloride and bromide extracts. (Figure 4.2.C). It is also unlikely that a square based pyramidal configuration is adopted since these are expected to give rise to absorptions at lower wavelengths[40]. It is thus suggested that the following equilibrium takes place between two octahedral or tetragonally distorted octahedral complexes.

$$\underset{\text{I}}{\overline{CuX_2(OCOX)_3(H_2O)}} \rightleftarrows \underset{\text{II}}{\overline{CuX_2(OCOX)_4}} + H_2O$$

$$X = Cl, Br \qquad \ldots (4.7)$$

With increasing oxime concentration the water is substituted for the fourth oxime. From the relative position of the two ligands in the spectrochemical series[41], the crystal field splitting caused by a nitrogen donor ligand is greater than that caused by water (Figure 4.3) and therefore the absorption spectrum will shift to lower wavelengths as equilibrium (4.7) shifts to the right. The blue colour in the bromide system is then probably due to the predominance of species II, while species I will be the main component of green solutions.

4.1.3 The Effect of Copper Concentrations

The effect of copper concentration on extraction was studied to ascertain that no polymerization of the extracted copper complex took place. Extraction curves in the form of log D versus log $\{Cl\}$ plots at different initial aqueous copper concentrations and constant oxime concentrations are shown in Figure 4.4 (A). They indicate that extraction decreases with increasing copper concentration. This dependence was found to be an artificial effect caused by the consumption of extractant to an extent that the oxime concentration was no longer in excess and could no longer be considered to be constant.

$$\begin{aligned}[oxime] &= [oxime]_{initial} - [oxime]_{consumed}\\ &= [oxime]_{initial} - 3{,}5\ [Cu]_{organic}\end{aligned}$$

Figure 4.3 -

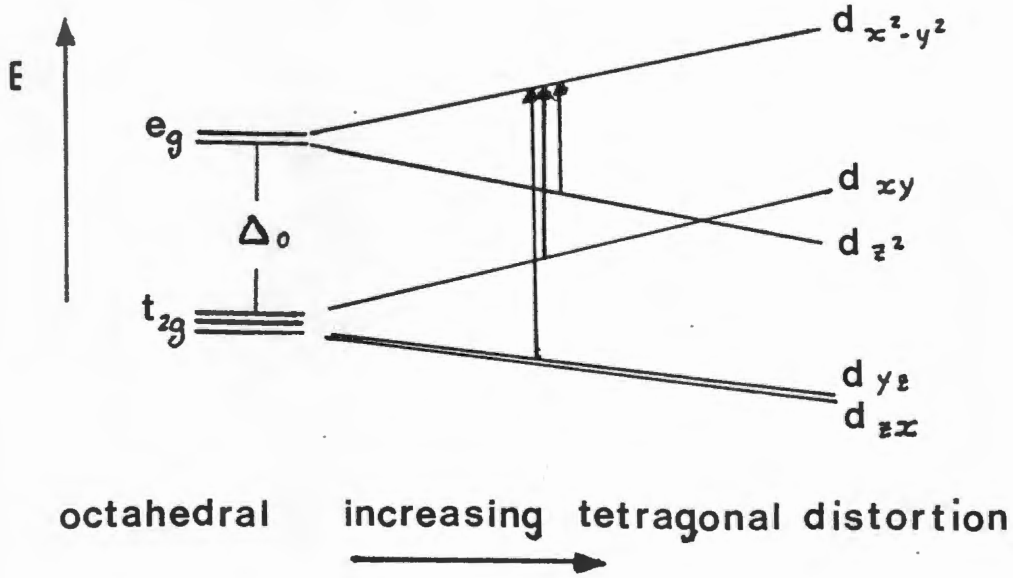

If the above correction is introduced then the curves are superimposed (Figure 4.4(B)), as predicted from extraction equations (4.2).

4.1.4 The Effect of pH

Aqueous solutions of pH ranging from 3 to 0, but having a constant chloride concentration were contacted with octanal oxime solutions. Details are shown in Figure (4.5). Extraction from chloride solutions

Figure 4.4 (A) - log D dependence on initial aqueous Copper concentration ([OCOX] = 0,1M, [NaCl] = 0,05 - 4,0M, [HCl] = 10^{-3}M (+,◒) [HNO_3] = 1,6 x 10^{-3}M (◆)

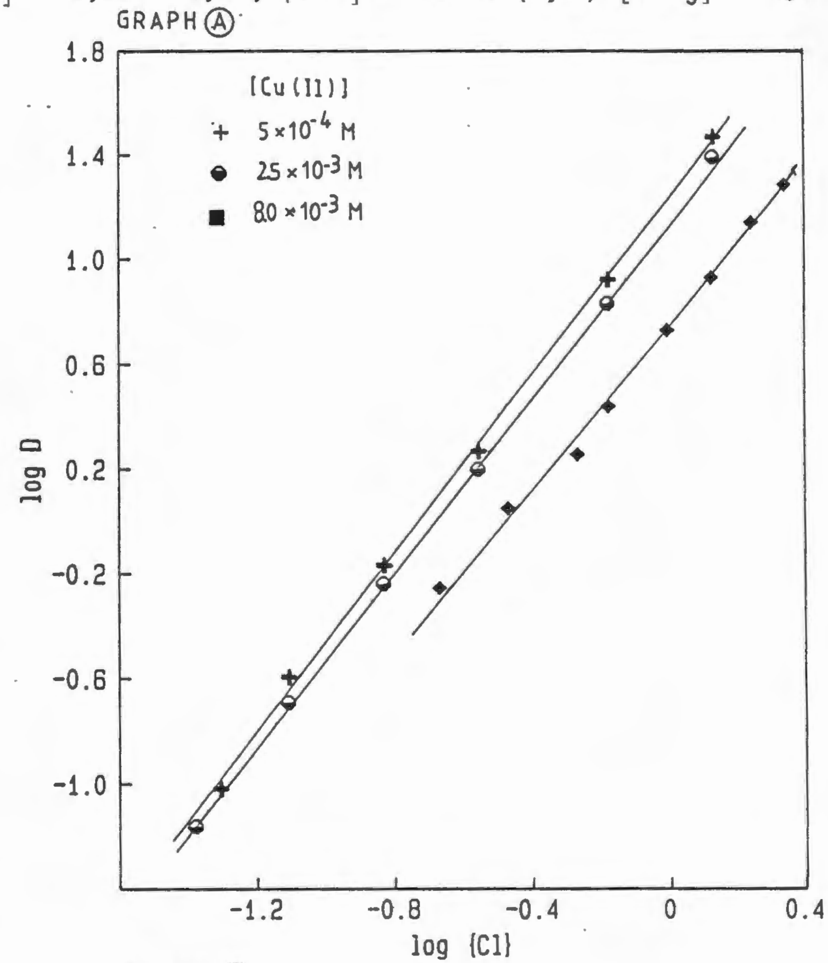

Figure 4.4 (B) - Log D terms corrected for Oxime consumed

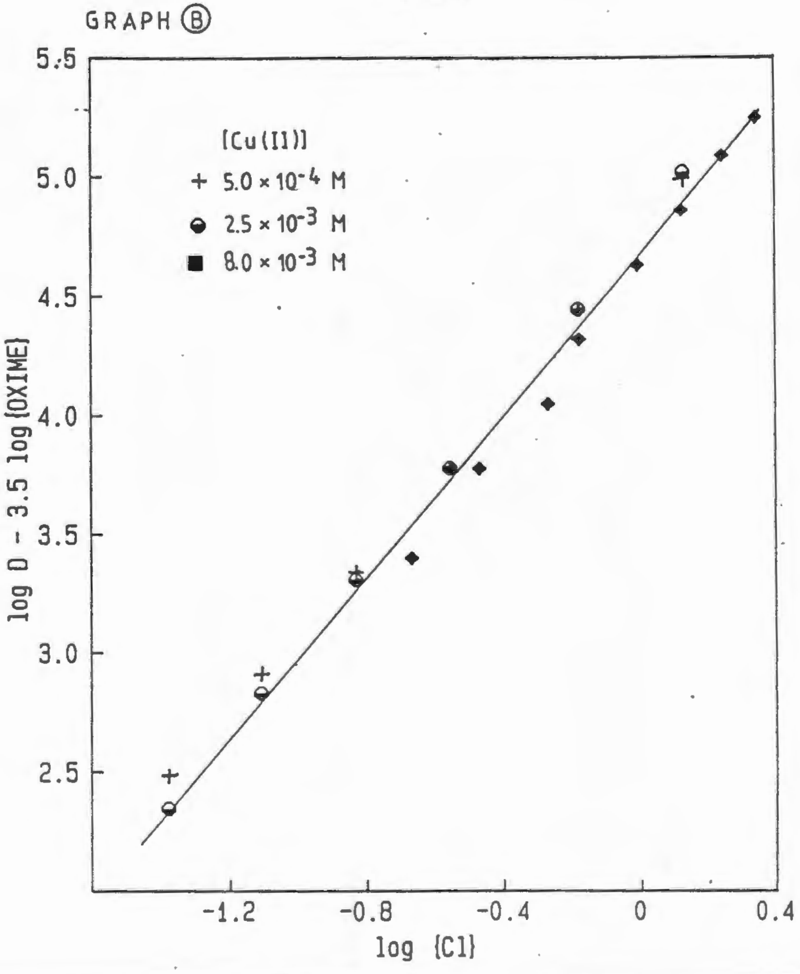

should ideally be independent of pH. This is true for the pH region used in previous extraction studies (~ 3 pH units). Below pH of approximately 2, extraction decreases considerably (Figure 4.5). Two main factors may contribute to this decrease. First, octanal oxime is a Lewis base by virtue of its nitrogen lone pair which is available for coordination to any Lewis acid and therefore a proton. Thus as the hydrogen ion concentration is increased, protons begin to compete with the copper ions and the effectiveness of the oxime as an extractant is decreased. Secondly, the protonated extractant will have a greater tendency to become partially soluble in the aqueous phase and this would also contribute to the decrease in the distribution ratio.

4.1.5 The Stoichiometry of the Reaction

In addition to the slope analysis results discussed above, further confirmation of the stoichiometry of the extracted complexes was obtained by various methods.

i) The metal to chloride ratio was determined by analysis of the organic extracts under different conditions. Results are summarized in Table 3 and it is clear that the extracted complex maintains a 2 to 1 chloride-to-metal ratio in all cases. Experimental details are given in Section (2.3.2).

Table 4.1 - Halogen-to-Copper Ratios in Various Extraction Systems

$[Cu^{2+}]_{aqi}$	[NaCl]	[KBr]	Solvent	Extractant	Halogen-to-Copper Ratio
0,004M	2,0M	-	Toluene	0,2M OCOX	2,19
0,008M	2,0M	-	Toluene	0,2M OCOX	2,16
0,004M	2,0M	-	n-heptane	0,2M OCOX	2,08
0,006M	2,0M	-	n-heptane	0,2M OCOX	2,09
0,004M		2,0M	Toluene	0,2M OCOX	2,14
0,008M		2,0M	Toluene	0,2M OCOX	2,09
0,008M	2,0M	-	Toluene	0,2M OCOX	2,05
0,008M	2,0M	-	n-heptane	0,2M 2EHO	2,15
0,008M	-	2,0M	Toluene	0,2M 2EHO	2,11

Figure 4.5 - Effect of pH on the extraction of Cu(II) from Chloride solutions with Octanal Oxime ($[Cu^{2+}]_i$ = 5 x 10^{-4}M, [Cl] = 1,0 M)

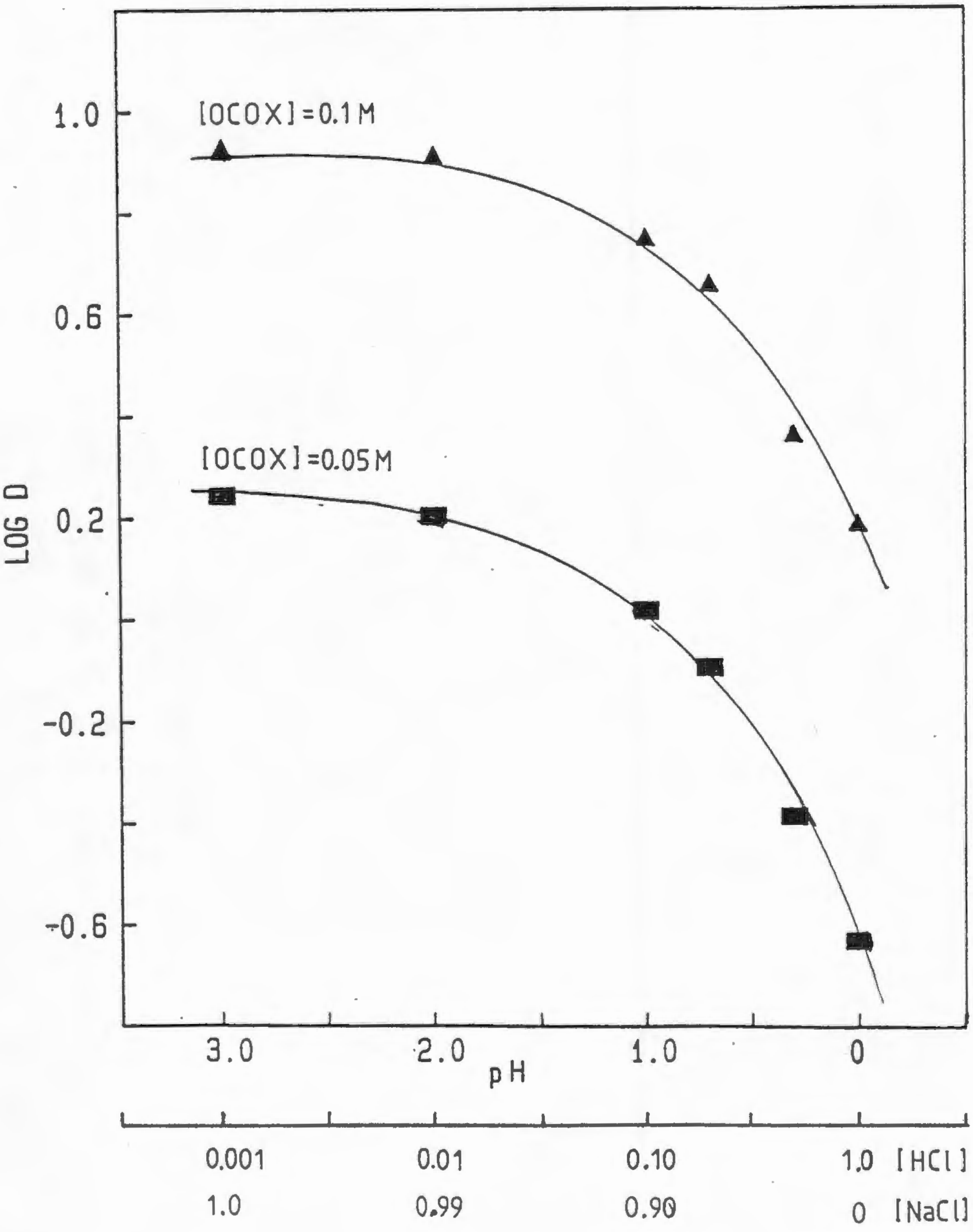

ii) In order to determine the oxime-to-metal ratio in the extracted complex, a metal loading curve was obtained by a method outlined in Section (2.3.3). Plots of the copper concentration in the organic phase versus the initial copper concentration in the aqueous phase for extraction from chloride and bromide media are shown in Figure 4.6 and 4.7 respectively.

The chloride curve (Figure 4.6), first flattens out at copper loadings of approximately 1,45 x 10^{-2}M in organic solutions of 0,05M octanal oxime, giving an oxime-to-copper ratio of 3,44. This could indicate formation of both $CuCl_2(OCOX)_3$ and $CuCl_2(OCOX)_4$ complexes, confirming deductions made in section 4.1.2. As the copper concentration in the aqueous phase is increased beyond 1,5M, higher loadings, representing formation of $CuCl_2(OCOX)_2$, are obtained. The experimental conditions under which $CuCl_2(OCOX)_2$ is observed, however, are so different from those used in previous experiments that it is unlikely that they model the extraction equilibrium. More specifically, extraction curves were obtained at a ligand-to-metal ratio of 6,2 to 100 (i.e. $[Cu^{2+}]_i$ = 0,008M, $[OCOX]$ = 0,05 to 0,8M), while at $[Cu^{2+}]_i$ = 1,5M this ratio is 0,03. So, one can only draw valid comparisons from the initial part of the curve.

Another disadvantage of this type of method is that if the ligands do not form strongly held complexes then it will be difficult to distinguish a definite plateau region. This is the case for the bromide loading curve (Figure 4.7).

iii) The water content of some $CuCl_2$/oxime extracts was determined by the Karl-Fisher method (Section 2.6). Allowances were made for both the amount of water taken up by the oxime and the amount of Karl-Fisher reagent used up by the copper[42]. This last correction is necessary because of the reduction of Cu(II) by the iodide ion as follows :

$$2\ Cu(II) + 2e^- \rightleftarrows Cu(I)$$

$$2\ I^- \rightleftarrows I_2 + 2e^-$$

Figure 4.6 - Loading of Copper from Chloride solutions into 0,05M Octanal Oxime in Toluene. Constant parameters : ([NaCl] = 4,0M, [HNO_3] = 2 x 10^{-3}M)

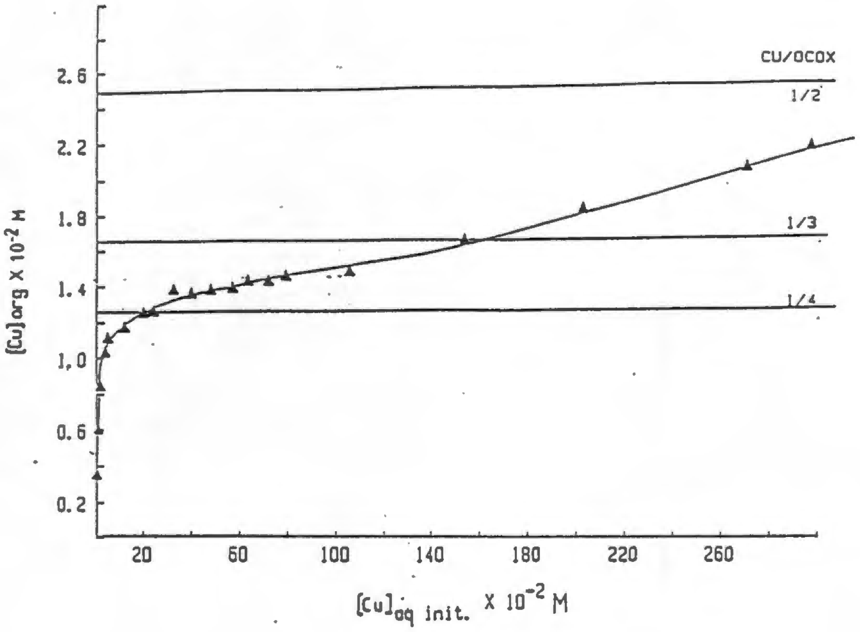

Figure 4.7 - Loading of Copper from Bromide solutions into 0,05M Octanal Oxime in Toluene. Constant parameters : ([KBr] = 3,6M, [HNO_3] = 2 x 10^{-3}M)

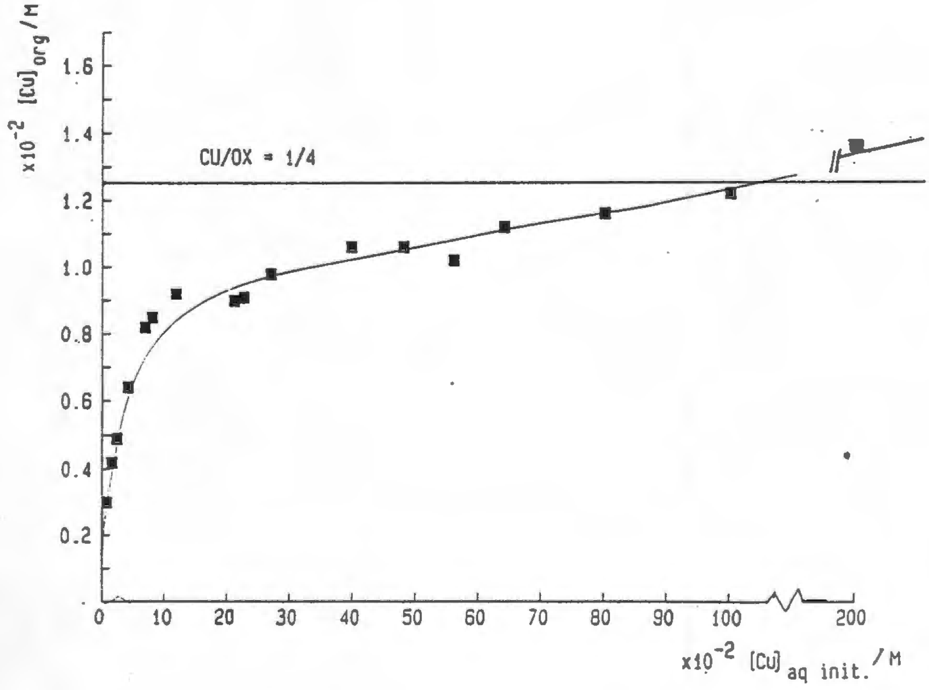

therefore $[H_2O]$ (true) = $[H_2O]$ (measured) - $[H_2O]$ (oxime) + 1/2 $[Cu(II)]$ (organic)

Results are shown in Table 4.2, and it is evident that very little water is taken up by the complex itself. An average value of one water molecule per metal ion was obtained, which is in agreement with the proposed formation of $CuCl_2(OCOX)_3(H_2O)$. The results were not sensitive to oxime concentration.

Table 4.2 - Water Content of Organic Phases

$[Cu]_{org}$/M	Solvent	$[H_2O]$ (Measured)	H_2O/Cu
-	Toluene	0,049	-
-	0,2M OCOX	0,090	-
-	0,4M OCOX	0,110	-
-	0,8M OCOX	0,170	-
0,0251	0,2M OCOX	0,101	0,92
0,0246	0,4M OCOX	0,112	0,58
0,0163	0,8M OCOX	0,175	0,80

4.2 Extraction of Copper with 2-Ethylhexanal Oxime and 2-Methyl Propanal Oxime

The extraction of copper from chloride solutions with 2-ethylhexanal oxime (2EHO) and methyl propanal oxime (MPO) was undertaken to see what effect increased steric crowding around the metal ion would have on the structure of the extracted complex.

Figure 4.8 - Structures of some Aliphatic Oximes

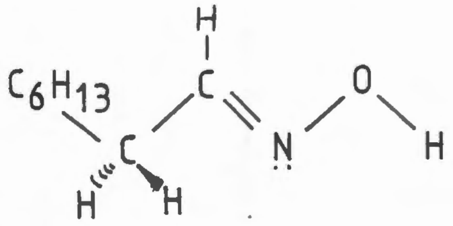

Octanal oxime

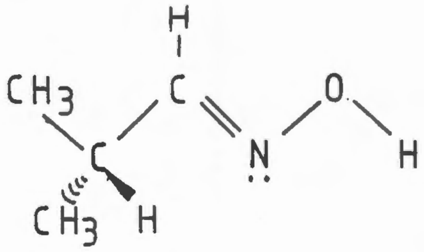

2-methyl propanal oxime

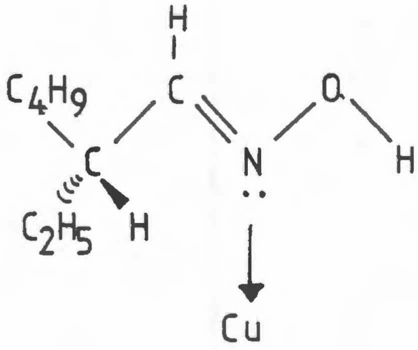

2-ethyl hexanal oxime

The above extractants were chosen so that steric hindrance about the N-Cu bond was increased, in the order OCOX < MPO < 2EHO, by increasing the size of the alkyl group bonded to the carbon, β to the coordinating nitrogen. It was found that extraction decreases with increased steric hindrance either due to the structure of oxime or by increasing the size of the halogen bonded to the copper ion. This is illustrated by the chloride activity values at 50% extraction (Table 4.3). The weaker extractants require higher chloride activites to reach a 50% extraction.

Table 4.3 - Chloride Activities Values at 50% Extraction of Copper into 0,2M Oxime Solutions

Oxime	Medium	{Cl}
OCOX	Cl	0,12
OCOX	Br	0,30
EHO	Cl	0,95
EHO	Br	1,41

The structure of the oxime did not have a marked effect on the nature of the extracted complex. As can be seen from the plots of log D versus $\log[2EHO]_{monomer}$ (Figure 4.9) and log D versus log {Cl} (Figure 4.10), approximate slopes of three and two respectively were obtained for both chloride and bromide complexes. Methyl propanal oxime extraction curves could not be obtained because the extracted complex(es) is(are) partially soluble in the aqueous phase. Furthermore $CuCl_2(MPO)_4$ easily precipitates out of solution, which proves that under certain conditions formation of a complex with four oxime molecules is possible. Elemental analysis results for the complex are shown in Table 4.4.

Figure 4.9 - log D dependence on 2-Ethylhexanal Oxime concentration for the extraction of Copper from Chloride (●) and Bromide (■) solutions. Constant parameters : $[Cu^{2+}]_i$ = 8 mM, $[HNO_3]$ = 1,6 x 10^{-3}M, $\{Br^-\}$ = 0 or $\{Cl^-\}$ = 0

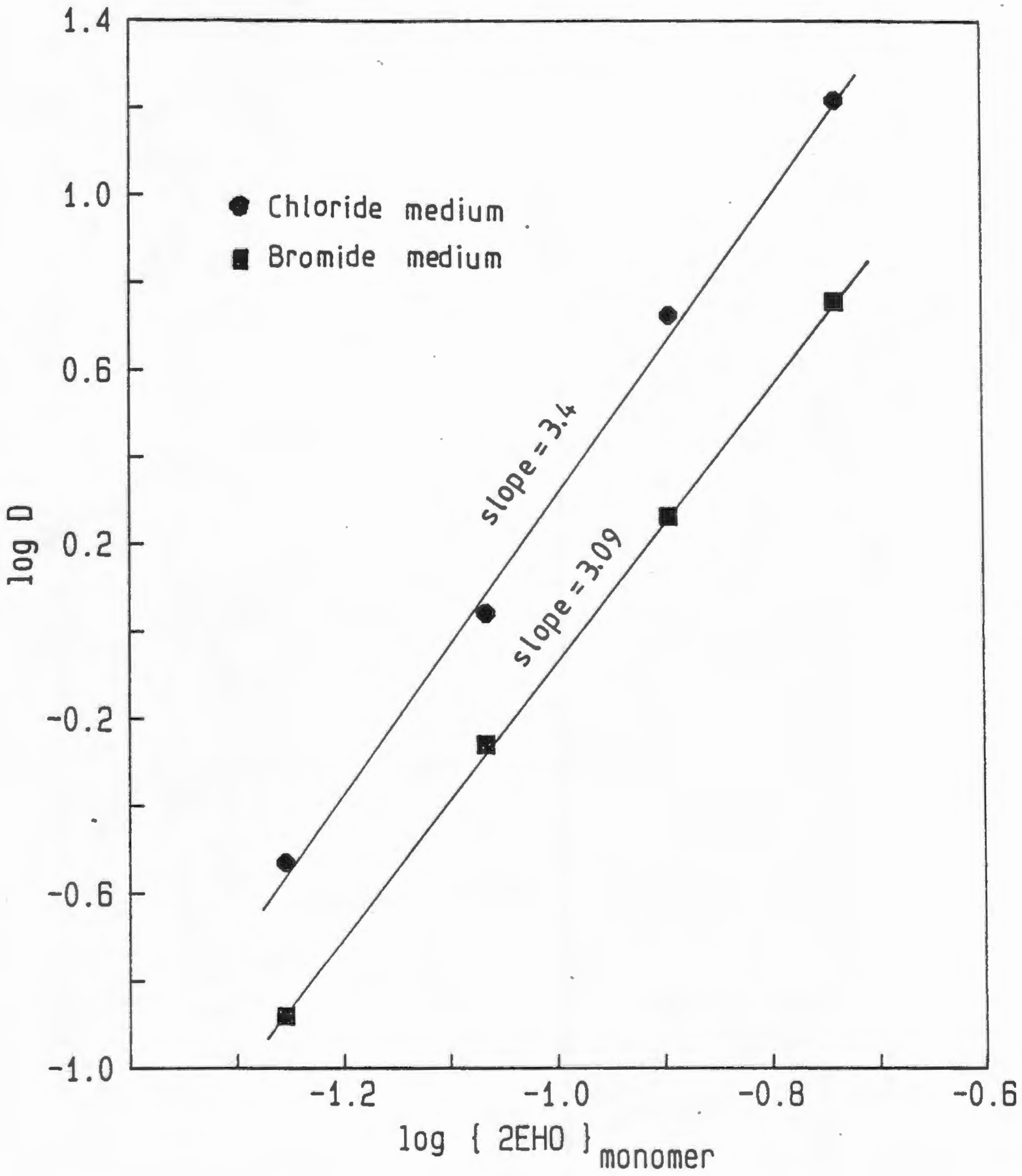

Figure 4.10 - log D dependence on Chloride concentration for the Extraction of Copper from Chloride (Graph A) and Bromide (Graph B) solutions. Constant parameters : $[Cu^{2+}]_i$ = 8 mM, $[HNO_3]$ = 1,6 x 10^{-3}M

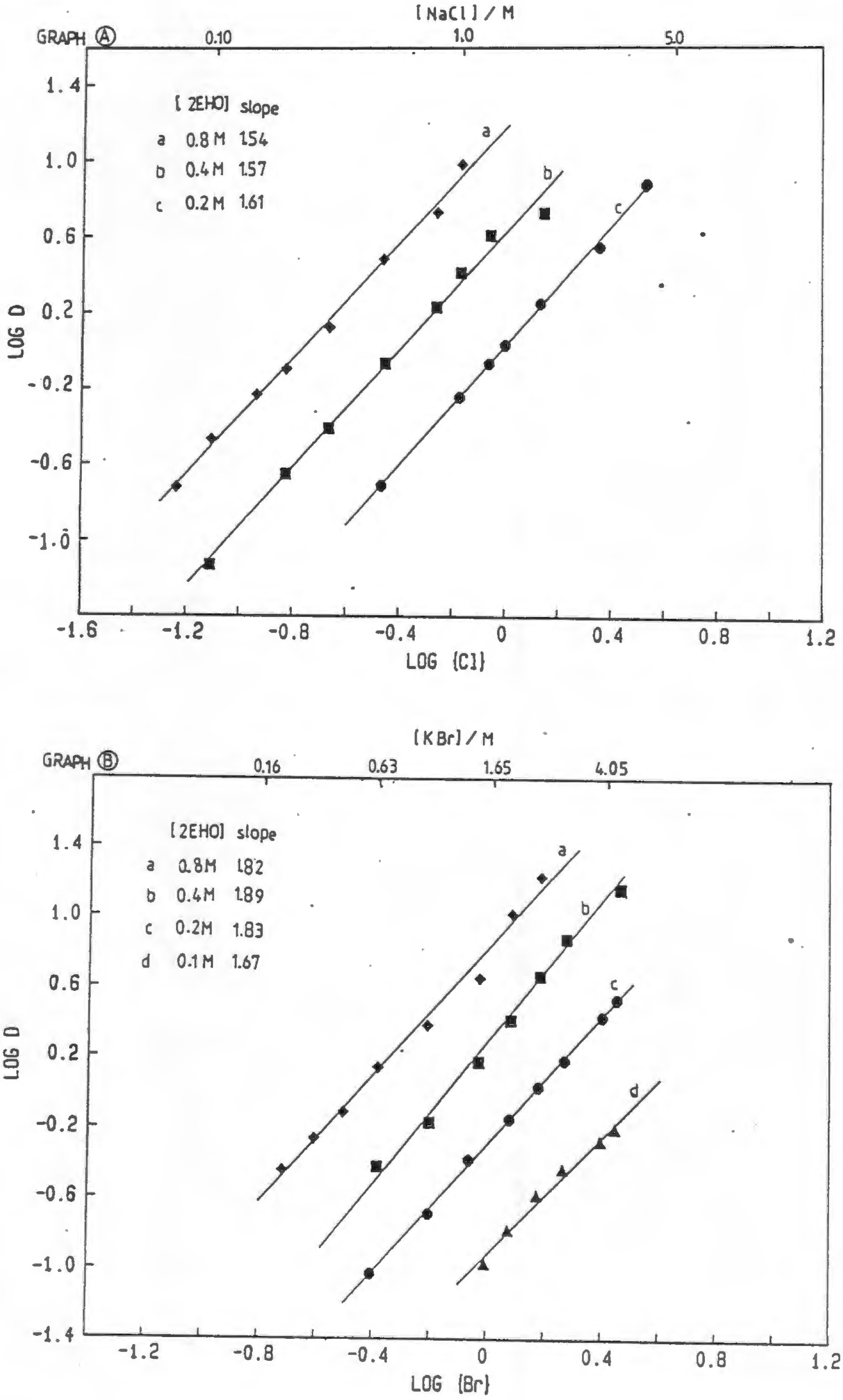

Table 4.4 - Elemental Analysis Results for $CuCl_2(MPO)_4$

Element	Calculated, %	Observed, %
Cu	13,1	13,0
Cl	14,6	14,0
N	11,6	11,6
C	39,8	39,2
H	7,5	7,3

To summarize, the overall extraction reaction is

$$Cu^{2+} + 2\ X^- + 3\ \overline{OX} \leftrightarrows \underset{I}{\overline{CuX_2(OX)_3(H_2O)}} + \overline{OX} \leftrightarrows \underset{II}{\overline{CuX_2(OX)_4}}$$

$X^- = Cl^-, Br^-$

OX = OCOX, MPO, 2EHO

The equilibrium is governed by Le Chatelier's principle and thus formation of complex II will be favoured by high extractant concentrations. At pH lower than two, protonation of octanal oxime, inhibiting the extraction of copper, becomes an important factor.

CHAPTER 5

CHAPTER 5

SOLVENT EXTRACTION OF COPPER FROM CHLORIDE SOLUTIONS WITH n-OCTYL-3-PYRIDINE CARBOXYLATE AND ACORGA CLX-20

ACORGA CLX-20, a pyridine dicarboxylic ester, has been patented for the selective extraction of copper from chloride solutions [24]. It functions as a nitrogen donor via a mechanism (5.1), which is similar to that of extraction of $CuCl_2$ with octanal oxime.

$$Cu^{2+} + 2Cl^{-} + \overline{2\ ACORGA} \rightleftharpoons \overline{CuCl_2(ACORGA)_2} \qquad \ldots.\ (5.1)$$

It was thus decided to compare the extraction reaction of these two reagents. ACORGA CLX-20 was not used for detailed studies because it is not availabe as a very pure reagent. An analogue, n-octyl-3-pyridine carboxylate (NOPC), was synthesized. The difference between the two reagents lies in the number of ester groups attached to the pyridine ring. A monosubstituted pyridine was opted for, due to the availability of starting material. Experimental details are given in Section (2.1).

Figure 5.1 - Structure of ACORGA CLX-20 and n-octyl-3-pyridine carboxylate

n-octyl-3-pyridine carboxylate

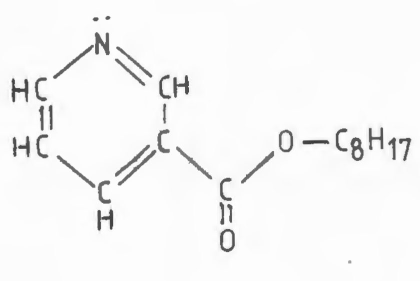

ACORGA CLX-20

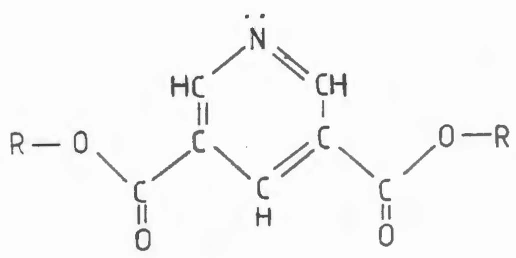

5.1 The Effect of Chloride Concentration

Two typical extraction curves for ACORGA CLX-20 and N-octyl-3-pyridine carboxylate are shown in Figure 5.2.

Figure 5.2 - Extraction of Copper with ACORGA CLX-20 and n-octyl-3-pyridine carboxylate. ([ACORGA CLX-20] = 0,82M; [NOPC] = 0,96M, $[Cu^{2+}]_i$ = 8 mM)

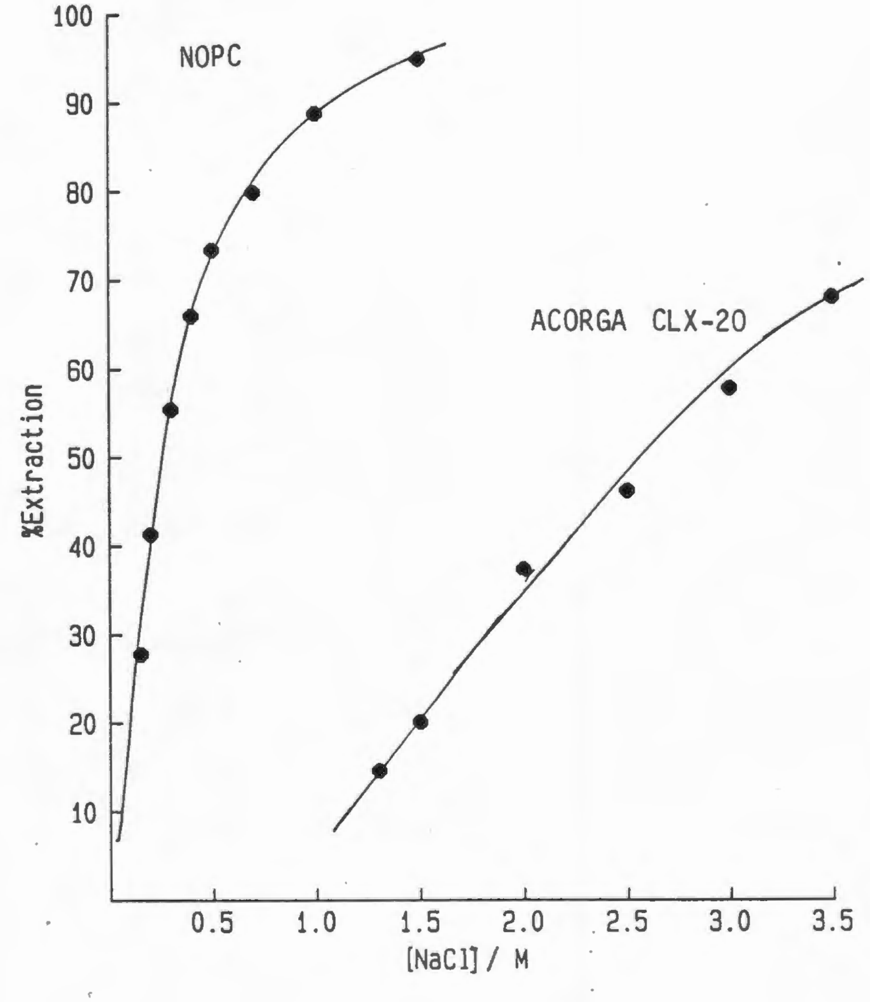

ACORGA CLX-20 is the weaker extractant of the two and therefore extracts from higher chloride concentrations. This is due to the two carboxylic ester groups which withdraw electron density from the co-ordinating nitrogen to a greater extent than in NOPC which possesses only one such group. The second ester group also introduces an extra alkyl chain and thus the overall solubility of both the reagent and the extracted complex in the organic phase is expected to improve.

5.2 The Stoichiometry of the Extraction Reaction

5.2.1 Slope Analysis

Metal distribution experiments were again used to determine the effect of both chloride and extractant concentration (Section 2.3.1). Following the slope analysis method outlined in Section (4.1), logarithmic plots of the distribution coefficient versus chloride activity (Figure 5.3 and 5.4), and extractant concentrations (Figure 5.5) were obtained. ACORGA CLX-20 was used as supplied by ICI, and its percentage purity was determined by a non-aqueous acid-base titration (Section 2.1).

The plots in Figures 5.3-5.5 all have slopes of approximately two. It must be noted that in this instance no correction for the extractant concentration was necessary as these reagents do not associate in toluene. No deviations from ideal behaviour could be detected in vapour pressure osmometry measurements. So it is clear that the extracted complex is of the form $CuCl_2(EXT)_2$, where EXT = NOPC, ACORGA CLX-20.

5.2.2 Analysis of Organic Extracts

Confirmation of the stoichiometry of the extracted n-octyl-3- pyridine complex was obtained from its metal loading curve (Section 2.3.3), shown in Figure 5.6.

Figure 5.3 - Extraction of Copper from Chloride solutions with n-octyl-3-pyridine Carboxylate. Constant parameters : $[Cu^{2+}]_i$ = 8mM, $[HNO_3]$ = 1,6 x 10^{-3} M

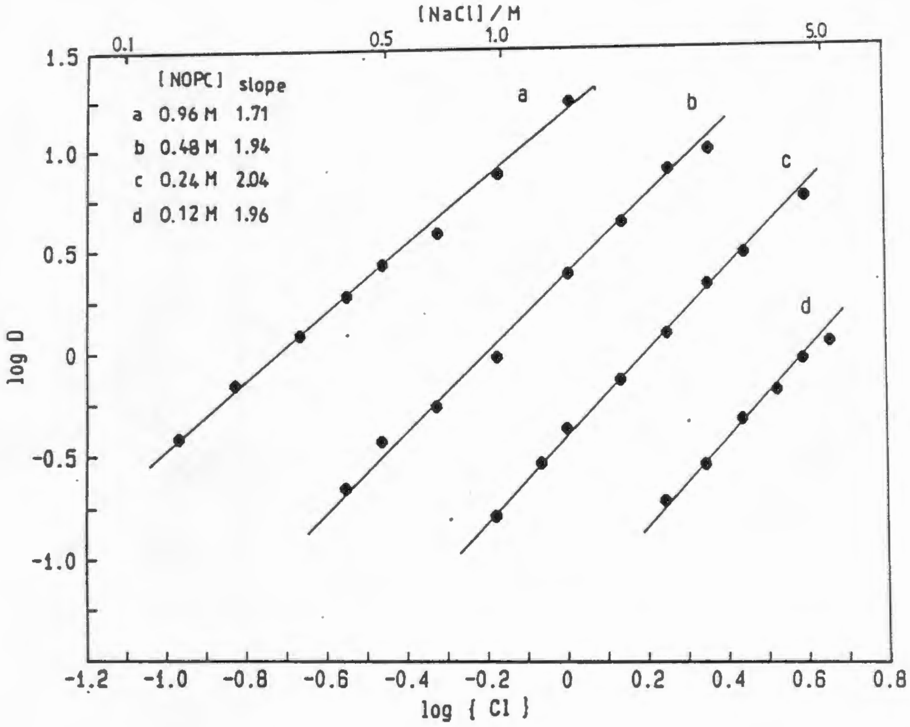

Figure 5.4 - Extraction of Copper from Chloride solutions with ACORGA CLX-20. Constant parameters : $[Cu^{2+}]_i$ = 8 mM, $[HNO_3]$ = 1,6 x 10^{-3} M

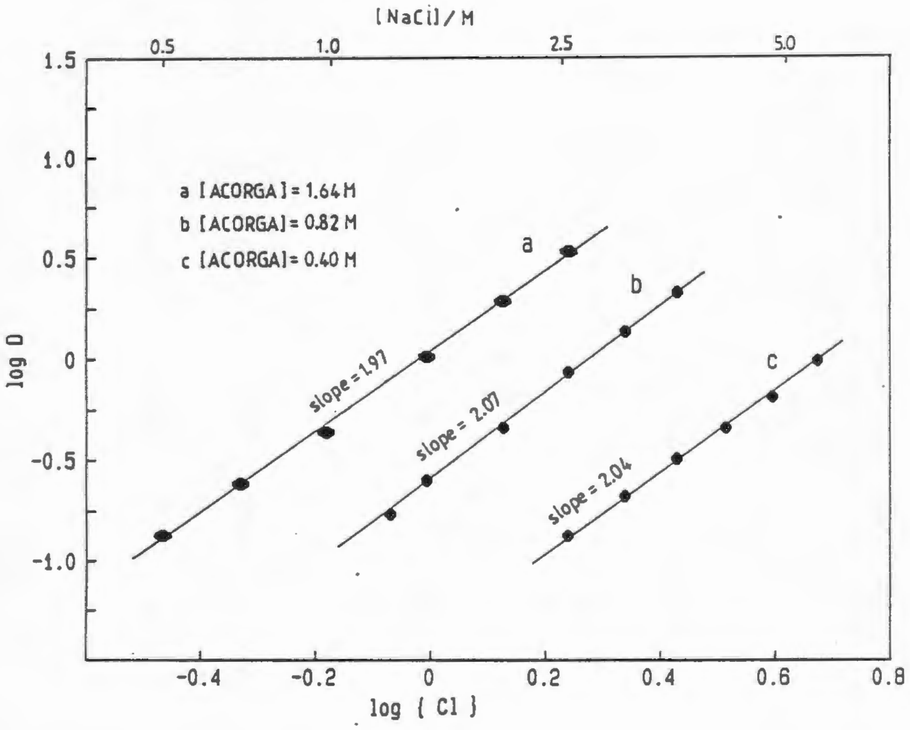

Figure 5.5 - log D Dependence on extractant concentration. Constant parameters : $[Cu^{2+}]_i$ = 8 mM, $[HNO_3]$ = 1,6 x 10^{-3} M, [NaCl] = 1,0 M

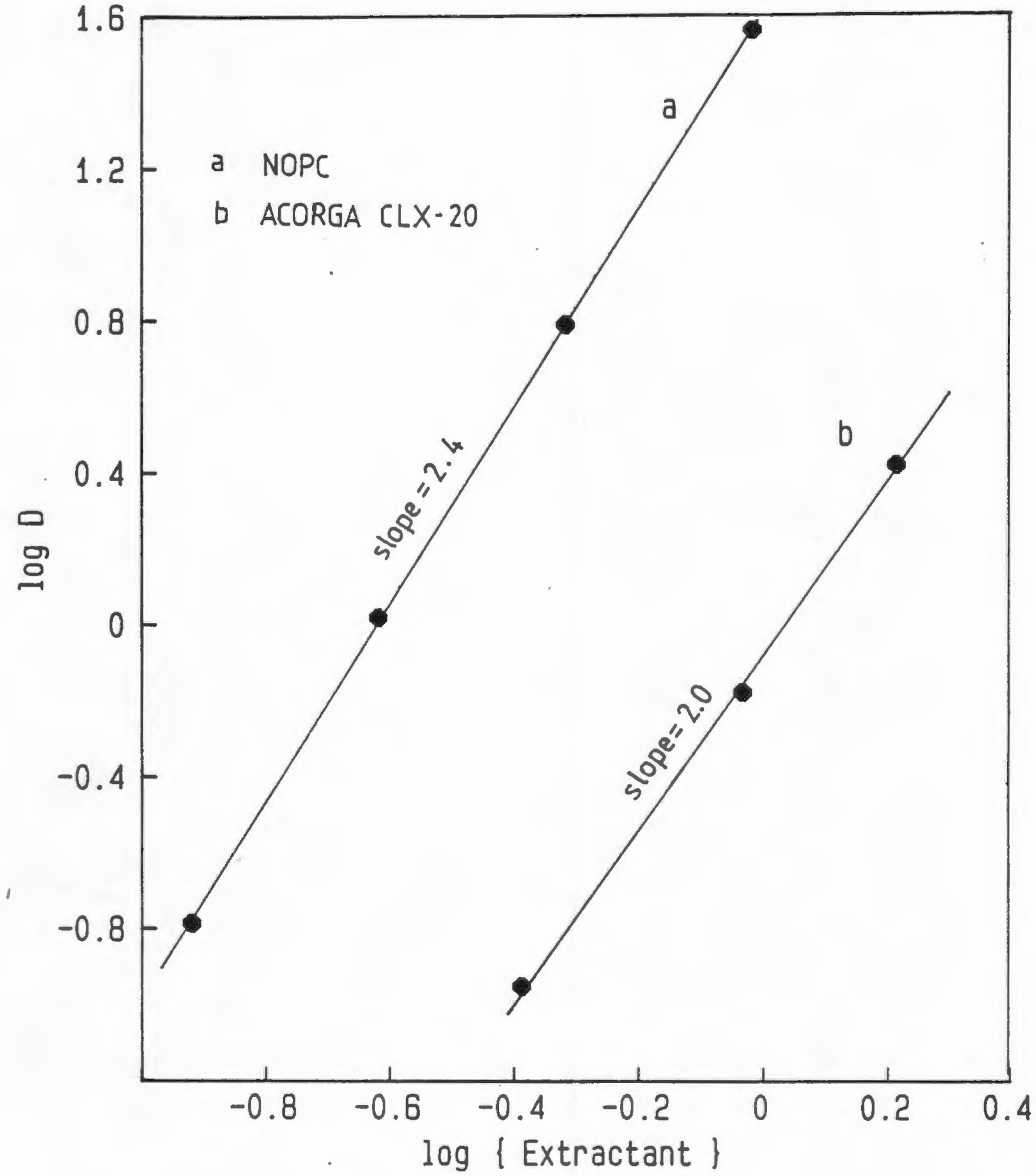

Figure 5.6 - Loading of Copper from Chloride solutions into 0,05M n-octyl-3-pyridine carboxylate. $[NaCl] = 4{,}0M$, $[HNO_3] = 2 \times 10^{-3}$ M

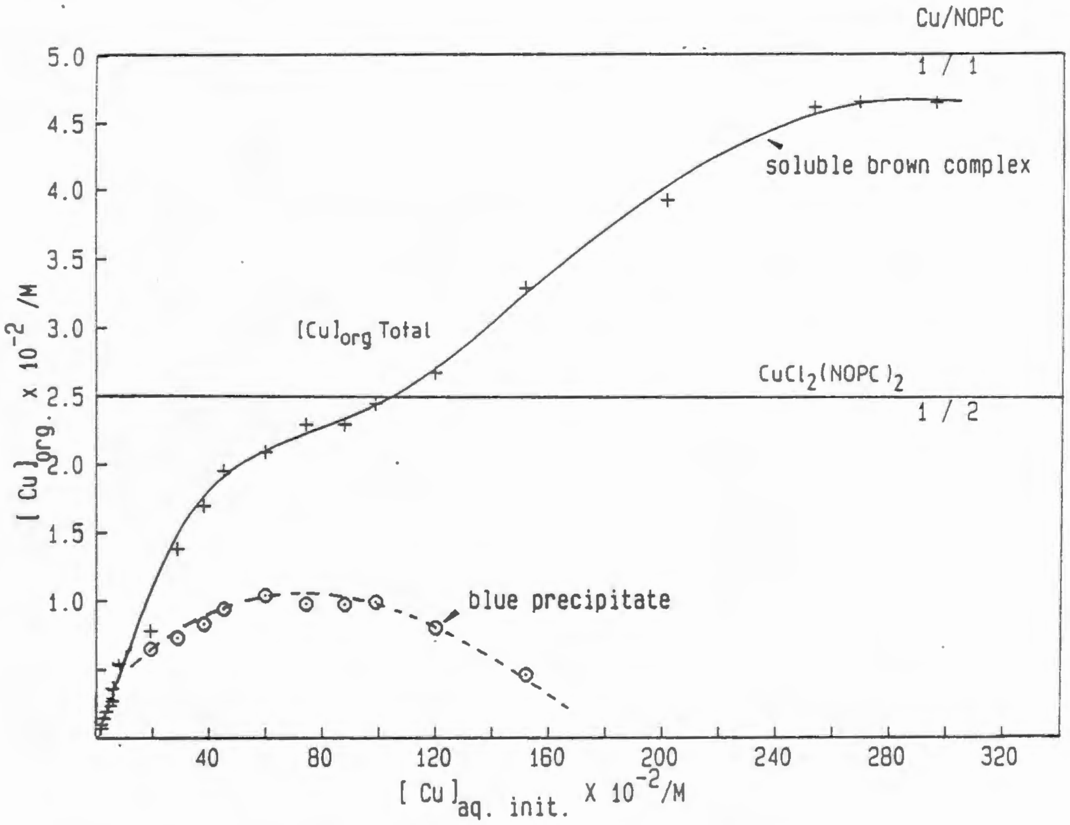

It was found that as the concentration of copper in the aqueous phase was progressively increased (Cu(aq) > 0,1M), the extracted complex precipitated in the organic phase as a light-blue complex. This precipitate was filtered and the elemental analysis results confirm its $CuCl_2(NOPC)_2$ stoichometry.

Table 5.1 - Elemental Analysis for $CuCl_2(NOPC)_2$

Element	Calculated, %	Observed, %
Cu	10,5	10,4
Cl	11,7	12,0
C	55,5	54,0
N	4,6	5,5
H	7,0	7,0

The interesting aspect, however, is that the curve (Figure 5.6) initially levels off at the expected copper-to-ligand ratio of one to two and as the aqueous phase is further loaded with copper, the blue precipitate redissolves (dashed curve), and the organic phase turns into a brown clear solution. The brown complex seems to have a copper-to-ligand ratio of one to one, as is indicated by the second plateau. A possible structure can be envisaged where the chlorines act as bridging ligands (Figure 5.7).

Figure 5.7 - Postulated Dimer structure

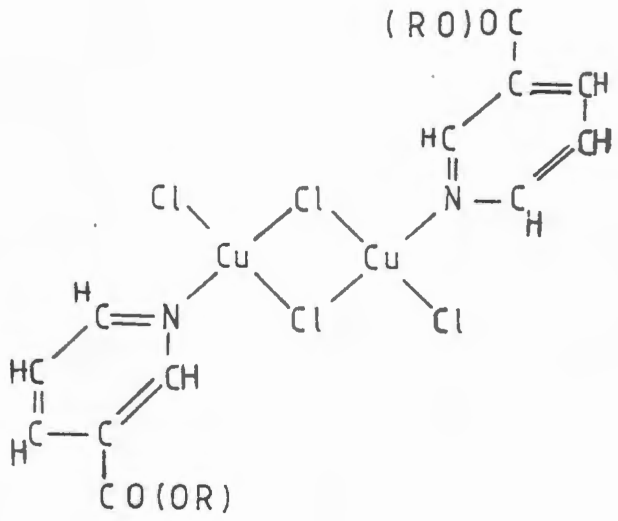

The phenomenon that with excess copper different complexes are formed was also observed by Prins et al [30], in their studies of the extraction of copper (II) with 4-t-butyl-1,2,6-cyclohexanetrione tri-oxime (H_3BHT) in pentanol. At low copper loadings a complex of the form $Cu(H_2BHT)_2 \cdot 2H_2O$ precipitated in the organic phase and when excess copper was used a new soluble chelate $[Cu_nL_n]$ was formed.

5.3 The Effect of pH

To determine the effect of pH on extraction, solutions of constant chloride concentrations (NaCl + HCl), containing different amounts of acid were contacted with solutions of n-octyl-3-pyridine carboxylate in toluene (Figure 5.8). Even although the chloride concentration remained constant, the chloride activity varied by approximately 0,09 log units, due to the increased acid content. (i.e. chloride activity is greater in HCl solution than in NaCl)[38, 61]. Figure 5.8 shows that extraction increases with decreasing pH and that this increase is greater than would be predicted by the change in chloride activity (dashed line). This discrepancy is at its worst for more dilute extractant solutions. For example, the 0,2M(NOPC) curve is steeper than the 0,4M. In fact, at 0,48 Molar extractant there is no noticeable effect of pH. This is illustrated by Figure 5.9 where the two curves for the extraction of copper from NaCl and HCl media are superimposed, even though the NaCl curve was obtained at constant pH 3 and the HCl curve at a pH range of 0,5-0.

A possible explanation is that there are two mechanisms by which extraction occurs : one is the solvating mechanism already mentioned and it is the predominant one. The other is the extraction of copper anionic species by the protonated extractant.

$$\text{i.e. } \mathrm{CuCl_2} + \overline{\mathrm{2L}} \overset{K_1}{\rightleftarrows} \overline{\mathrm{CuCl_2L_2}} \qquad \text{.... (1)}$$

$$\mathrm{CuCl_3^-} + \overline{\mathrm{LH^+}} \overset{K_2}{\rightleftharpoons} \overline{\mathrm{(CuCl_3)(LH)}} \qquad \text{.... (2)}$$

$$\overline{\mathrm{L}} + \mathrm{H^+} \overset{K_b}{\rightleftarrows} \overline{\mathrm{LH^+}}$$

In deciding whether mechanism (2) is favoured by high extractant concentrations :

Figure 5.8 - Effect of pH on extraction of Copper from Chloride solutions with n-octyl-3-pyridine carboxylate. Constant parameters : $[Cl]_{total}$ = 1,0M, $[Cu^{2+}]_i = 5 \times 10^{-4}$M

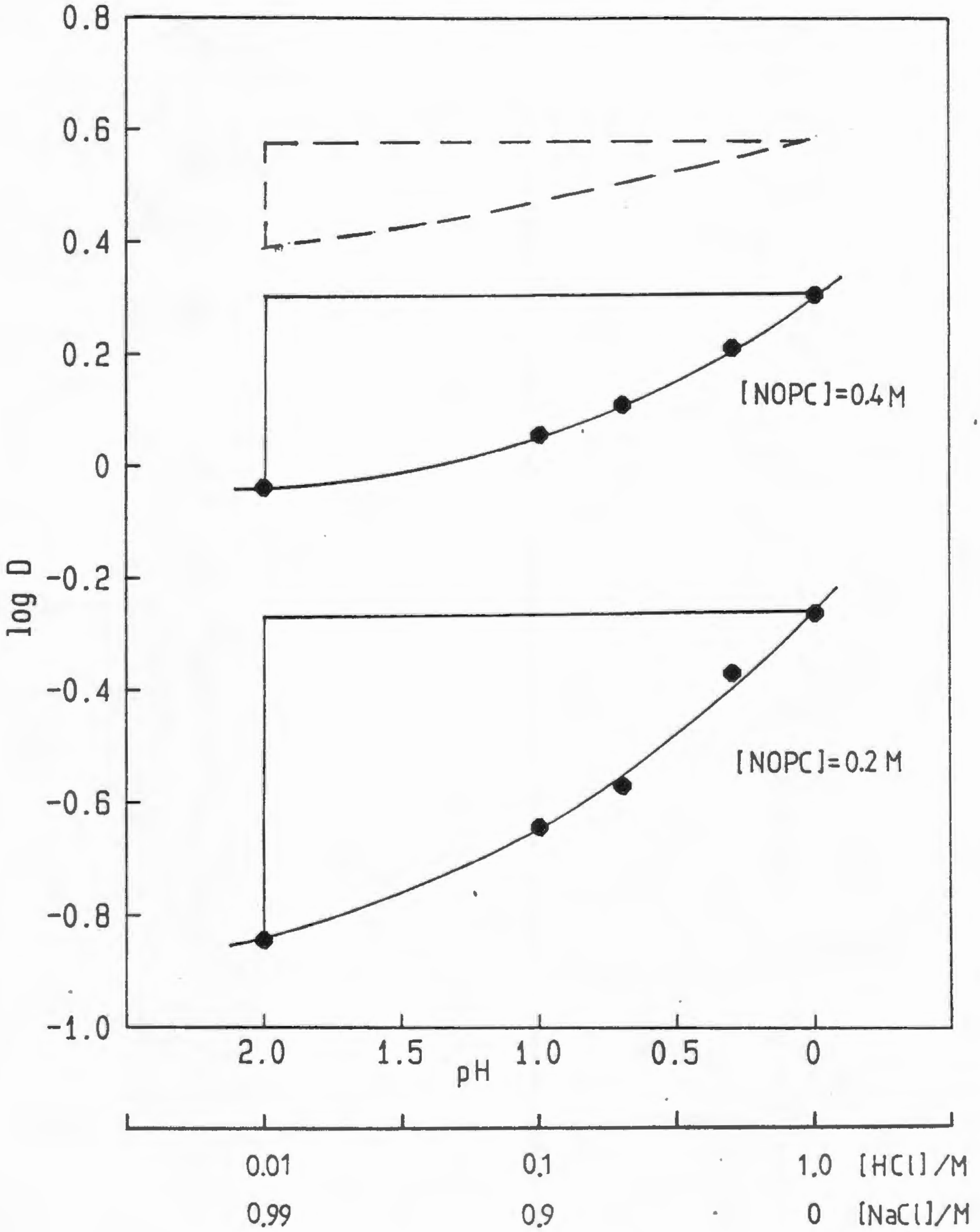

Figure 5.9 - Extraction of Cu(II) from NaCl and HCl solutions with n-octyl-3-pyridine carboxylate. Constant parameter : [NOPC] = 0,48M ● ([HCl] = 0,3-1,4 M, $[Cu^{2+}]_i$ = 5 x 10^{-4} M, $[HNO_3]$ = 1 x 10^{-3}M, pH variable) ■ ([NaCl] = 0,4-3,0M, $[Cu^{2+}]_i$ = 8 x 10^{-3}M, $[HNO_3]$ = 1,6 x 10^{-3}N, pH ≃ 3)

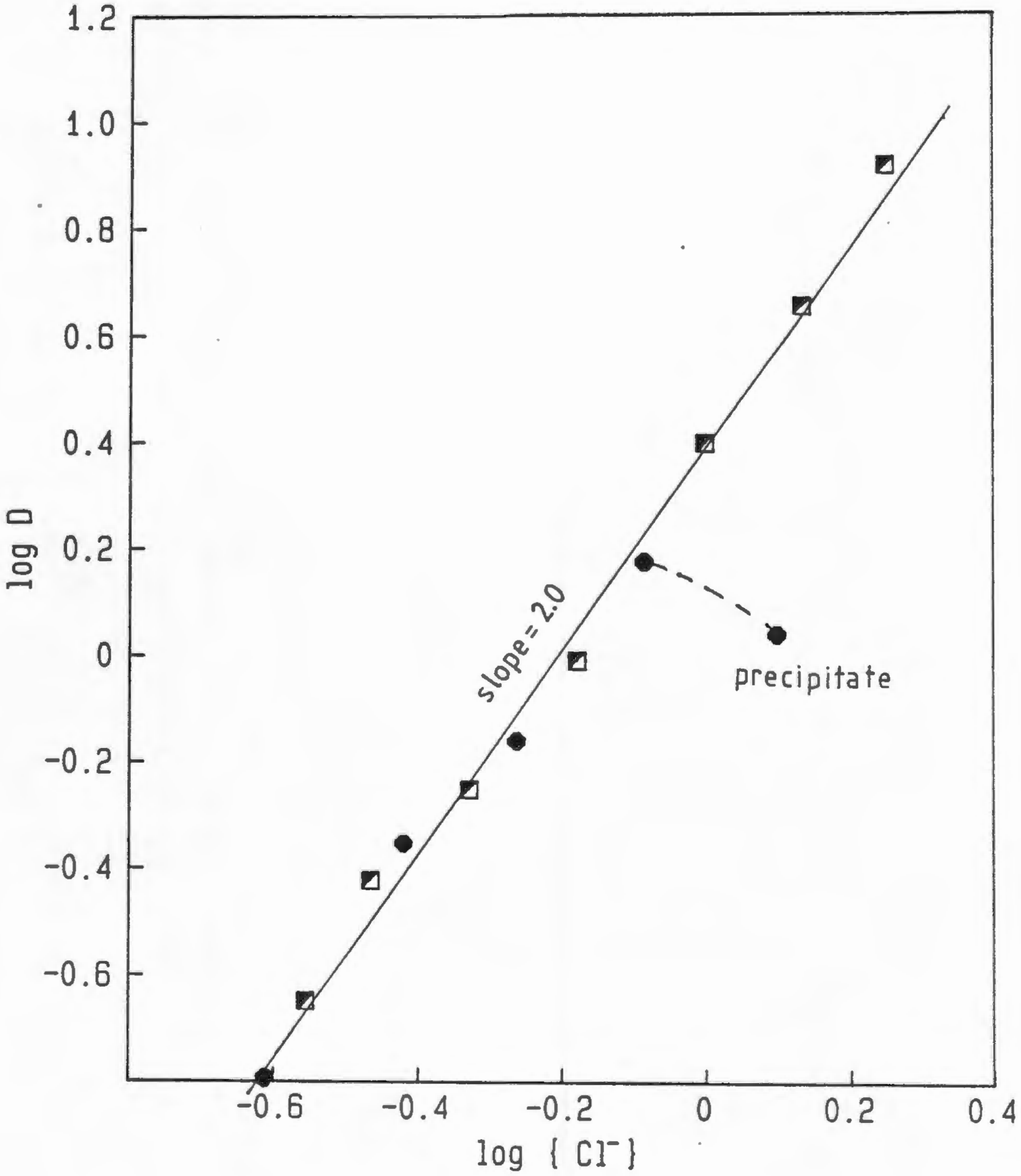

$$[CuCl_2L_2] \quad = \quad K_1\ [L]^2\ [CuCl_2]$$

$$[(CuCl_3)(LH)] = K_2\ [CuCl_3]\ K_b\ [L]\ [H^+]$$

$K_1\ [CuCl_2] > K_2\ [CuCl_3]$ since (1) is the main extraction mechanism. Because (1) has a second order dependence on $[L]$ and (2) a first order dependence, formation of $(CuCl_3)(LH)$ will be least noticeable at high extractant concentrations as was demonstrated in Figure (5.8-9).

To conclude : ACORGA CLX-20 and n-octyl-3-pyridine carboxylate extract copper from chloride solutions in the following manner :

$$Cu^{2+} + 2Cl^- + \overline{2\ L} \leftrightarrows \overline{CuCl_2L_2}(H_2O)_x$$

N-octyl-3-pyridine carboxylate becomes partially protonated above pH 2 and starts extracting anionic copper species. In addition $CuCl_2(NOPC)_2$ precipitates above 0,005M concentrations. The two carboxylic ester groups in the ACORGA CLX-20 reagent increase the solubility of the extracted complex in the organic phase and reduce its affinity for the proton.

CHAPTER 6

CHAPTER 6

THE EXTRACTION OF SOME BASE METALS FROM CHLORIDE SOLUTIONS WITH OCTANAL OXIME, N-OCTYL-3-PYRIDINE CARBOXYLATE AND ACORGA CLX-20

Solvent extraction applied to extractive metallurgy is used primarily to upgrade leach liquors for electrowinning and therefore the selectivity of the extractant is one of its most important properties. Selectivities are based on different mechanisms and rates of extraction, synergistic effects or changes in co-ordination and therefore an understanding of the extraction reaction is useful.

Ni(II) and Co(II) are extracted via a solvation mechanism similar to that of Cu(II). The treatment of data follows the pattern outlined in section 4.1 and will not be discussed in detail.

6.1 Extraction of Cobalt (II) with Octanal Oxime and N-octyl-3-pyridine Carboxylate

Octanal oxime extracts Cobalt (II) at lower chloride concentrations than n-octyl-3-pyridine carboxylate as shown in Figure 6.1. In the region of octanal oxime extraction the aqueous cobalt (II) solutions contain mainly the octahedral, $Co(H_2O)_6^{2+}$ and $CoCl(H_2O)_5^{+}$ species while at the higher chloride concentrations where n-octyl-3-pyridine carboxylate extracts, tetrahedral $CoCl_4^{2-}$ is the main component [44]. The species diagram is shown in Figure 6.2. The colour of the aqueous solution changes from light pink where the predominant species are octahedrally co-ordinated to bright blue for tetrahedral co-ordination.

The extracted cobalt/OCOX complex has a pink colour and its UV-VIS absorption spectrum (Figure 6.3) is consistent with octahedral symmetry. (Main peak at 520nm, $\varepsilon \simeq 9$)[45]. In contrast, the complex extracted with n-octyl-3-pyridine carboxylate is bright blue and has a characteristic tetrahedral symmetry [45] (λ = 620 nm, $\varepsilon \simeq 348$). Logarithmic dependencies of the distribution coefficient on the chloride activity for both extractants

Figure 6.1 - Extraction of Co(II) from Chloride solutions with n-octyl-3-pyridine carboxylate and octanal oxime. $[Co^{2+}]_i$ = 8mM, $[HNO_3]$ = 1,6 x 10^{-3}M, [Ext] = 0,2M

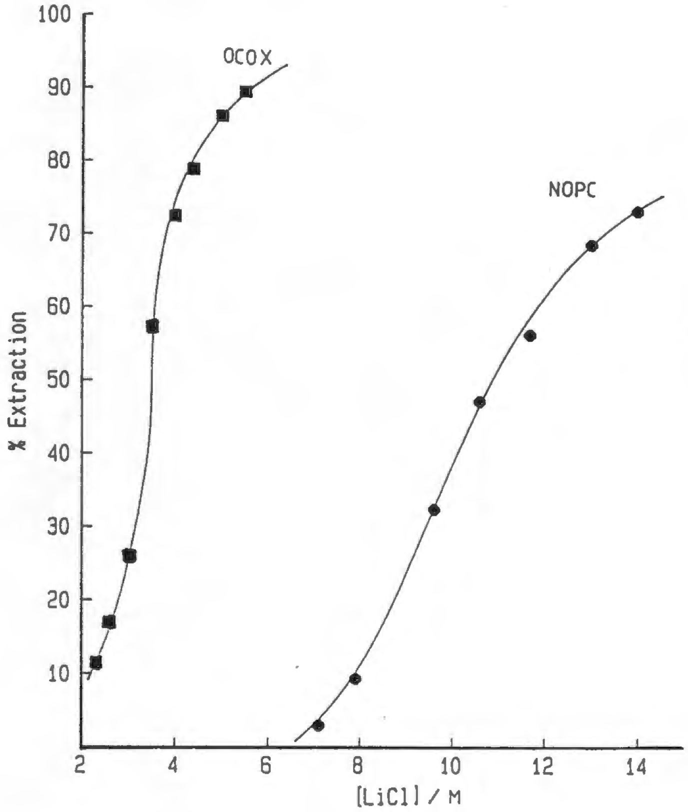

Figure 6.2 - Abundances of the indicated Cobalt complexes as a function of HCl molality. Reproduced from Reference 44

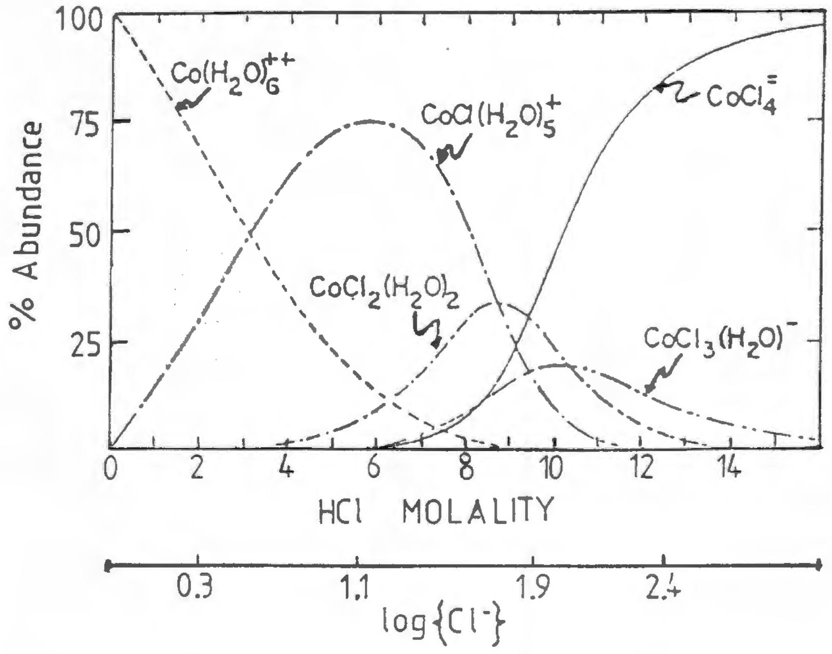

Figure 6.3 - UV-VIS Absorption spectra of Cobalt (II) extracts of Octanal Oxime and n-octyl-3-pyridine carboxylate. (OCOX : [Co] = 1,29 x 10^{-3}M, ℓ = 5cm, $\varepsilon \approx 9$ at λ = 520nm) (NOPC : [Co] = 2,8 x 10^{-3}M, ℓ = 1cm, $\varepsilon \approx 350$ at λ = 620 nm)

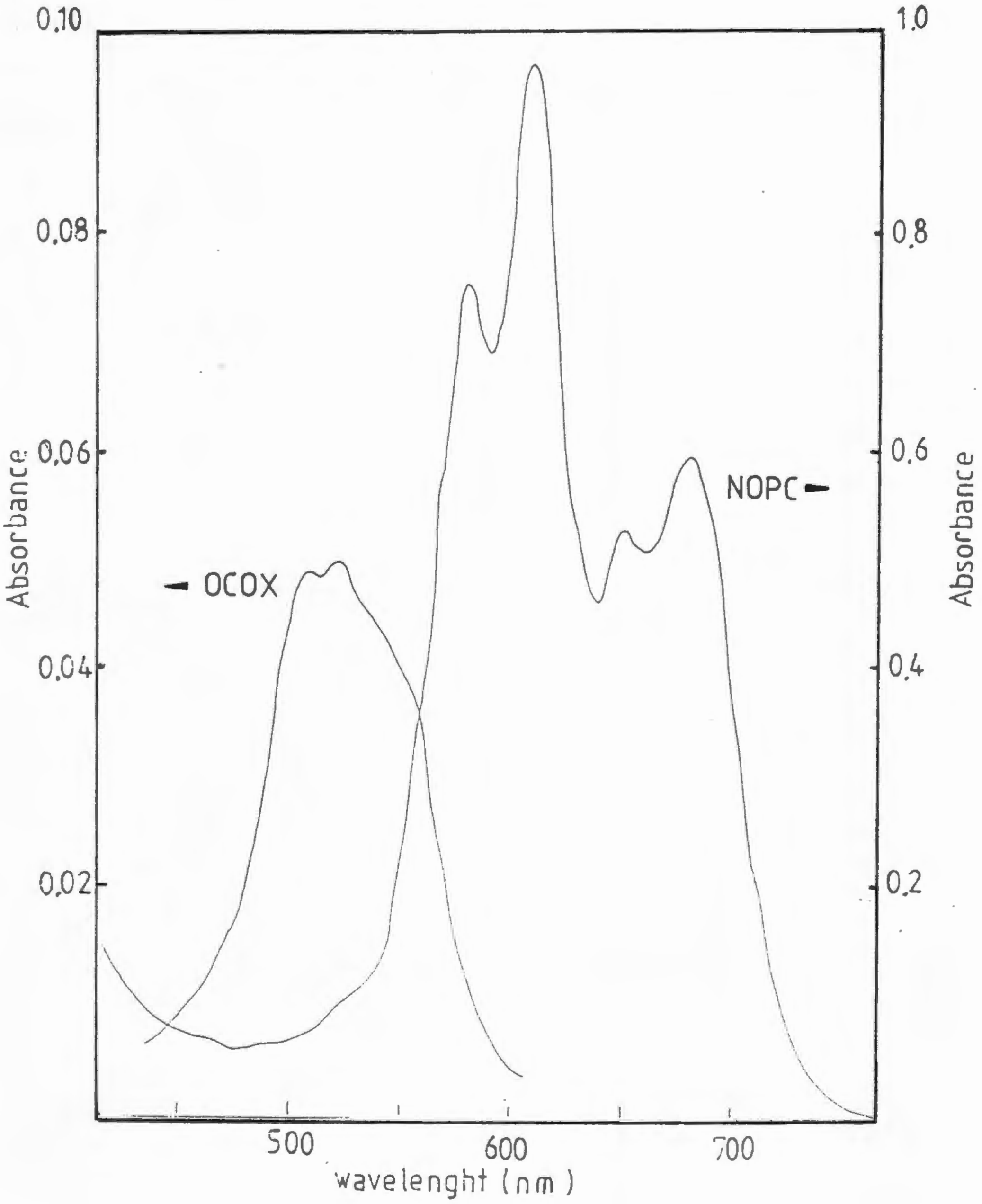

are shown in Figure 6.4. The log D versus log {Cl} curves for OCOX have slopes which are higher than two. In the NOPC case, extraction occurs at very high chloride concentration and therefore the slope analysis technique cannot be applied because of salting effects. Direct analyses of organic extracts (2.3.2) were thus undertaken. Results (Table 6.1) confirm that $CoCl_2$ is extracted in both cases.

Table 6.1 - Chloride to Cobalt Ratio in Organic Extracts
Aqueous Concentration (8mMCo^{2+}, 1,6mM HNO_3)

[NaCl] /	[LiCl]	[Ext]	$[Cl^-]$ / $[Co^{2+}]$
3,2M		0,4M OCOX	2,04
4,5M		0,4M OCOX	2,05
	9,7M	0,2 NOPC	1,94
	12,0M	0,2 NOPC	2,00
	14,0M	0,2 NOPC	2,08

The dependence of the distribution coefficient on the concentration of OCOX monomer is shown in Figure 6.5 and a slope of approximately four is obtained. N-octyl-3-pyridine carboxylate extracts cobalt as a tetrahedral complex with two chloride ions neutralizing the charge. It is most probable that two NOPC solvating ligands make up the co-ordination number of four.

The extraction of cobalt thus proceeds as follows :

$$Co^{2+} + 2Cl^- + \overline{4\ OCOX} \rightleftarrows \underset{\text{(Octahedral)}}{\overline{CoCl_2(OCOX)_4}} \qquad \ldots\ldots (6.1)$$

$$Co^{2+} + 2Cl^- + \overline{2\ NOPC} \rightleftarrows \underset{\text{(Tetrahedral)}}{\overline{CoCl_2(NOPC)_2}} \qquad \ldots\ldots (6.2)$$

Figure 6.4 - Log D dependence on Chloride concentration for the extraction of Cobalt (II) with OCOX and NOPC. Constant parameters $[Co^{2+}]_i$ = 8mM, $[HNO_3]$ = 1,6 x 10^{-3}M.

◑ ([OCOX] = 0,4M, NaCl)
● ([OCOX] = 0,2M, LiCl)
○ ([OCOX] = 0,1M, LiCl)
◒ ([NOPC] = 0,2M, LiCl)

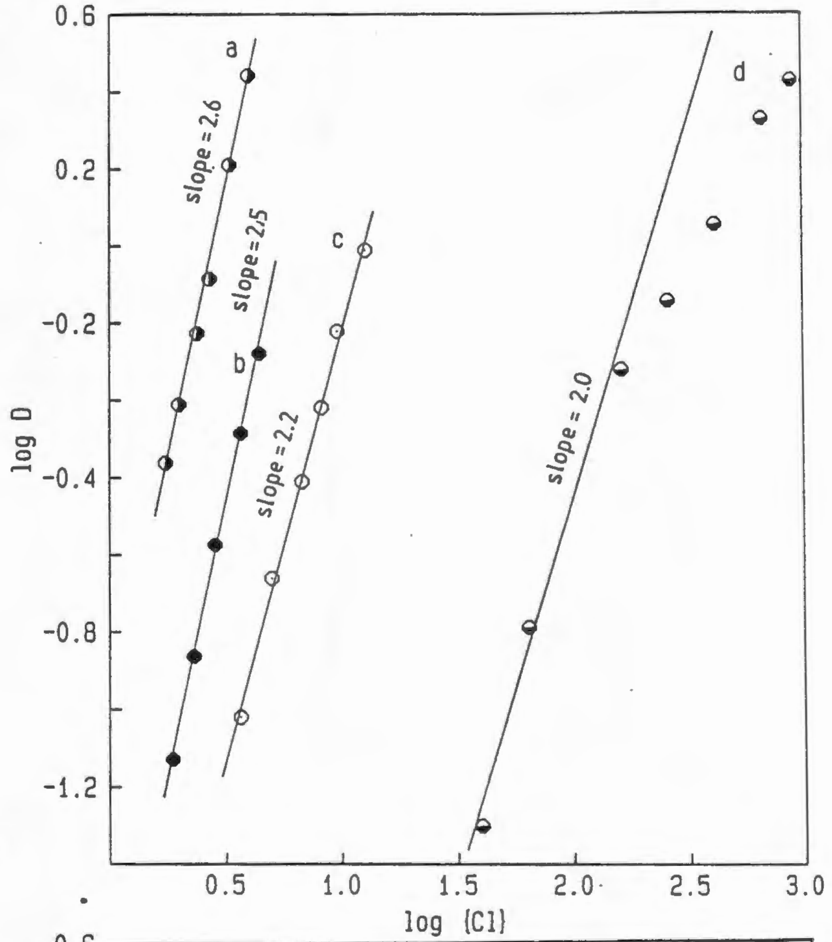

Figure 6.5 - Log D dependence on the Oxime Monomer concentration for extraction of Cobalt (II).
Constant parameter
{Cl} = 0,6

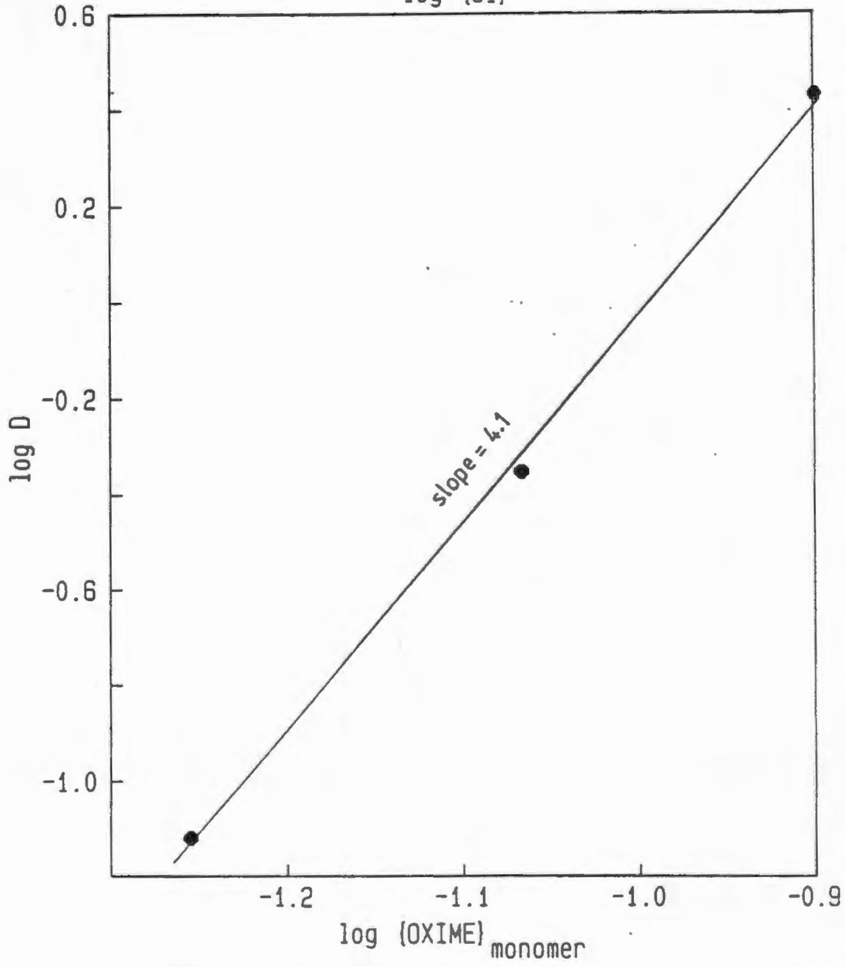

6.2 Extraction of Nickel (II)

Slope analysis data for the extraction of nickel (II) from chloride solutions is consistent with the presence of $NiCl_2(OCOX)_3$ in the organic phase for the extraction with octanal oxime and $NiCl_2(NOPC)_2$ for extraction with n-octyl-3-pyridine carboxylate. Log-log plots of D versus chloride activity and extractant concentration are shown in Figures 6.6 and 6.7 respectively.

The UV-VIS absorption spectra of both complexes are typical of an octahedral, Ni(II) d^8 ion, namely : two peaks in the 350-750 nm region with very low molar absorbances, due to the two transitions [46].

$^3A_{2g} \rightarrow {}^3T_{ig}$ (P) ~ 400 nm region

$^3A_{2g} \rightarrow {}^3T_{ig}$ (F) ~ 600 nm region

The spectra are shown in Figure 6.8, together with that of $[Ni(H_2O)_6]Cl_2$ and $NiCl_2(MPO)_4$ for comparison purposes. $NiCl_2(MPO)_4$ precipitates out of solution when a (5,0 NaCl, 8mM Ni(II), 1.6mH HNO_3) solution is contacted with a 0,4 Molar solution of 2-methyl propanal oxime. The analyses results are shown in Table 6.2.

Table 6.2 - Analysis of $NiCl_2(MPO)_4$

Element	Calculated %	Observed %
Ni	12,1	11,9
Cl	14,8	14,7
C	11,7	11,6
N	40,1	37,2
H	7,5	7,5

The spectra for $NiCl_2$ complexes of OCOX, MPO and NOPC are all similar to the one obtained for $[Ni(H_2O)_6]Cl_2$, indicating that all these will have an octahedral geometry. Their peaks are shifted to lower wavelengths as is

Figure 6.6 - log D dependence on Chloride concentration for the extraction of Ni(II) with OCOX (Graph A) and NOPC (Graph B)

$[Ni^{2+}]_i = 8mM$
$[HNO3] = 1,6 \times 10^{-3}$

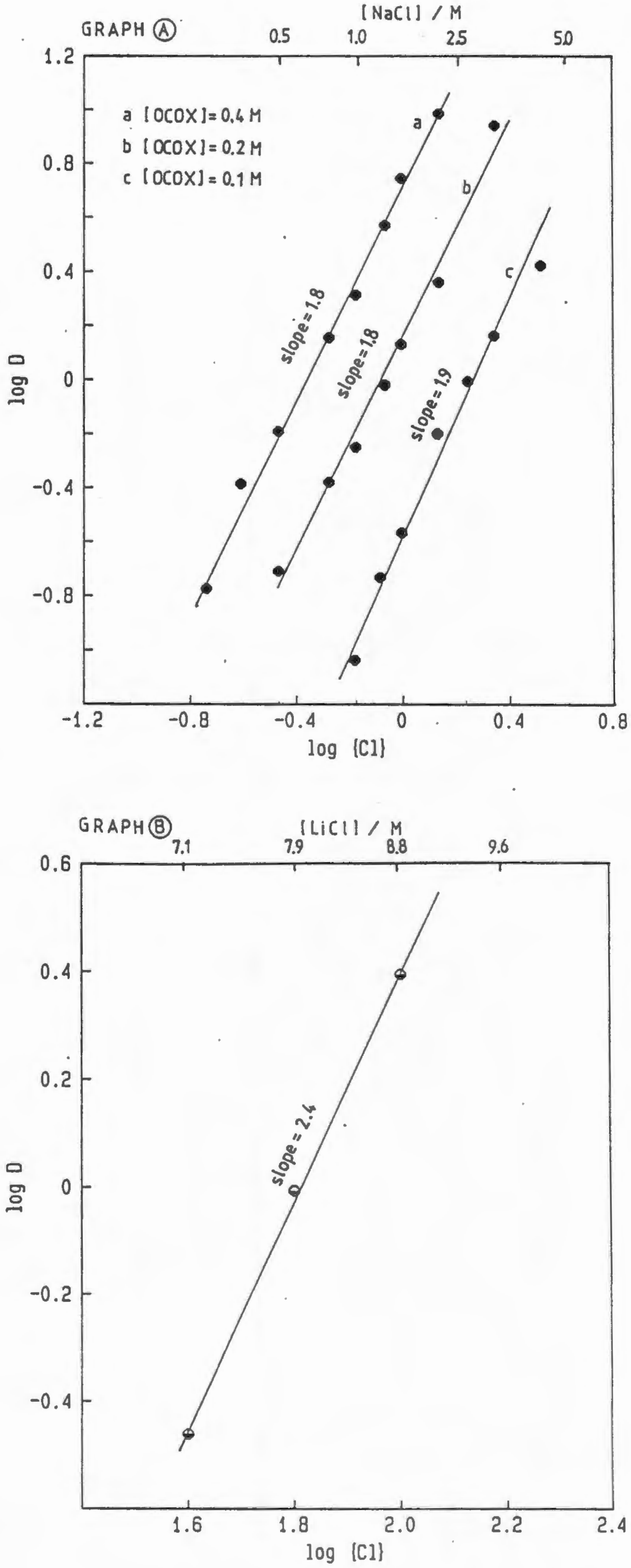

$[NOPC] = 0,2M$
$[Ni^{2+}] = 8mM$
$[HNO_3] = 1,6 \times 10^{-3}M$

Figure 6.7 - Log D dependence on extraction concentration for the extraction of Ni(II). ([OCOX] = 0,1-0,4M, [NaCl] = 1,5M, $[Ni^{2+}]_i$ = 8mM $[HNO_3]$ = 1,6 x 10^{-3}M) ([NOPC] = 0,08-0,2M, $[Ni^{2+}]_i$ = 1,27 x 10^{-3}M, [LiCl] = 9,6M)

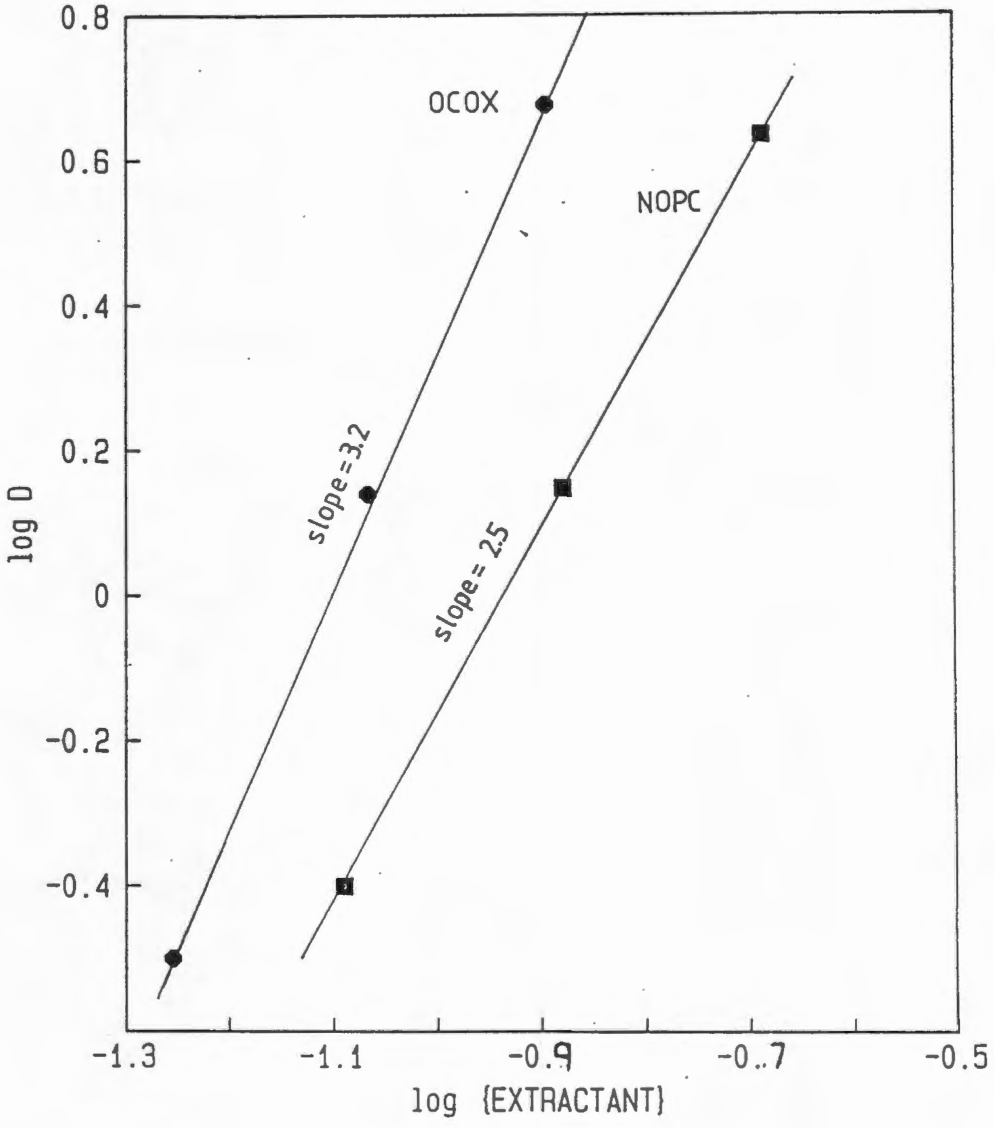

expected from the relative positions of nitrogen donor ligands and water in the spectrochemical series. To complete the required co-ordination number of six, water will be present in the complexes to varying degrees.

i.e. $NiCl_2(MPO)_4$
$NiCl_2(OCOX)_3(H_2O)$
$NiCl_2(NOPC)_2(H_2O)_2$

Figure 6.8 - UV-vis Absorption spectra for various Ni(II) complexes

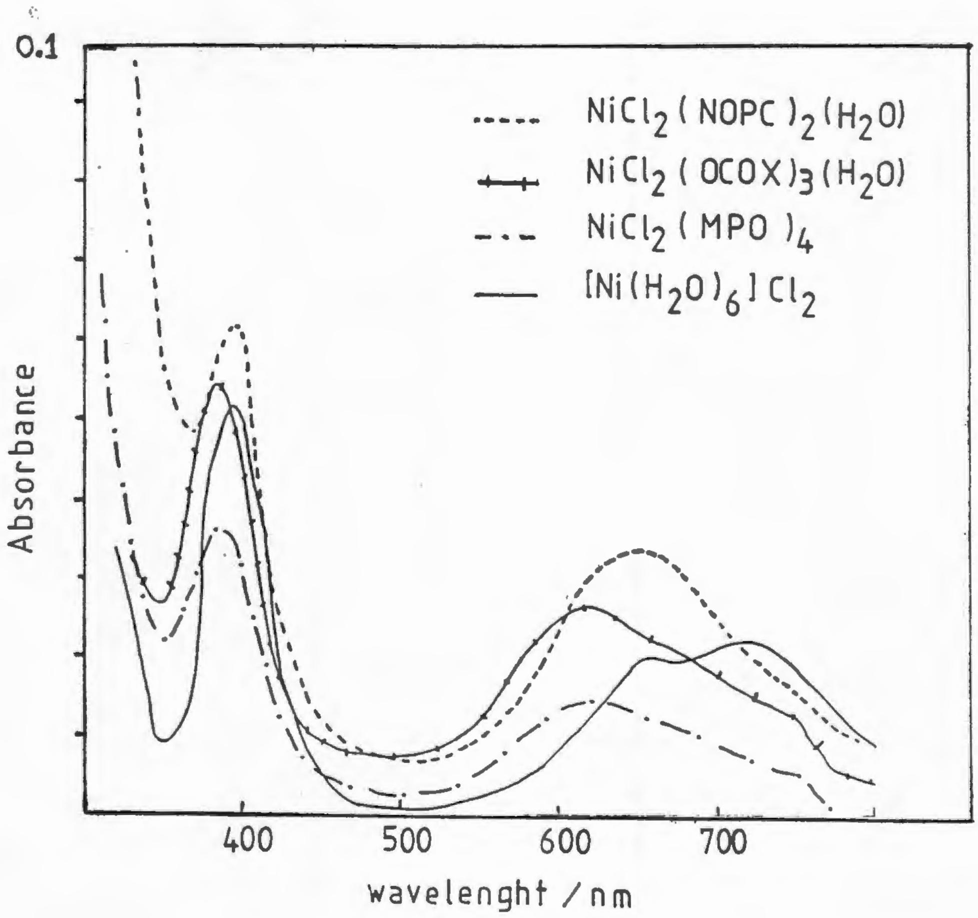

6.3 Extraction of Iron (III)

The hexaquairon (III) ion is very easily hydrolized and only exists in its hydrated form at very low pH. Partially hydrolized iron (III) solutions have colours ranging from yellow to brown and are well known for their instability. In addition to the soluble hydroxy species arising from the complex equilibria shown below, polymerization of dimers as well as oxolation occurs.[47] At higher pH, ferric oxide and oxyhydroxide precipitate.

$$Fe^{3+} + H_2O \rightleftarrows Fe(OH)^{2+} + H^+ \qquad \text{.... (6.3)}$$

$$2\ Fe(OH)^{2+} \rightleftarrows (Fe(OH))_2{}^{4+} \qquad \text{.... (6.4)}$$

$$Fe^{3+} + 2H_2O \rightleftarrows Fe(OH)_2{}^{+} + 2H^+ \qquad \text{.... (6.5)}$$

In chloride solutions species of the type $(FeCl_n{}^{3-n})$[48] are also present and it is suggested by Dousman et al[49] that bridged chloride species play an active role in the precipitation of FeOOH. It is clear then, that the initial hydrogen ion concentration in the aqueous phase will directly affect distribution ratios and should therefore be maintained constant for the study of the effect of chloride and extractant concentration. At high chloride concentrations, however, (i.e. above 5,0M LiCl) it was found to be difficult to adjust the pH to a constant value by addition of base, because as soon as the pH reached a value of ~ 2,2, a very fine orange precipitate appeared and was accompanied by a pH drop which seemed to be fairly insensitive to further small additions of base.

This was also observed by Dousman et al[49], and a diagram taken from their paper on "The influence of chloride ions on the formation of iron (III) oxyhydroxide" is reproduced here.

Figure 6.9 - Titration curves[49] : pH vs ml added base for a 6,25 x 10^{-2}M Fe(III) Solution. Curve A : Cl/Fe = 0,3 Curve B : Cl/Fe = 12,8. Reproduced from reference 44.

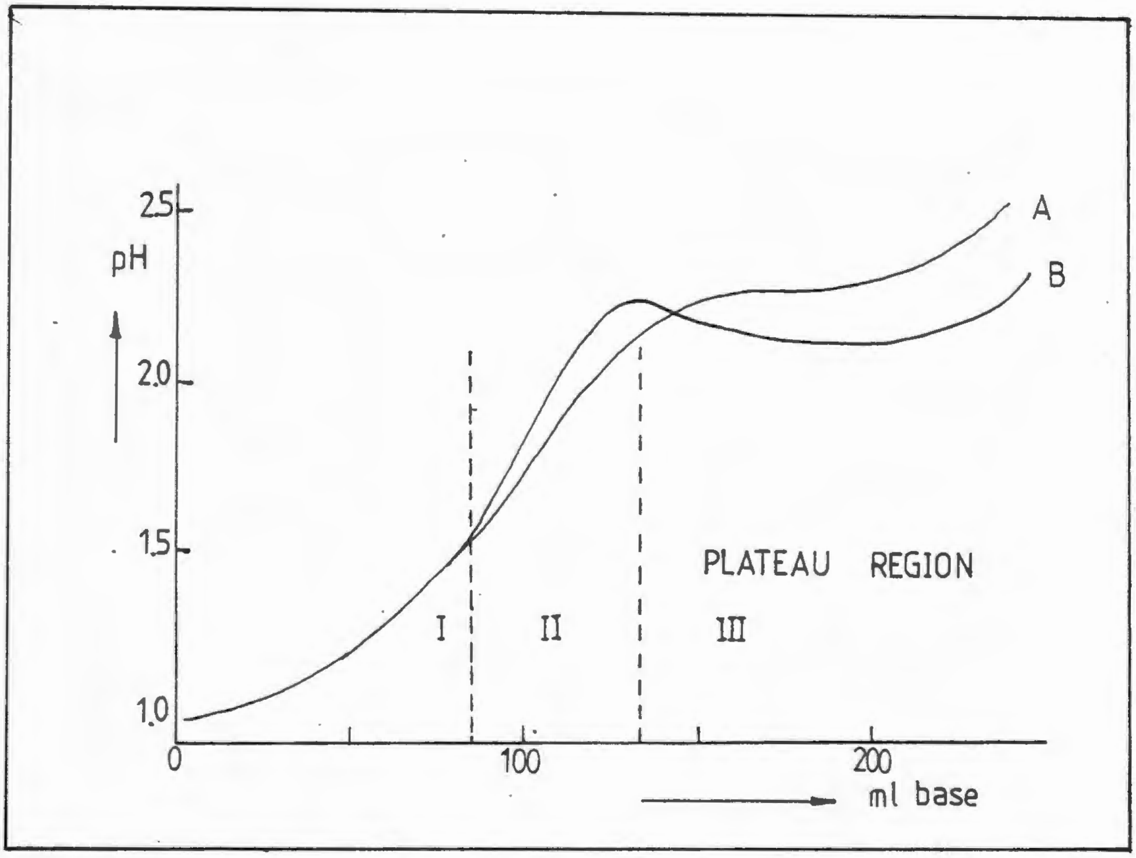

The diagram shows the effect of Cl/Fe ratio on the shape of the titration curve, and it can be seen that at the higher chloride concentration there is a plateau region where the pH is insensitive to addition of base.

Due to these complications, experiments were set up at various chloride concentrations with a fixed initial amount of acid and the approximate pH range determined. Table 6.3 shows the lithium chloride and acid concentrations used and their respective pH ranges.

Table 6.3 - pH Values of Fe^{3+} (8mM) Solutions at Various Acid and Chloride Concentrations

[LiCl]	0,1 HNO_3	10^{-2} HCl	5 x 10^{-3} HCl	10^{-4} HCl
5,0	< 0	0,6	1,1	1,6
5,5	< 0	0,2	0,9	1,5
6,4	< 0	0,0	0,7	1,4
7,1	< 0	< 0	0,4	1,4
7,9	< 0	< 0	0,1	1,3

a) Extraction of Fe^{3+} with ACORGA CLX-20

The extraction of iron (III) from lithium chloride solutions with ACORGA CLX-20 at different acid concentrations is shown in Figure 6.10. It can be seen that extraction only takes place to any considerable extent at pH lower than ~ 0,5 and chloride concentrations higher than 5,5M LiCl. This suggests that extraction is taking place via the following reactions :

$$\overline{RNH^+} + FeCl^-_4 \rightleftarrows \overline{(RNH)^+ (FeCl_4)^-} \quad \text{.... (6.6)}$$

$$Fe^{3+} + 4Cl^- \rightleftarrows FeCl^-_4 \quad \text{.... (6.7)}$$

$$\overline{RN} + H^+ \rightleftarrows \overline{RNH^+} \quad \text{.... (6.8)}$$

where high chloride and hydrogen ion concentrations will push the equilibria to the right. This position is supported by the following :

1. Extraction increases with increasing chloride concentration and decreasing pH.

2. The plot of log D versus log $\{Cl^-\}$ for the extraction of iron from lithium chloride solutions containing 0,1M HNO_3, has a slope of 3,55, indicating the possible extraction of $FeCl^-_4$ into the organic phase.

Figure 6.10 - Extraction of Fe(III) from Lithium Chloride solutions with ACORGA CLX-20 (0,2M)

Aqueous solutions :
$[Fe^{3+}]_i$ = 8mM
$[LiCl]$ = 5,0-8,0M

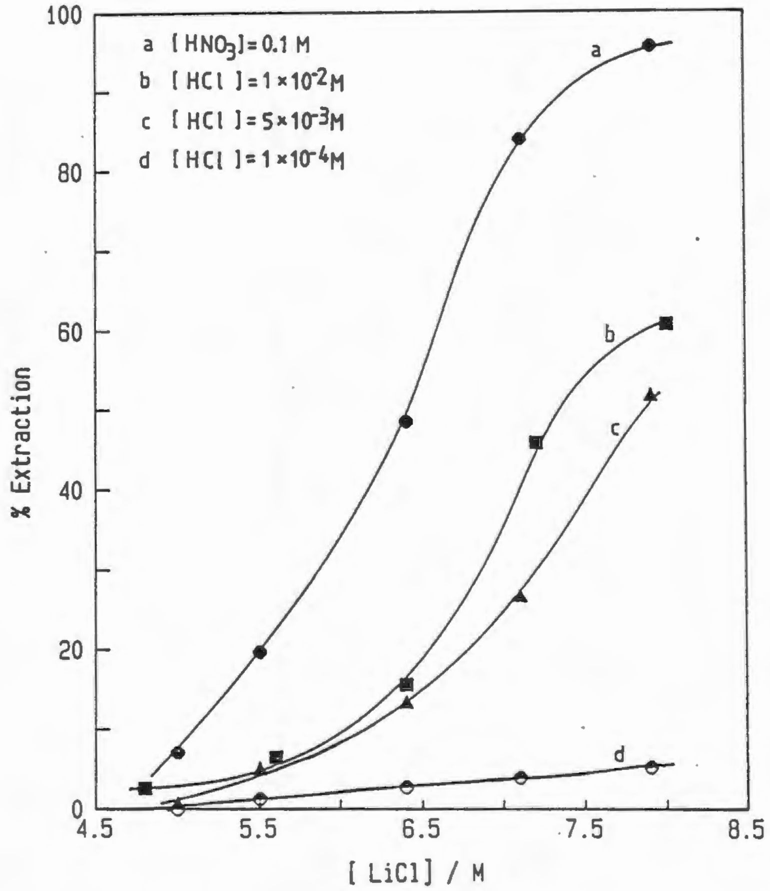

Figure 6.11 - Extraction of Fe(III) from Lithium Chloride solutions with Octanal Oxime (0,2M)

Aqueous solutions :
$[Fe^{3+}]$ = 8mM
$[LiCl]$ = 5,0-8,0M

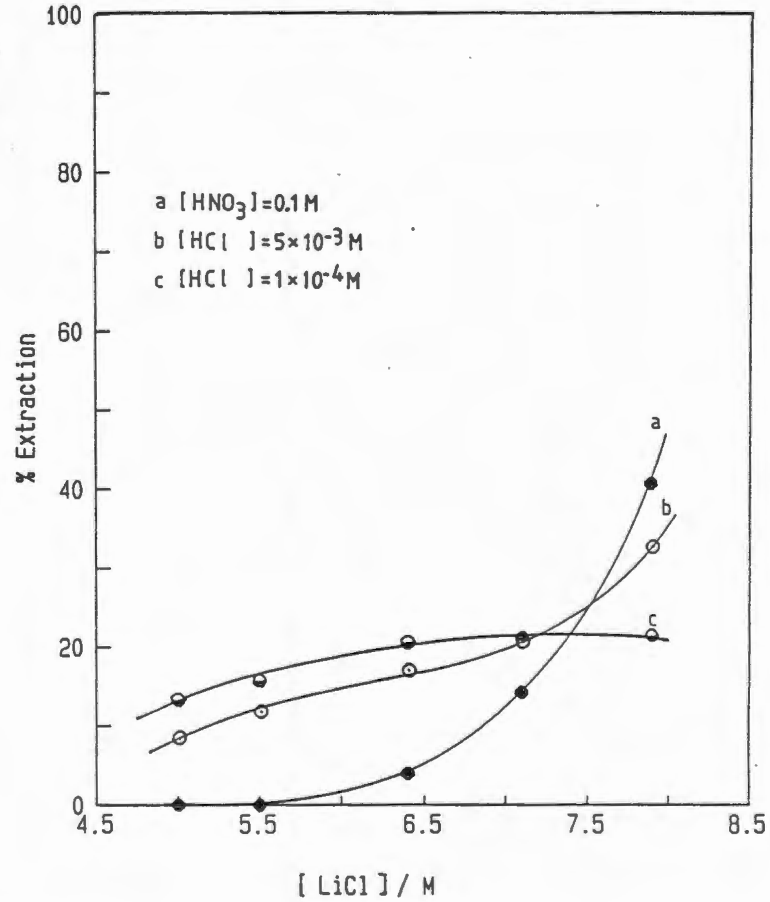

3. The increase in extraction is accompanied by an increase in the percentage protonation of extractant (Table 6.4). The percentage protonation of the extractant was determined as described in Section (2.3.5).

Table 6.4 - Extraction of Iron (III) from LiCl Solutions Containing 5×10^{-3} HCl and 8mM Fe^{3+} into 0,2M ACORGA

[LiCl], M	Extraction, %	Protonation, %	$[RNH^+]$*,M
6,4	13,2	1,73	0,0034
7,1	26,6	4,28	0,0084
7,9	51,8	7,83	0,0156

* Concentration of protonated ACORGA

b) Extraction of Iron with Octanal Oxime

Curves for the extraction of iron (III) from lithium chloride solutions with octanal oxime are shown in Figure 6.11. At the highests chloride concentration (7,9M LiCl), the extraction decreases with increasing pH as was the case with ACORGA, indicating that extraction is taking place via the ion association reaction. At the lower chloride concentrations, however, the extraction improves as the pH is increased.

Two reactions can be proposed :

A) Extraction by Solvation

$$FeCl_3 + x\ RNOH \rightleftarrows FeCl_3(RNOH)_x \qquad \ldots (6.9)$$

$RNOH = (C_7H_{15})CHNOH$ (Octanal Oxime)

B) Extraction by Cation Exchange

$$FeCl_2^+ + RNOH + x\ (RNOH) \rightleftarrows FeCl_2(RNO)(RNOH)_x + H^+ \quad \ldots (6.10)$$

Reaction (A) would be independent of pH only when no protonation occurred, as seen in the case of copper (4.1.4), and the log D versus pH curve would have the shape of curve A (dashed line) Figure 6.12. If (B) is the extraction reaction then a linear dependence with slope = 1 is expected. The extraction as a function of pH is shown in Figure 6.12, but it does not shed much light on the matter because a precipitate is formed at the interface at pH ~ 1,4 and thereafter extraction results do not represent an equilibrium situation.

6.4 Extraction of Cu, Fe, Pb and Zn with ACORGA CLX-20

The solvent extraction of copper from chloride solutions is pertinent to the recovery of non-ferrous metals from complex sulphide ores. These ores contain mainly copper, iron, lead and zinc. The loading of copper was tested with a feed solution containing these metals in the proportion expected from the leaching of a complex ore with ferric chloride

$$CuFeS_2 + 4FeCl_3 \rightleftarrows CuCl_2 + 5FeCl_2 + 2S$$
$$ZnS + 2FeCl_3 \rightleftarrows ZnCl_2 + 2FeCl_2 + S$$
$$PbS + 2FeCl_3 \rightleftarrows PbCl_2 + 2FeCl_2 + S$$

Experimental details of loading (Figure 6.13(A)) and stripping (Figure 6.13(B)) isotherms are given in Section 2.3.4, and feed solution compositions are given in Table 6.5.

Table 6.5 - Feed Solution Compositions ($g\ell^{-1}$)

Solution	Cu	Fe	Zn	Pb	[HCl]	Total Cℓ
A	25,2	167,5	19,6	<10 (sat)	0,1M	7,6M
B	25,4	167,5	19,6	<10 (sat)	0,5M	8,0M

The shape of the extraction isotherm is very favourable and only two stages are required to fully load a 25 $g\ell^{-1}$ copper solution at an organic-to-aqueous ratio of 2,5, as shown in Figure 6.13(A). The amount of

Figure 6.12 - Extraction of Fe(III) with Octanal Oxime as a function of pH. Aqueous solutions $[Fe(III)]_i$ = 8mM, [LiCl] = 5,5M

(A) Log D vs pH

(B) % Extraction vs pH

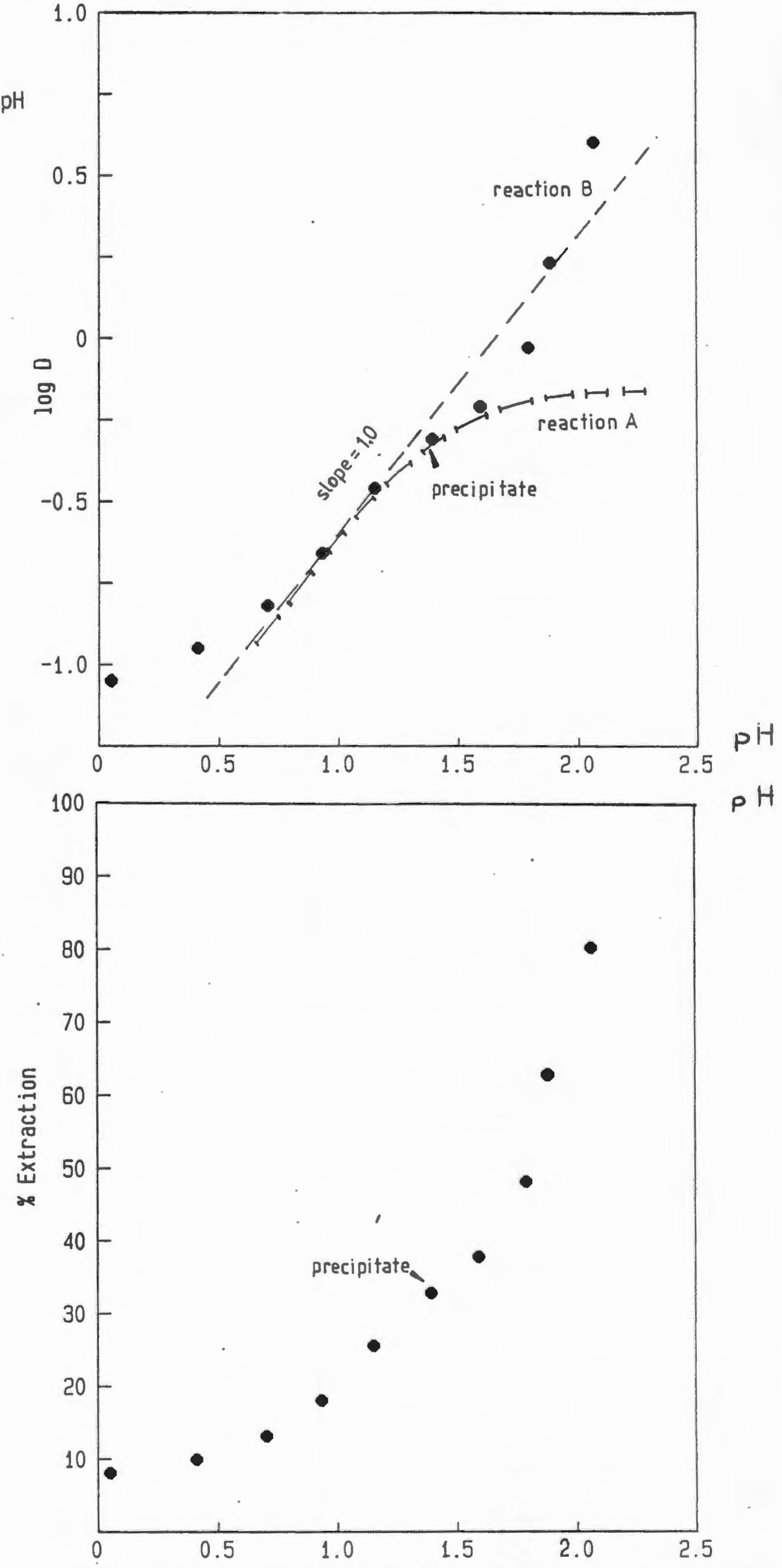

acid present in the feed solution, although having no effect on the copper extraction, is important to keep all the iron in solution. The stripping (Figure 6.13(B)) is not so efficient and 3 stages are necessary to reduce the loaded organic from 10,5 $g\ell^{-1}$ to 3 $g\ell^{-1}$, at a phase ratio of 2,5 to 1 (org/aq). If the phase ratio is decreased (dashed line) then only one stage is required but then the copper concentration of the strip liquor only increases by 7,5 $g\ell^{-1}$. Concentrated solutions are required for the electrowinning step and therefore the initial copper concentration in the strip liquor is already 25 $g\ell^{-1}$ and increases to 44,5 $g\ell^{-1}$ with the higher phase ratio (2,5) as shown in Figure 6.13 (B).

Having established favourable conditions for extraction, batch counter-current experiments were run as described in Section 2.7. These are designed to maximize the loading of copper by contacting clean solvent with aqueous solution from which most of the copper has already been extracted.

It was found that if feed solution B was used, no iron precipitation was observed at first contact but in the subsequent second and third stages large amounts precipitated out of solution. This is due to the decrease of acid in the aqueous phase as a result of extractant protonation as was observed in Section 6.3. This problem was overcome by reducing the total chloride concentration. Results are shown in Table 6.6.

Figure 6.13(A) - Copper extraction isotherm for 26% by volume ACORGA CLX-20 in Shellsol 2325 $[Cu]_i = 25\ g\ell^{-1}$. Curve A : $[Cl]_{total} = 7,6M$. Curve B : $[Cl]_{total} = 8,0M$

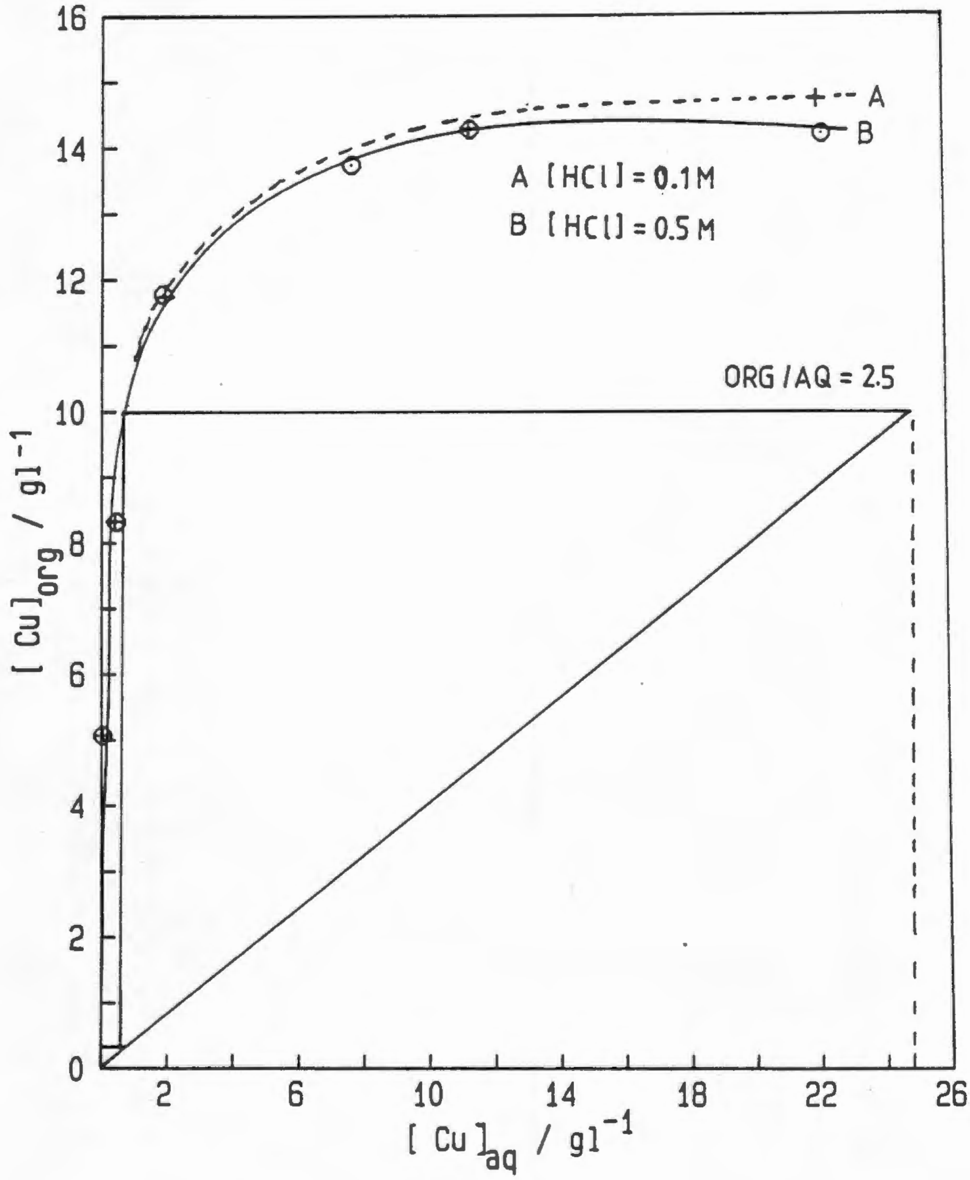

Figure 6.13(B) - Copper stripping isotherm. Organic phases loaded with 14,3 gℓ^{-1} Copper, contacted with strip liquor containing 25 gℓ^{-1} Cu, 0,15M HCl

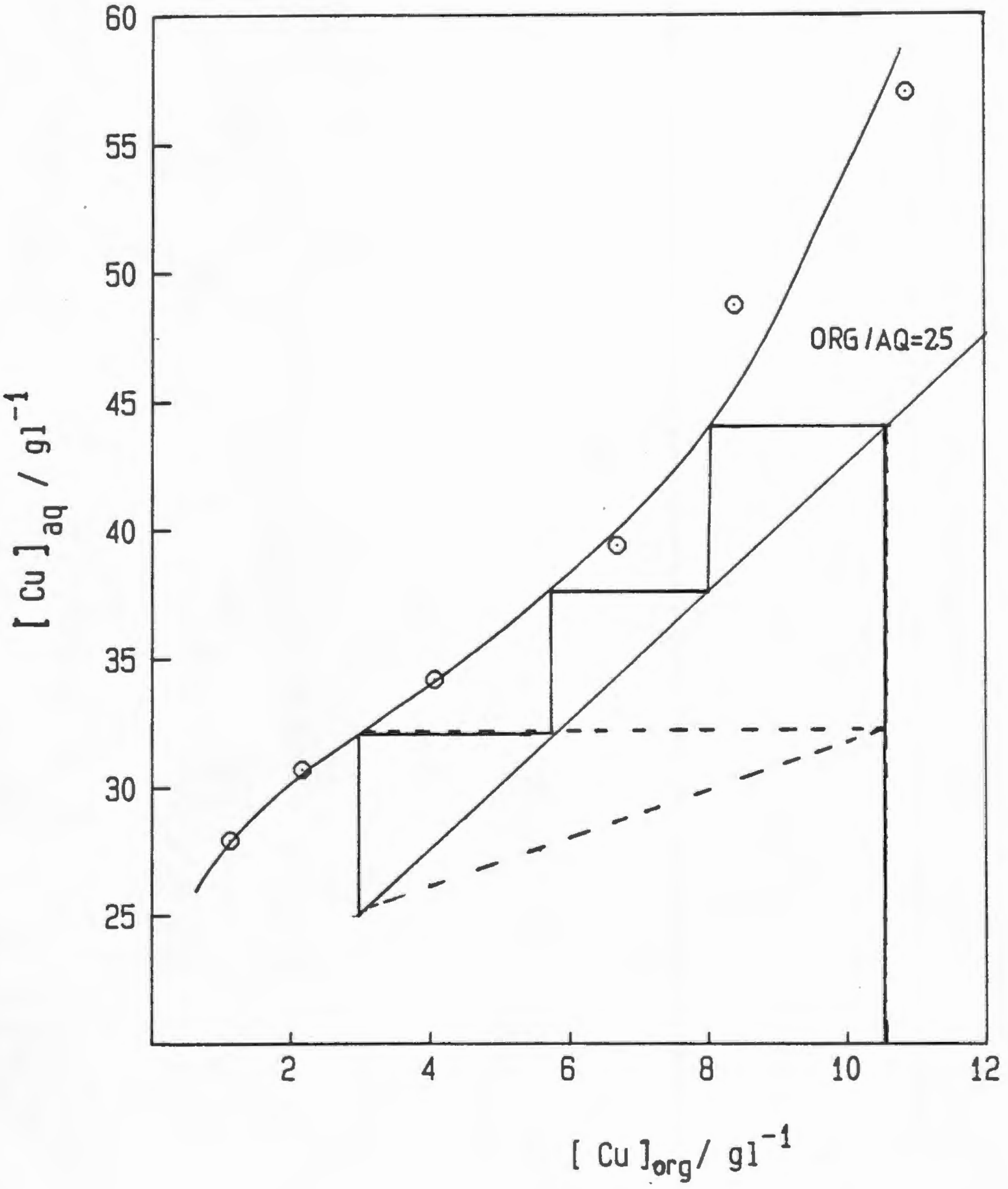

Table 6.6 - Batch Counter-Current Extraction with 26% by Volume ACORGA CLX-20. Organic/Aqueous = 2,5; 3 Stages; 5 Cycles

$g.l^{-1}$	Cu	Fe	Zn	Pb	[HCl]	$[Cl]_{total}$
Feed	22,3	117,2	16,3	< 10	0,5M	6,0M
Loaded Organic						
Cycle 1	8,41	0,41	0,25	0,037		
Cycle 2	8,64	0,50	0,25	0,056		
Cycle 3	8,84	0,54	0,35	0,096		
Cycle 4	8,94	0,51	0,32	0,109		
Cycle 5	8,94	0,66	0,35	0,108		

The poor selectivity between Cu and Fe can be best understood in terms of the metal extraction curves at various lithium chloride concentrations (Figure 6.14).

ACORGA extracts of Cu^{2+}, Fe^{3+} and Zn^{2+} are green, yellow and colourless respectively. Copper (I) is extracted as a brown complex. Cu(I) is easily oxidized to Cu(II) in air and therefore special precautions had to be taken. Cu(I) solutions were made up with CuCℓ and Cu metal added to reduce any Cu(II) present. (Section 2.3.1). All solutions and flasks were flushed with N_2. Only two samples (marked *) in Figure 6.14 had green organic extracts indicating that partial oxidation had taken place. Extraction of copper (I) decreases with increasing chloride concentration due to formation of $CuCl_2^-$ and $CuCl_3^{2-}$ species at the expense of the extractable neutral CuCl. Zn(II) is only extracted at high chloride concentrations. The main problem is in the separation of Cu(II) and Fe(III). It must be noted that most of the iron will be present as Fe(II) which is not extracted to such a great extent.

Figure 6.14 - Extraction curves for Cu(I), Cu(II), Fe(III), Fe(II) and Zn (II) with ACORGA CLX-20 in Shellsol 2325 ([Metal] = 0,05M, [HCl] = 0,1M [ACORGA] = 26% by volume)

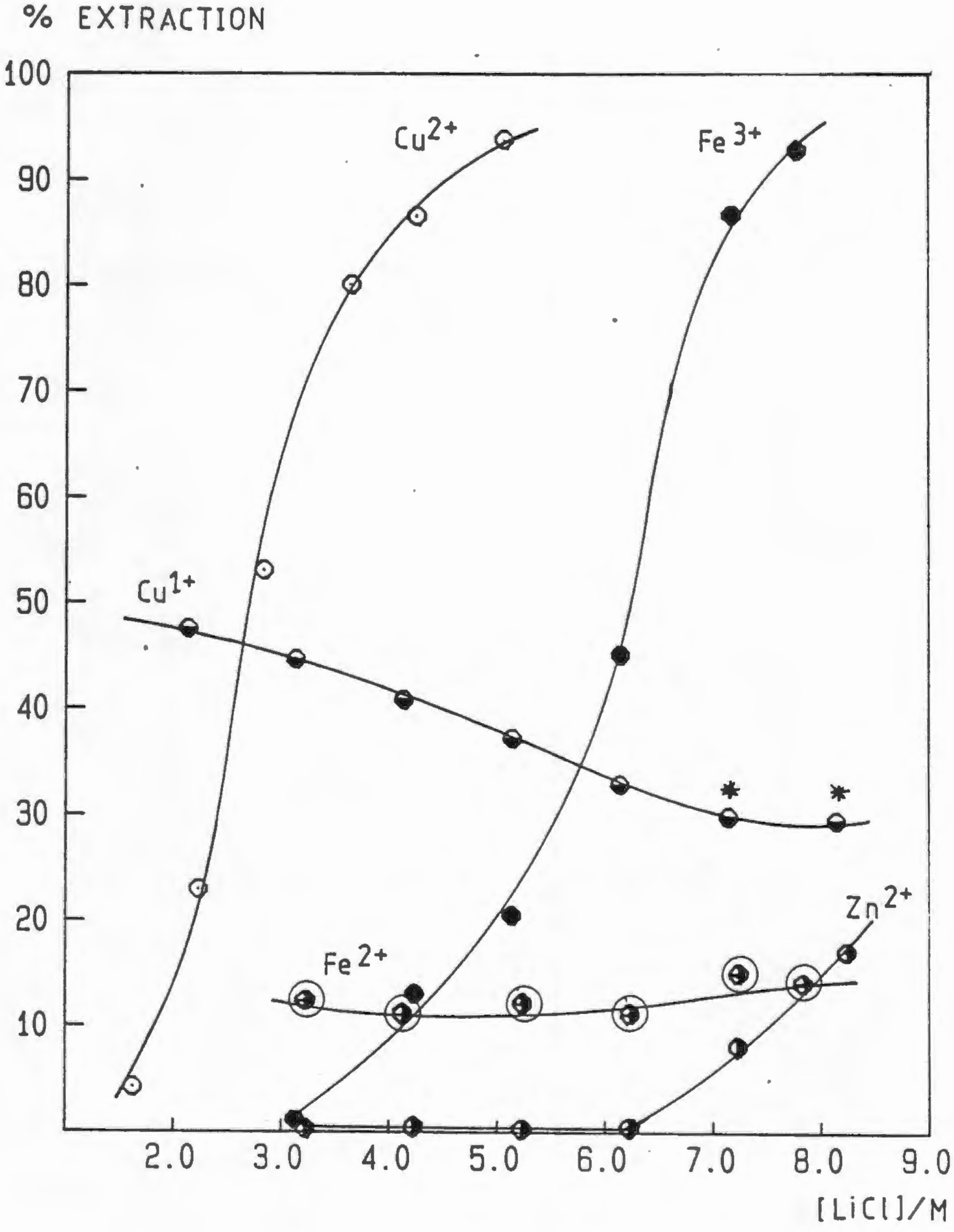

There is however another equilibrium that must be taken into account[50]

$$Cu(II) + Fe(II) \leftrightarrows Cu(I) + Fe(III) \qquad .... (6.11)$$

According to Le Chatelier's principle the equilibrium will shift to the right by either extraction of Cu(I) or Fe(III) or by stabilization of the Cu(I) or Fe(III) metal ions, e.g. by formation of $FeCl_4^-$ and $CuCl_2^-$ favoured by high chloride concentrations.

There is a further complication. A certain amount of acid (0,5M) is required to keep the iron in solution in the aqueous phase. High chloride concentrations, however, will increase the activity of the proton and some acid will be extracted into the organic phase. This problem is compounded by repeated contact of the aqueous phase with fresh organic as happens in counter-current extractions. This is the reason for the precipitation of iron from 8M chloride solution in the second and third stages.

Thus high chloride concentrations (e.g. 8M) have the following disadvantages :

1. Stabilise higher metal-chloro species and therefore increase amount of extractable $FeCl_4^-$.

2. Increased proton activity which causes increased protonation of extractant and thus increased extraction of iron by the ion-association mechanism (equation 6.3). As a consequence the amount of acid present in the aqueous phase decreases and iron precipitates.

At lower chloride concentrations (e.g. 6M) the consumption of acid is reduced and precipitation is not a problem but the extraction of Cu(I) is increased. This shifts equilibrium 6.8 towards formation of Fe(III) which is then also extracted.

To summarize :

Cobalt and Nickel are extracted by the solvation mechanism where

$$M^{2+} + 2Cl^- + x\,\overline{OCOX} \leftrightarrows \overline{MCl_2(OCOX)_x(H_2O)_{4-x}}$$

$x = 3$ for Ni^{2+}, $x = 4$ for Co^{2+}

$$M^{2+} + 2Cl^- + 2\,\overline{NOPC} \leftrightarrows \overline{MCl_2(NOPC)_2\,(H_2O)_x}$$

$x = 0$ for Co^{2+}, $x = 2$ for Ni^{2+}

Fe^{3+} is extracted mainly by the ion-association mechanism, which is favoured by high chloride and hydrogen ion concentrations. This is the main reason for the poor selectivity of ACORGA CLX-20 for copper over iron.

$$FeCl_4 + \overline{LH^+} \leftrightarrows \overline{(FeCl_4)(LH)}$$

where L = OCOX, NOPC, ACORGA CLX-20.

CHAPTER 7

CHAPTER 7

CONCLUSIONS

The extraction curves for Cu^{2+}, Ni^{2+}, Co^{2+} and Zn^{2+} from chloride solutions with both octanal oxime and n-octyl-3-pyridine carboxylate are shown in Figure 7.1. The respective complexes formed in the organic phase are also depicted. The metals are extracted in the order predicted by the Irving-Williams stability series for octahedral compounds[59].

$$\text{i.e.} \quad Zn(II) < Cu(II) > Ni(II) > Co(II)$$

Octanal oxime extracts from lower chloride concentrations than n-octyl-3-pyridine carboxylate. This is not expected on the basis of their relative pKa measured in ethanol (Appendix 2). N-octyl-3-pyridine carboxylate has an higher affinity for protons and should therefore also form stronger complexes with metal ions. The stability of the octanal oxime complexes can be explained in terms of the stoichiometry of the extraction reaction. As seen previously, three to four oxime ligands are coordinated to the metal ions of copper, nickel and cobalt, while only two n-octyl-3-pyridine carboxylate ligands are present in the corresponding metal/NOPC complexes. This decrease in the extractant stoichiometry is due to the bulkiness of the NOPC ligand. The steric crowding is well illustrated by the difference in configuration between the two cobalt complexes. The one has four oxime molecules and two chloride ions in its inner coordination shell while the other, in addition to having only two NOPC molecules has expelled two water molecules and adopted a tetrahedral configuration.

A valid comparison of extractant strength can be drawn between n-octyl-3-pyridine carboxylate and ACORGA CLX-20, since their extraction reactions have the same stoichiometry, (i.e. formation of $CuCl_2(Ext)_2$) and complexation occurs via the nitrogen in the pyridine ring in both cases. The measured pKa, in 80% ethanol, was 2,17 for n-octyl-3-pyridine carboxylate and 1,87 for ACORGA CLX-20. (Appendix 2). The lower value for ACORGA is expected because of a decrease in electron donating capacity of the pyridine nitrogen caused by the addition of a second ester group.

Figure 7.1 - Extraction curves for various divalent metals

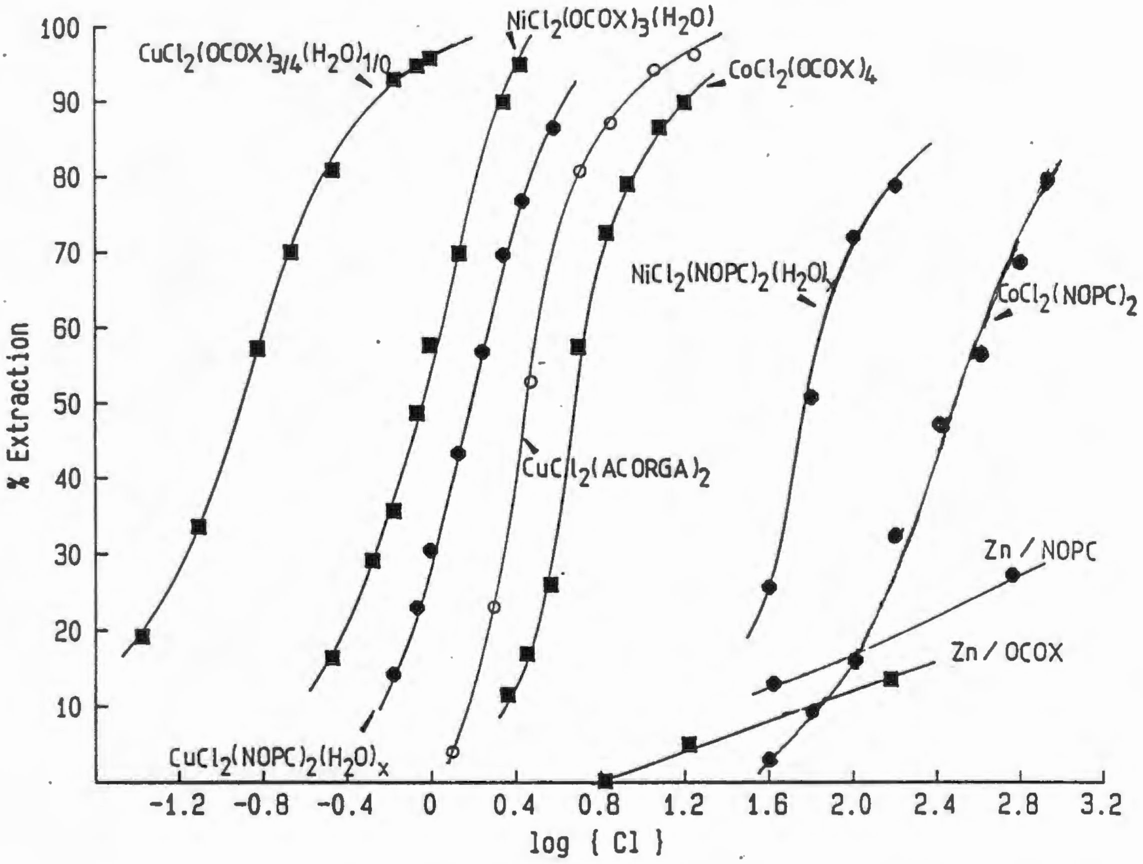

●[n-octyl-3-pyridine]= 0 2 M

○[ACORGA CLX-20]= 048 M

This in turn is reflected in the extractant strength and thus ACORGA CLX-20 extracts copper from higher chloride concentrations than n-octyl-3-pyridine carboxylate (Figure 7.1).

Extraction of iron (III) from chloride solutions of low pH occurs by a mechanism in which the protonated extractant associates with the negatively charged $FeCl_4$- species. Typical extraction curves for octanal oxime, n-octyl-3-pyridine carboxylate and ACORGA CLX-20 are shown in Figure 7.2. Since the ion association mechanism is dependent on the tendency of the extractant to be protonated, one expects the extraction to follow the basicity trend

i.e. % Extraction of NOPC > OCOX > ACORGA CLX-20

The observed sequence is :

% Extraction of NOPC > ACORGA CLX-20 > OCOX

Figure 7.2 - Extraction of Fe(III) with OCOX, NOPC and ACORGA CLX-20

$[Fe^{3+}]$ = 8mM
$[HNO_3]$ = 0,1M
[Extractant] = 0,2M

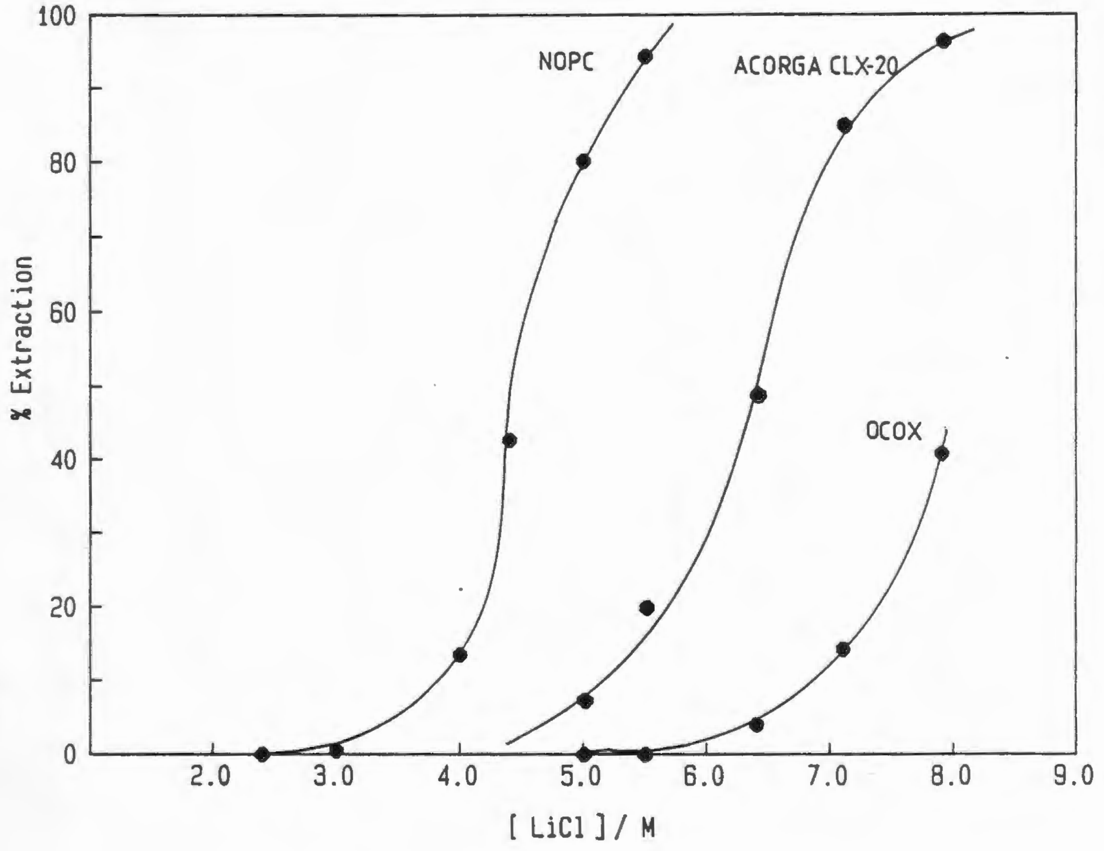

The low extraction values obtained for octanal oxime are probably due to its increased solubility in water, when protonated. The other two extractants will be affected to a lesser extent because they have larger carbon chains, making them more soluble in the organic phase. This difference is illustrated by the behaviour of OCOX and NOPC under different pH (Figure 4.5 and 5.8). The extraction of copper with OCOX decreased at low pH (< 2) while that of NOPC increased under similar conditions. Since the solvating mechanism is not affected by pH an ion-association reaction must be responsible for the increase in extraction in the NOPC case. This route of extraction is not open for octanal oxime if the protonated oxime is soluble in the aqueous phase.

From a practical point of view, octanal oxime would not be a useful extractant because of its solubility in water at pH lower than two. Furthermore it can be seen in Figure 7.1 that selective extraction of copper would require a controlled chloride concentration in the 0,1 to 0,4 Molar range, which is difficult to maintain because of the higher chloride concentrations present in the leach liquors. Moreover, weaker extractants are more easily stripped by contact with water or with solutions of low chloride content.

N-octyl-3-pyridine ester has two main problems as an extractant. First, the extracted copper complex precipitates in the organic phase at concentrations higher than 0,05M and secondly it is a relatively strong base and has therefore the highest affinity for $FeCl_4^-$ at low pH as already discussed. These two problems are partially overcome by ACORGA. Its behaviour as a copper extractant, from simulated ferric chloride leach liquors of complex sulphide ores, is governed by the following factors :

1. Amount of acid present in aqueous phase to keep the iron in solution. Too much acid however promotes extraction of $FeCl_4^-$.

2. Amount of chloride required for efficient extraction of copper and separation from Fe(III).

To summarize :

Extraction of copper (II) from chloride solutions with octanal oxime occurs via the general mechanism :

$$\mathrm{Cu^{2+} + 2Cl^{-} + \overline{3\ OCOX} \rightleftarrows \underset{\text{I}}{\overline{CuCl_2(OCOX)_3(H_2O)}} + \overline{OCOX} \rightleftarrows \underset{\text{II}}{\overline{CuCl_2(OCOX)_4}}}$$

The equilibrium is governed by Le Chatelier's principle and thus formation of complex II will be favoured by high extractant concentrations. The association of octanal oxime in toluene has been taken into account and formation constants for dimers and trimers have been calculated using vapour pressure osmometry techniques. Non-thermodynamic stability constants for the formation of aqueous copper-chloro species ($CuCl^+$,$CuCl_2$) have also been calculated.

N-octyl-3-pyridine carboxylate extracts copper by a similar mechanism :

$$\mathrm{Cu^{2+} + 2Cl^{-} + 2\ \overline{(EXT)} \rightleftarrows CuCl_2\ \overline{(EXT)}_2}$$

Ni(II) and Co(II) are extracted by a solvating mechanism while extraction of Fe(III) occurs by formation of an ion-associated complex.

Octanal oxime and n-octyl-3-pyridine carboxylate are unsuitable as copper extractants; octanal oxime mainly because it becomes partially soluble in the aqueous phase at pH less than two and n-octyl-3-pyridine carboxylate has an high affinity for Fe(III) at low pH. ACORGA CLX-20 is therefore the most suitable of the extractants studied for treating leach liquors obtained from chloride leaching of complex sulphide ores. From an aqueous solution containing 6,0M chloride; 0,5M HCl; 25 $g\ell^{-1}$ Cu; 117 $g\ell^{-1}$ Fe; 16,3 $g\ell^{-1}$ Zn and ~ 10 $g\ell^{-1}$ Pb; 100; 1,4; 5,4 and 2,5 percent extraction of Cu, Fe, Zn and Pb respectively were obtained using a 26% by volume ACORGA solution and a 2,5 organic to aqueous phase ratio.

APPENDICES

APPENDIX I

CALCULATION OF APPROXIMATE STABILITY CONSTANTS FOR THE FORMATION OF $CuCl^+$ AND $CuCl_2$

In Chapter 4 it was shown that extraction of copper with octanal oxime from chloride solutions takes place through the transfer of $CuCl_2$ from the aqueous to the organic phase. The formation of other charged copper-chloro species ($CuCl_n{}^{2-n}$) has been neglected, largely because stability constants for these complexes are not readily available. Literature values range from 0,1 to 4 for β_1 and from 0,2 to 4,9 for β_2, depending on experimental conditions and method[51] (Table I.1)

Table I.1 - Selected Literature Values for Stability Constants for Formation of ($CuCl_n{}^{2-n}$) Complexes at 25 °C

I (Mol dm^{-3}), Medium	Method	β_1	β_2	β_3	β_4	Ref
1,0, $HClO_4$	Spectrophotometric	1,30	0,23			52
2,0, $NaClO_4$	Spectrophotometric	1,30				53
1,0, $HClO_4$	Spectrophotometric	1,69				54
5,0, $NaClO_4$/NaCl	Spectrophotometric	4,00	4,7	1,96	0,23	55
5,0, $NaClO_4$	Spectrophotometric	1,86	1,0			51

The equilibrium formation of $CuCl_n{}^{2-n}$ can be expressed by :

$$Cu^{2+} + nCl^- \rightleftarrows CuCl_n{}^{2-n} \qquad \text{.... (I.1)}$$

$$\beta_n = \{CuCl^{2-n}\} / \{Cu^{2+}\} \{Cl\}^n$$

$$= \frac{{}^{M}\,CuCl_n}{{}^{M}\,Cu \cdot {}^{M}\,Cl^n} \times \frac{{}^{\gamma}\,CuCl_n}{{}^{\gamma}\,Cu \cdot {}^{\gamma}\,Cl^n} \qquad \text{.... (I.2)}$$

Since some activity coefficients in expression (I.2) are unknown one has to make the assumption that the ratio $\gamma_{CuCl_n}/\gamma_{Cu}$ remains constant under the experimental conditions used, and that a non-thermodynamic constant (β_n*) can be calculated by using the activity of chloride ions in sodium chloride solutions.

It must be stressed that these experiments were not run under constant ionic medium conditions for the following reason : Two concepts are generally used[56] in the determination of "stoichiometric" equilibrium constants.

1. Constant ionic strength concept which contends that "in dilute solutions, the acitivity coefficient of a given strong electrolyte is the same in all solutions of the same ionic strength". This only holds for dilute solutions ($u < 0{,}15m$) and therefore cannot be applied.

2. Constant ionic medium concept in which a "large excess of inert electrolyte is used and the activity coefficients of chemical species are considered to be constant". In this work NaCl is used as the electrolyte but the chloride ion is actively involved in the extraction reaction. Furthermore, extraction of copper with reagents other than octanal oxime occur from such concentrated chloride solutions that NaCl is no longer sufficiently soluble and LiCl has to be used. Under these conditions comparison of data in terms of chloride activities is more realistic.

β_n* values can thus be calculated from extraction data by incorporating expression (I.2) into equation (4.7) for the distribution coefficient, which becomes

$$D = \frac{K_{EXT}\ \{Cl\}^2\ \{OX\}^n}{1 + \sum \beta_n^*\ \{Cl\}^n} \qquad \text{.... (I.3)}$$

At a given oxime concentration, and assuming only formation of $CuCl^+$ and $CuCl_2$

$$D = A\ \{Cl^-\}^2\ /\ (1 + \beta_1^*\ \{Cl^-\} + \beta_2^*\ \{Cl^-\}^2) \qquad \text{.... (I.4)}$$

Thus, there are only three constants to be optimised. Data obtained for the extraction of copper from aqueous solution containing ($[\mathrm{Cu}^{2+}]_i$ = 5 x 10^{-4}M, [NaCl] = 0,01-5,0M) into octanal oxime solutions of toluene (0.05-0,4M) was treated by least squares analysis (Figure I.1) and the following stability constants were obtained :

$$\beta_1{*} = 1{,}81$$
$$\beta_2{*} = 0{,}66$$

These compare well with literature values given in Table I.1.

Figure I.1 - Extraction of Copper from Sodium Chloride solutions with Octanal Oxime. Aqueous solutions ($[\mathrm{Cu}^{2+}]_i$ = 5 x 10^{-4}M, $[\mathrm{HNO}_3]$ = 2 x 10^{-3},[NaCl] = 0,01-5,0M). Theoretical curves (full lines) calculated from : $\log D = \text{const.} + 2 \log \{\mathrm{Cl}^-\} + \log (1 + \beta_1 \{\mathrm{Cl}\} + \beta_2 \{\mathrm{Cl}\}^2)$ $\text{const} = K_{EXT} + 3{,}5 \log \{\text{oxime}\}$

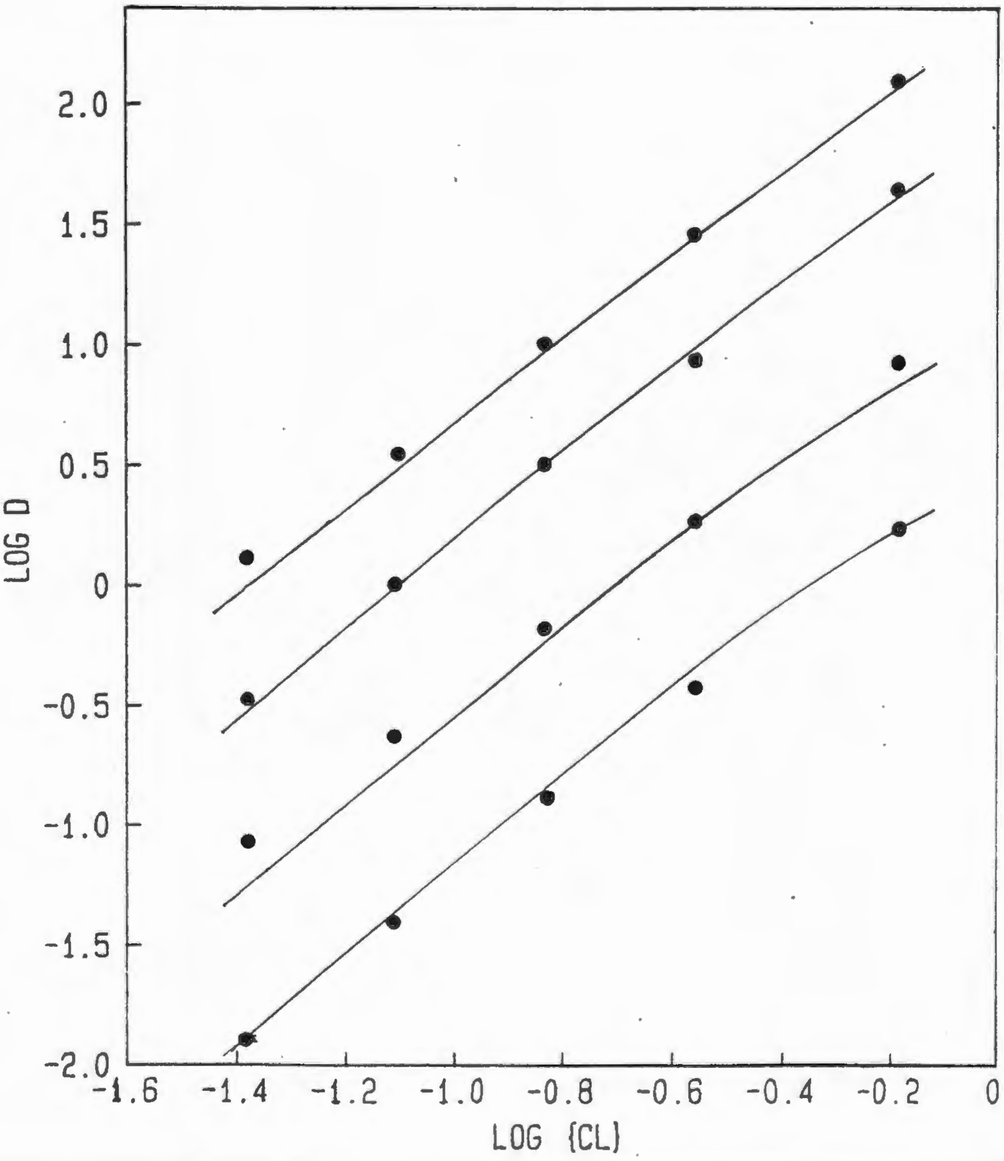

APPENDIX II

THE RELATIVE pKa's OF OCTANAL OXIME, N-OCTYL-3-PYRIDINE CARBOXYLATE AND ACORGA CLX-20 IN 80% ETHANOL

OCOX, NOPC and ACORGA CLX-20 solutions of ethanol were titrated against $HClO_4$ as described in Section 2.4.

The above extractants are weak bases and thus react as follows :

$$HL^+ \overset{Ka}{\rightleftarrows} H^+ + L \qquad \text{.... (II.1)}$$

L = Extractant

from equation (II.1) and the definition of the acid association constant, Ka, one obtains an expression for the pKa

$$pKa = pH + \log \frac{[HL^+]}{[L]} \qquad \text{.... (II.2)}$$

The extractants were titrated against $HClO_4$
and therefore

$$\text{added} \quad [ClO_4^-] = [HL^+] + [H^+] \qquad \text{.... (II.3)}$$

$$\text{also} \quad [L]_{Total} = [L] + [HL^+] \qquad \text{.... (II.4)}$$

substituting (II.3) and (II.4) into equation (II.2)

$$pKa = pH + \log \frac{[ClO_4^-] - [H^+]}{[L]_{Total} - [ClO_4^-] + [H^+]}$$

and therefore a plot of pH versus $\log \dfrac{[ClO_4^-] - [H^+]}{[L]_{Total} - [ClO_4^-] + [H^+]}$

will have a slope of -1 and intercept = pKa.

Such plots are shown in Figure II.1 and the pKa's are tabulated below. The pKa for hydroxyquinoline obtained by this method is also shown for comparative purposes.

	pKa in 80% EtOH
8-hydroxyquinoline	4,34
n-octyl-3-pyridine carboxylate	2,17
octanal oxime	1,92
ACORGA CLX-20	1,87

Figure II.1 - Determination of the relative pKa of OCOX, NOPC and ACORGA CLX-20 by titration with $HClO_4$

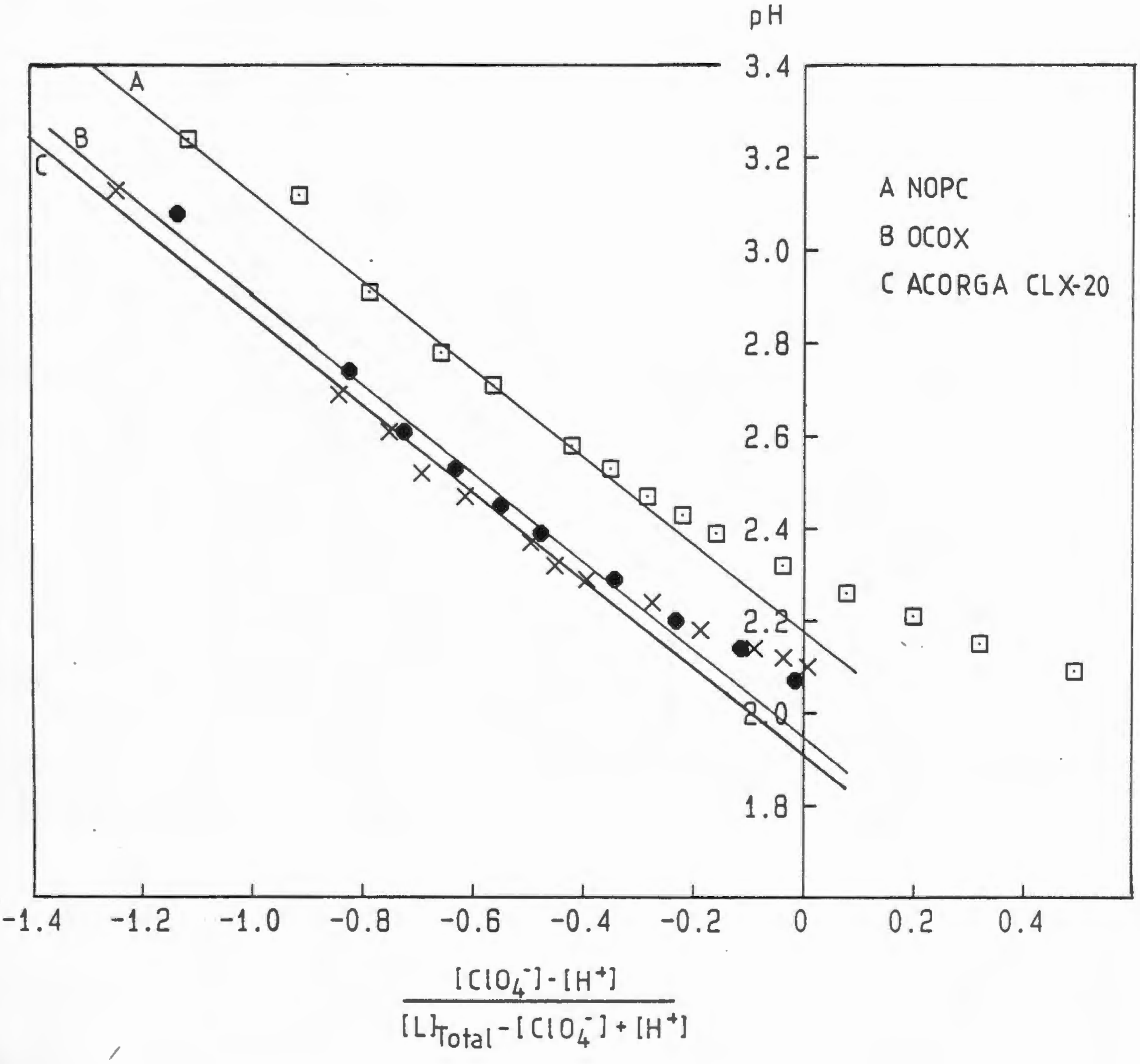

APPENDIX III

DETERMINATION OF THE SOLUBILITY OF EXTRACTANTS IN WATER

The solubility of OCOX, NOPC and ACORGA CLX-20 in water was determined by a method used by Preston et al[57] (Section 2.5). Ethanolic solutions of known extractant concentration are added to a well stirred aqueous phase. If the absorbance is monitored at a wavelength where the extractant does not absorb considerably then a discontinuity in gradient is obtained at the solubility limit, due to increased absorption resulting from light scattering by dispersed organic droplets. A typical plot of Absorbance versus Volume of extractant added is shown in Figure III.1.

The solubility is then calculated

Solubility = (end point (mℓ)/total volume water) x [extractant]

The aqueous solutions used corresponded in pH to the aqueous phases employed in the extraction studies (i.e. 0,0016M HNO_3). The highest solubility was measured for octanal oxime, but it can be neglected when compared with extractant concentrations used in the organic phase (i.e. 0,05-1,0M).

Solubility of extractants in aqueous phases of pH ~ 3

	ppm	M
Octanal oxime	35,1	$2,45 \times 10^{-4}$
n-octyl-3-pyridine carboxylate	30,9	$1,31 \times 10^{-4}$
ACORGA CLX-20	9,4	$3,12 \times 10^{-5}$

Figure III.1 - Solubility titration for NOPC, in 2,0 M NaCl, 1,6 x 10^{-3}M HNO_3. Absorance measured at 280 nm. [NOPC] = 5,232 mg mℓ$^{-1}$

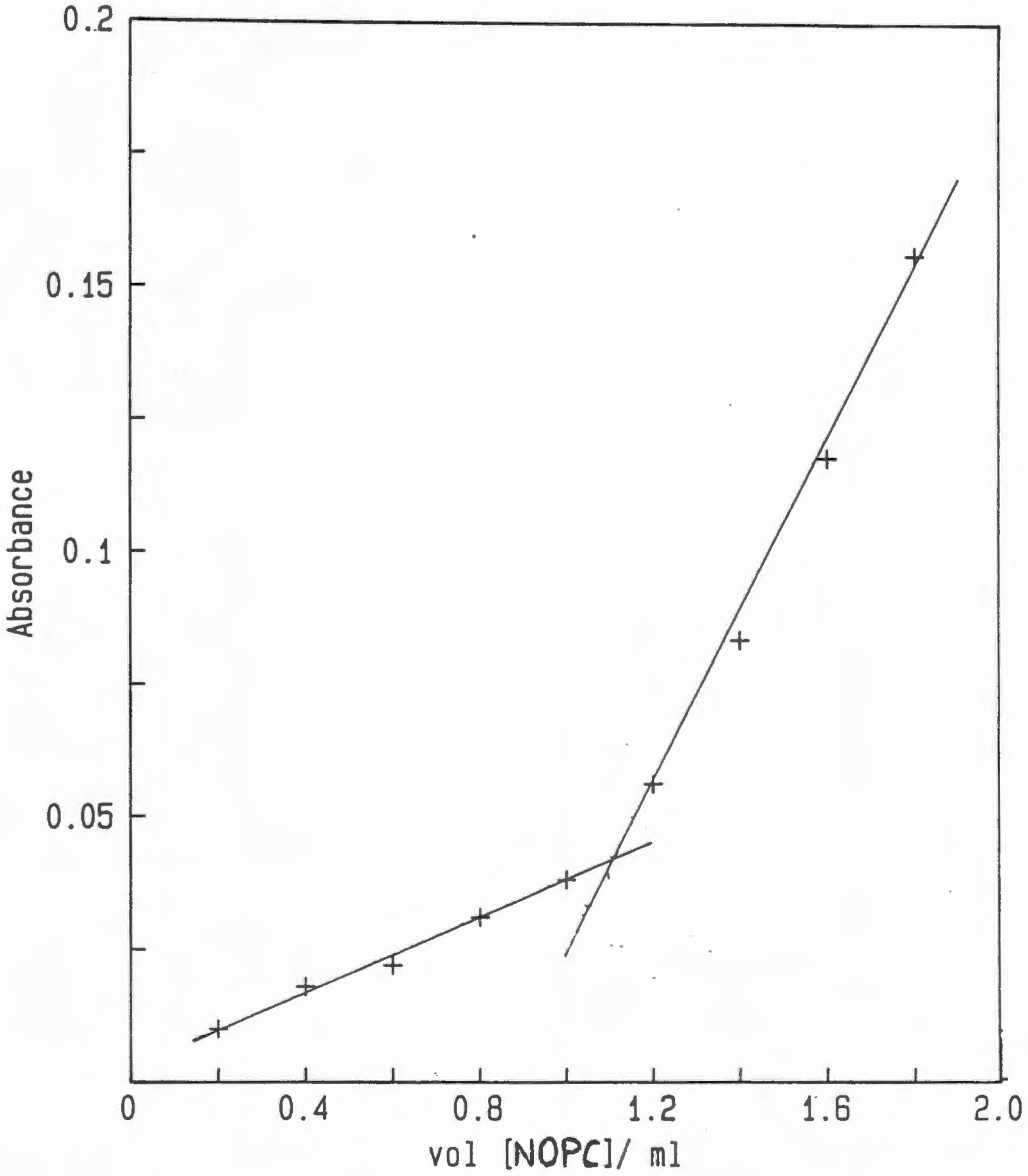

REFERENCES

REFERENCES

1. Kirk-Othmer, **Encyclopaedia of Chemical Technology,** Third ed. Vol. 6, pp 819-852, John Wiley and Sons, New York, 19$_7$8.

2. Cases J.M. Finely Disseminated Complex Sulphide Ores. In **Complex Sulphide Ores** Jones M.J. Ed. (London : IMM, 1980) pp. 234-47.

3. Barbery G., Fletcher A.W., Sirois L.L. Exploitation of Complex Sulphide Deposits : A Review of Processing Options from Ore to Metal. Reference 2, pp. 135-150.

4. Beck R.D., Chamart J.J. The Broken Hill Concentrator of Black Mountain Mineral Development Co. (Pty.) Ltd., South Africa, Reference 2, pp 88-99.

5. Roberts A.N., Burns C.J., Cameron A.W. Metallurgical Development at Woodlawn Mines, Australia, Reference 2, pp 128-134.

6. Guzman A. Process Design for a Bolivian Complex Sulphide Ore containing Casserite, Reference 2, pp 171-177.

7. Paynter J.C. A Review of Copper Hydrometallurgy, **J. South African Inst. Min. Metall.,** November 1973, pp 158-170.

8. Subramanian K.N., Jennings P.H., Review of the Hydrometallurgy of Chalcopyrite Concentrates. **Can. Metall. Quart.** Vol. 11, Number 2, 1972, pp 387-400.

9. Cambell M.C., Ritcey G.M. Applications of Chloride Metallurgy to Base-Metal Sulphide and Uranium Ores at CANMET. In **Extraction Metallurgy '81** (London : IMM 1981) pp 76-90.

10. Flett D.S., Spink D.R. Solvent Extraction of Non-Ferrous Metals : A Review 1972-1974, **Hydrometallurgy,** Vol. 1 (1976) pp 207-240.

11. Flett D.S. Solvent Extraction in Copper Hydrometallurgy : A Review, **Trans. Instn. Min. Metall.** Sec. C., 83 (1974), pp 30-38.

12. Andersen E., Boe G.H., Danielssen T., Finne P.M. Production of Base Metals from Complex Sulphide Concentrates by the Ferric Chloride Route in a Small, Continuous Plant, Reference 2, pp 186-192.

13. Kordosky G.A., Sudderth R.B., House, J.E. Copper Recovery by Solvent Extraction : A Changing Industry and its Effects on Reagents Development. In **Extraction Metallurgy '85,** (London : I.M.M. 1985) pp 1057-1074.

14. Ashbrook A.W. Commercial Chelating Solvent Extraction Reagents III Oximes : Spectra, structure and Properties, **Hydrometallurgy,** Vol. 1, 1975, pp 5-24.

15. van der Zeeuw A.J., Kok R. Ideas and Practice in the Design of Solvent Extraction Reagents. In ISEC '77 : **Proceedings International Solvent Extraction Conference,** Toronto, September 1977, Vol. 1, pp 17-23.

16. Kordosky G.A., SieraKoski J.M., House J.E. The LIX 860 Series : Unmodified Copper Extraction Reagents. **ISEC '83 : Proceedings International Solvent Extraction Conference,** Denver, August/September 1983, pp 191-192.

17. Flett D.S., Okuhara D.N., Spink D.R. Solvent Extraction of Copper by Hydroxyoximes, **J. Inorg. Nucl. Chem.** Vol. 35, 1973, pp 2471-2487.

18. Chakravorthy A. Structural Chemistry of Transition Metal Complexes of Oximes. **Coord. Chem. Rev.** Vol. 13, 1974, pp 1-46.

19. Ashbrook A.W. Chelating Reagents in Solvent Extraction Processes : The Present Position. **Coord. Chem. Rev.** 1975, Vol. 16, pp 285-307.

20. Christie P.G., Lakshmanan V.I., Lawson G.J. The Liquid-Liquid Exctraction of Copper (II) and Iron (III) from Chloride Solutions using LIX 64N in Kerosene. In ISEC '74 **Proceedings International Solvent Extraction Conference,** Lyon, September 1974, Vol. 1, pp 685-697.

21. Lakshman V.I., Lawson G.J., Nyholm P.S. The Extraction of Copper (II) and Iron (III) with KELEX 100 from Aqueous Media Containing Chloride Ions. Reference 20, Vol. 1, pp 699-709.

22. Aggett J., Billinghurst, M.W. Solvent Extraction of Pyridine Complexes of Copper (II). **J. Inorg. Nucl. Chem.** 1969, Vol. 31, pp 513-525.

23. Lenarcik B., Bezak E. Studies on Extraction of Transition Metal Complexes cf. 3,4-Dimethylpyridine and 3,5- Dimethylpyridine with Oxygen-Containing Solvents. **Sep. Science and Technol,** Vol. 17 (7), 1980, pp 945-959.

24. Dalton C.F., Price R., Quan P.M. Novel Solvent Extractants for Chloride Leach Systems, Reference 16, pp 189-190.

25. Sato T., Adachi K., Kato T. Nakamura T. The Extraction of Divalent Manganese, Cobalt, Copper, Zinc and Cadmium from Hydrochloric Acid Solutions by Tri-n-Octylamine. **Sep. Science and Technol,** 1982, Vol. 17, pp 1565-1576.

26. Sekine T., Hasegawa Y. In **Solvent Extraction Chemistry : Fundamentals and Applications,** Dekker M. Inc. Ed (New York 1977) pp. 432-435.

27. Stary J. In **The Solvent Extraction of Metal Chelates,** Pergamon Press 1964, pp 101-109.

28. Uhlig E., Bechet J. Metal Extraction and Complex Formation by α-Amino Oximes. Z. **Anorg. Allg. Chem.** (1984) Vol. 518, pp 187-196.

29. Paping L.R.H., Beelen T.P.M., Rummens C.P.J., Prins R. Extraction of Cu(II) and Ni(II) by Camphorquinone Dioxime, **Polyhedron,** 1982, Vol. 1 No. 6, pp 503-510.

30. Paping L.R.M., Beelen T.P.M., Mols M., Prins R. Extraction of Copper (II) and Nickel (II) by Cyclic Trioximes and Cyclic Furazan Oximes. **Polyhedron,** 1984, Vol. 3, No. 4, pp. 479-484.

31. Preston J.S. Solvent Extraction of Base Metals by Mixtures of Organophosphoric Acids and Non-Chelating Oximes, **Hydrometallurgy,** 1983, Vol. 10, pp 187-204.

32. Preston J.S. Solvent Extraction of Nickel and Cobalt by Mixtures of Carboxylic Acids and Non-Chelating Oximes, **Hydrometallurgy,** 1983, Vol. 11, pp. 105-124.

33. Preston J.S. Non-Chelating Oximes in the Solvent Extraction of Base Metals, Reference 16, pp. 357-358.

34. Geiseler G., Stöckel E. The Use of the Mecke-Kempter Equation for the Interpretation of Association Equilibria, **Spectrochimica Acta,** 1961, Vol. 17, pp. 1185-1195.

35. Huang Chun-Hui., Bautista R.G. The Aggregation and Interaction of Tributyl Phosphate and Tricapryl Methyl Ammonium Nitrate in Hexane by Osmometry. **Sep. Science and Technol,** 1984, Vol. 19, pp 515-529.

36. Madariaga J.M., Aurrekoetxea M., Katime I. On the Interactions of Metal Extractant Reagents, **Chemica Scripta,** 1983, Vol. 22, pp 90-94.

37. Larramendi M.P.E. Study of the Synergistic Effect in the Extraction of Ni(II) with Mixtures of 5,8-diethyl-7-hydroxydodecane-6-oxime, Organophosphorous and Carboxylic Acids in Toluene, PhD Thesis, Bilbao University, 1982.

38. Marais Y., Kertes A.S. In **Ion Exchange and Solvent Extraction of Metal Complexes,** John Wiley and Sons (1969) pp 922-925.

39. Soukup R.W., Schnid R. Metal Complexes as Color Indicators for Solvent Parameters, **J. Chem. Educ.** Vol. 62, No. 6, 1985, pp 459-462.

40. Hathaway B.J., Billing D.E. The Electronic Properties and Stereochemistry of Nuclear Complexes of Copper (II) Ion. **Coordin. Chem. Rev.,** Vol. 5, 1970, pp 143-207.

41. Cotton F.A. Wilkinson G. In **Advanced Inorganic Chemistry,** John Wiley and Sons (1980), Fourth Edition, pp 663.

42. Mikhailov V.A. Volk V.N. The Extraction of Ammonium Chloride by Copper (II) Di-2-ethyhexyl Phosphate. **Russ. J. Inorg. Chem.** Vol. 30(3), 1985, pp 410-413.

43. Ciavatta L. Ferri D. Projection Maps for the Determination of Equilibrium Constants, **J. Inorg. Nucl. Chem.** Vol. 40, 1978, pp 519-524.

44. Zeltmann A.H. Matwityoff N.A. Morgan L.O. Nuclear Magnetic Resonance of Oxygen-17 and Chlorine-35 in Aqueous Hydrochloric Acid Solutions of Cobalt (II). I. Line Shifts and Relative Abundances of Solution Species, **J. Phys. Chem.,** Vol. 72, No. 1, 1968, pp 121-127.

45. Reference 41, pp. 768-773.

46. ibid, pp 785-788.

47. Dousma J. de Bruyn P.L. Hydrolysis-Precipitation Studies of Iron Solutions, I. Model for Hydrolysis and Precipitation from Fe(III) Nitrate Solutions. **J. Coll. Interf. Science,** Vol. 56, No. 3, 1976, pp 527-539.

48. Gamlen G.A. Jordan D.O. A Spectrophotometric Study of the Iron (III) Chloro-complexes, **J. Chem. Soc.** 1, 1953, pp 1435-1444.

49. Dousma J. van den Hoven T.J., de Bruyn P.L. The Influence of Chloride Ions on the Formation of Iron (III) Oxyhydroxide, **J. Inorg. Nucl. Chem.** Vol. 40, 1978, pp 1089-1093.

50. Preston J.S., Muir D.M., Parker, A.J. Cuprous Hydrometallurgy, Part VIII Solvent Extraction and Recovery of Copper (I) Chloride with Organic Nitriles from an Iron (III), Copper (II) Chloride, Two-Step Oxidative Leach of Chalcopyrite Concentrate. **Hydrometallurgy,** 5, 1980, pp 227-241.

51. Ashurst K.G., The Thermodynamics of the Formation of Chlorocomplexes cf Nickel and Copper (II) in Perchlrate Medium, NIM Report 1712, Randburg, S.A. (1975).

52. McConnel H., Davidson N., Spectrophotometric Investigation of the Copper (II) Chloro Complexes in Aqueous Solution of Unit Ionic Strength, **J. Am. Chem. Soc.,** Vol. 76, 1950, pp 3164-3167.

53. Lister M.W., Rosenblum P., Some Equilibrium Constants of Transition Metal Halides. **Can. J. Chem.** Vol. 38, 1960, pp 1827-1836.

54. Ashton L.A., Bullock J.I., Simpson P.W.G., The Association Constant of the First Chloro-Copper (II) Complex in Water to 100 ° C. **Polyhedron** Vol. 4, No. 7, 1985, pp 1323-1327.

55. Khan M.A., Schwing-Weill M.J., Stability and Electronic Spectra of the Copper (II) Chloro Complexes in Aqueous Solutions. **Inorg. Chem.** Vol. 15, No. 9, 1976, pp 2202-2205.

56. Sekine T., Hasegawa Y., In Solvent Extraction Chemistry, Reference 26, pp 32-34.

57. Foakes H.J., Preston J.S., Whewell R.J., Aqueous Phase Solubilities and Partition Data for Commercial Copper Extractants, **Anal. Chim. Acta.,** Vol. 97, 1978, pp 349-356.

58. Vogel's Textbook of Quantitative Inorganic Analysis, Fourth Edition, Longman, pp 261-280.

59. Irving H., Williams R.J.P., Order of Stability of Metal Complexes, **Nature,** No. 6, Vol. 162, 1984, pp 746-747.

60. Reference 58, pp 687-690.

61. Harned H.S., Owen B.B., Physical Chemistry of Electrolytic Solutions, Third Ed. Reinhal Publishing Corporation (1964) pp 731-735.

62. Reference 58, pp 374-377.

63. Reference 58, pp 363-366.